POST-TRANSLATIONAL MODIFICATIONS OF ARABIDOPSIS RECEPTOR-LIKE KINASES IN PLANT IMMUNITY AND DEVELOPMENT

A Dissertation

by

JINGGENG ZHOU

Submitted to the Office of Graduate and Professional Studies of
Texas A&M University
in partial fulfillment of the requirements for the degree of

DOCTOR OF PHILOSOPHY

Chair of Committee,	Ping He
Committee Members,	Michael V. Kolomiets
	Pingwei Li
	Gary R. Kunkel
Head of Department,	Gregory D. Reinhart

December 2015

Major Subject: Biochemistry

ABSTRACT

Arabidopsis BRI1-associated receptor kinase1 (BAK1) is a signaling partner of multiple receptors involved in plant immunity, growth and cell death control. BAK1 contains an extracellular leucine rich repeat (LRR) domain, transmembrane (TM) domain, juxta-membrane (JM) domain and kinase domain (K). Here we report the existence of at least one carboxyl-terminal BAK1 fragment (BAK1-C') consisting of TM, JM and K domains, originating from proteolytic cleavage. Production of BAK1-C' is largely reduced by brassinosteroid (BR)-induced BRI1-BAK interaction. An aspartic acid-to-alanine mutation at the site 287 (D287A) of BAK1 largely reduces BAK1 cleavage and BAK1D287A mutant is not able to activate multiple immune responses in *Arabidopsis* plants. Our data also indicate that the D287 site of BAK1 is required for its functions in BR signaling and cell death control. The D287A mutation of BAK1 does not affect BAK1 kinase activity, flagellin (flg22)-induced FLS2 (receptor for flg22)-BAK1 interaction or BR-induced BRI1 (receptor for BR)-BAK1 interaction. Taken together, our study suggests that the proteolytic cleavage of BAK1 may play roles in plant immunity, growth and cell death control.

The duration and intensity of immune responses must be tightly regulated to combat infections without causing deleterious side effects. The plant U-box E3 ubiquitin ligases PUB12/13 associates with FLS2 in a BAK1-dependent manner upon flg22 perception, and poly-ubiquitinates FLS2 for degradation, thereby down-regulating flagellin signaling. PUB13 consists of UND, U-box and ARM domains, and the ARM

domain interacts with the FLS2/BAK1. Over-expression of the ARM domain of PUB13 supresses FLS2-PUB13 association and FLS2 degradation, indicating that ectopic expression of the ARM domain of PUB13 *in planta* generates dominant negative effects via blocking the PUB12/13-mediated ubiquitination activity. Similarly to the *pub12pub13* mutant plants, the transgenic plants over-expressing the PUB13 ARM domain show enhanced immune responses compared to wild-type plants. Furthermore, *pub12pub13* mutant plants and PUB13ARM transgenic plants are more sensitive to stress-induced senescence. Thus, the resemblance between PUB13ARM transgenic plants and *pub12pub13* mutant plants provides evidences that the ectopic expression of the ARM domain of PUBs serves as an alternative method to dissect the overlapping functions of *PUB* genes.

ACKNOWLEDGEMENTS

I would like to thank my committee chair, Dr. Ping He, and my committee members, Dr. Michael V. Kolomiets, Dr. Pingwei Li, and Dr. Gary R. Kunkel, for their guidance and support throughout the course of this research.

I am grateful to the people who are involved in this project. Dr. Libo Shan for guiding the project, Dr. Dongping Lu, Guangyuan Xu, Dr. Scott A. Finlayson, Chenglong Liu and Xin Chen for performing various assays. Thanks also go to my colleagues and friends and the department faculty and staff for making my time at Texas A&M University a great experience.

Finally, thanks to my mother and father for their encouragement and to my girlfriend for her love.

NOMENCLATURE

BAK1	BRI1-associated receptor kinase1
BiFC	bimolecular fluorescence complementation
BIK1	Botrytis-Induced Kinase 1
BR	brassinosteroids
BRI1	brassinosteroid insensitive1
CDPK	Ca^{2+}-dependent protein kinase
Co-IP	co-immunoprecipitation
EF-Tu	elongation factor Tu
ETI	effector-triggered immunity
FLS2	flagellin-sensing 2
GFP	green fluorescence protein
GST	glutathione-S-transferase
HA	hemagglutinin
LPS	lipopolysaccharide
LRR	leucine-rich repeat
MAPK	mitogen-activated protein kinase
PAMP	pathogen-associated molecular pattern
PTI	PAMP-triggered immunity
RLK	receptor-like kinase
ROS	reactive oxygen species

SDS-PAGE	sodium dodecyl sulfate-polyacrylamide gel electrophoresis
WB	Western blot
WT	wild-type
½ MS	half-strength Murashige and Skoog medium

TABLE OF CONTENTS

Page

LIST OF FIGURES

Page

LIST OF TABLES

Page

CHAPTER I

INTRODUCTION AND LITERATURE REVIEW

Plants and animals rely on the innate immune system to fight against pathogen invasions. Unlike animals, plants lack an adaptive immune system and mobile defender cells. The first line of plant immune responses is initiated by detection of conserved pathogen- or microbe-associated molecular patterns (PAMPs or MAMPs) through pattern-recognition receptors (PRRs) (Boller and Felix, 2009; Macho and Zipfel, 2014). *Arabidopsis* flagellin-sensing2 (FLS2), a plasma membrane-localized receptor-like kinase (RLK), is a PRR of bacterial flagellin (Gomez-Gomez and Boller, 2000). A 22-amino-acid peptide corresponding to the N-terminus of flagellin, flg22, is perceived by FLS2 and induces FLS2 association with another plasma membrane-localized RLK, BAK1, which was originally identified as the plant growth hormone brassinosteroid (BR) receptor BRI1-associated kinase (Chinchilla et al., 2007; Heese et al., 2007; Li et al., 2002; Nam and Li, 2002). BAK1 is required for multiple MAMP-mediated responses and heterodimerizes with other PRRs, including bacterial elongation factor-Tu (EF-Tu) receptor EFR (Roux et al., 2011) and *Arabidopsis* Pep1 receptor AtPEPR1 (Postel et al., 2010). Upon perception of flg22, BIK1, a receptor-like cytoplasmic kinase in the FLS2-BAK1 complex, is rapidly phosphorylated by BAK1, and subsequently released from the FLS2-BAK1 complex (Lin et al., 2014; Lu et al., 2010; Zhang et al., 2010). BAK1 phosphorylates BIK1 at multiple tyrosine, serine and threonine residues and phosphorylation is indispensable for flg22-induced BIK1 release from FLS2 complex

(Lin et al., 2014; Lin et al., 2013; Xu et al., 2013). BIK1 directly phosphorylates the plasma membrane-localized respiratory burst oxidase homolog RBOHD, thereby contributing to flg22-triggered burst of reactive oxygen species (ROS) (Kadota et al., 2014; Li et al., 2014b). Perception of different MAMPs often elicits a series of overlapping immune responses, including membrane depolarization, ROS burst, cytoplasmic calcium transient, activation of Ca^{2+}-dependent protein kinases (CDPKs) and mitogen-activated protein kinase (MAPK) cascades, ethylene production, transcriptional reprograming, callose deposition and stomatal closure (Boller and Felix, 2009; Zhang and Zhou, 2010) (Fig. 1).

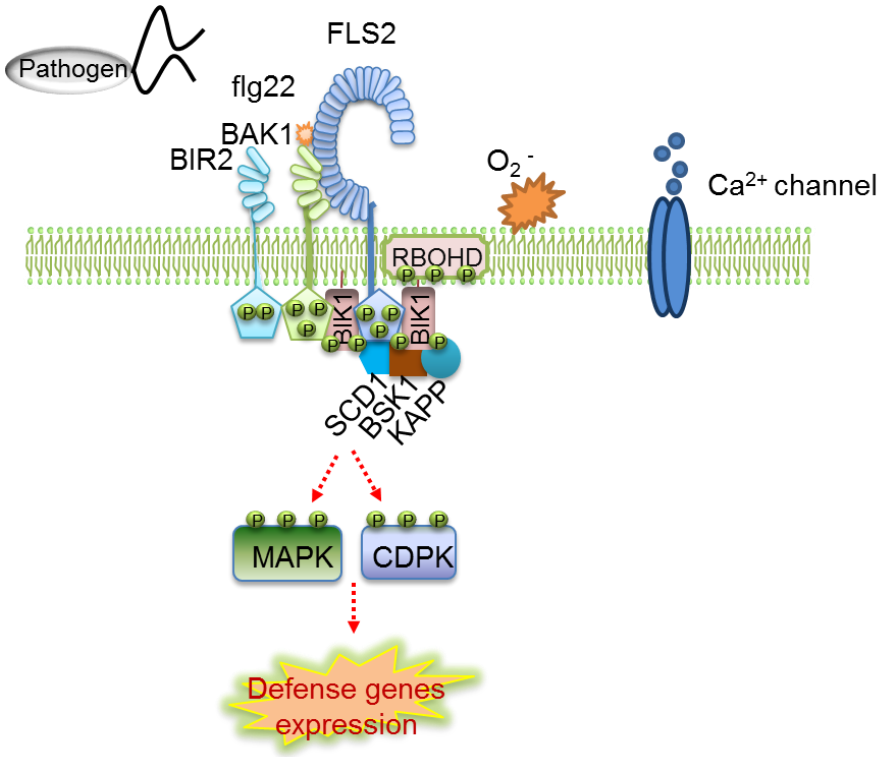

Figure 1. Flagellin induced immune responses in Arabidopsis

Plant genomes encode large numbers of cell membrane-localized RLKs to sense different signals from pathogen molecules to growth factors. Generally, RLKs have an extracellular ligand-perceiving domain, a transmembrane domain, a juxtamembrane domain, and a serine/threonine kinase domain. Mammalian cell surface receptor kinases usually contain a tyrosine kinase domain. There is a conserved aspartate in the catalytic motif of most kinases that is required for catalytic activity. The serine/threonine kinases usually have an arginine located before this catalytic aspartate. The kinases with such residues are termed as RD kinases. However, most plants RLKs implicated in pathogen detection are non-RD kinases that lack an arginine before the catalytic aspartate. They generally require additional partners to modulate their functions. An example is BAK1, which has been reported to interact with many RLKs, and is required for their activity (Greeff et al., 2012). Recently, it has been shown that Arabidopsis BAK1 together with BIK1 possess both serine/threonine kinase activity and tyrosine kinase activity in plant immunity (Lin et al., 2014). Arabidopsis genome consists of more than 600 RLKs, which are divided into 44 sub-families based on their N-terminal domains. Plant RLKs have been implicated in a lot of biologically important processes and signal pathways (Gish and Clark, 2011).

BAK1 is a multifunctional protein that plays important roles in plant growth and cell death control, in addition to plant immunity (Chinchilla et al., 2009). The steroid hormone brassinosteroids (BRs) play a major role in the growth and development in plants, and BR is sensed by the transmembrane serine/threonine protein kinase brassinosteroid insensitive 1 (BRI1). BAK1 plays a positive regulatory role in

modulating BRI1 receptor function (Nam and Li, 2002). Perception of BRs by BRI1 results in transphosphorylation and hetero-oligomerization with BAK1, and disassociation of the BRI1 kinase inhibitor1 (BKI1) and activation of BR signaling (Wang and Chory, 2006). BIK1 also acts as a negative modulator in BR signaling. BIK1 associates with BRI1, and is released from BRI1 upon BR perception (Lin et al., 2013). Recently, BAK1 together with cyclic nucleotide-gated channel 17 (CNGC17) were reported to promote plant growth when Phytosulfokine (PSK) is perceived by the leucine-rich repeat receptor kinase PSKR1. (Ladwig et al., 2015) Moreover, BAK1 was reported to negatively regulate cell death in a BR-independent manner, and *Arabidopsis* double knock-out mutant of *bak1* and its closest homolog *bak1-like 1 (bkk1)* exhibits a seedling lethality phenotype and constitutive defense responses (He et al., 2007a). *NbBAK1*-silenced *Nicotiana benthamiana* plants also display enhanced cell death symptom upon infection with the Oomycete pathogen *Hyaloperonospora parasitica (Heese et al., 2007).* The leucine rich repeat RLK (LRR-RLK) BIR1, defined as a BAK1-interating receptor-like kinase1, interacts with both BAK1 and BKK1 at the plasma membrane and negatively modulates cell death (Gao et al., 2009). These results suggest the activity of BAK1 in cell death control must be regulated by a mechanism other than interaction with receptor BRI1 (Fig. 2).

Ubiquitin consisting of 76 amino acids, is a highly conserved 8.6 kDa protein in eukaryotic cells. Ubiquitin molecule(s) could be covalently attached to proteins via its C-terminus, which is termed as ubiquitination or ubiquitylation. Ubiquitination is carried out in an ATP-dependent manner, and is a stepwise enzymatic reaction carried out by

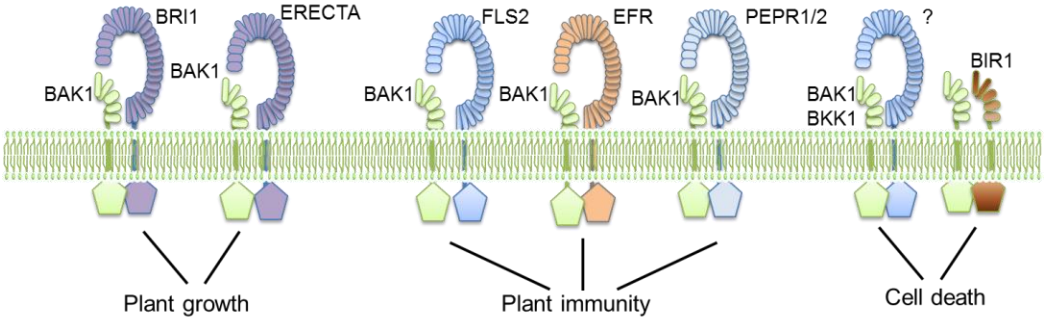

Figure 2. Multiple functions of BAK1.

an ubiquitin-activating enzyme (E1), an ubiquitin-conjugating enzyme (E2) and ubiquitin-ligase (E3) (Vierstra, 2009). The C-terminal glycine residue of a single ubiquitin can be linked to a target protein, known as monoubiquitination. Protein monoubiquitination can occur at more than one lysine residue of the target protein, known as multi-monoubiquitination. Successive addition of self-linked ubiquitin molecules can form a branched or linear ubiquitin chain, termed as polyubiquitination. All the seven lysine residues of ubiquitin can be used in the synthesis of polyubiquitin chain, resulting in a high-order complex chain. To be noted, protein ubiquitination is a reversible process as many enzymes could remove ubiquitin from the ubiquitinated proteins (Finley, 2009; Zhou et al., 2014).

Different types of protein ubiquitination modifications lead to different fates of the targeted proteins. Monoubiquitination of cell membrane-localized receptors usually serves as a signal for protein endocytosis and vesicle trafficking, leading to either protein degradation in lysosomes, or recycling back to the cell surface. As to polyubiquitination, different polyubiquitin chains play different roles in a variety of signaling pathways. Two of the well-studied examples are the K48- linked and K63-linked chains. The K48-

linked polyubiquitin chain usually directs the target proteins to the proteasome-dependent degradation, whereas the target proteins with K63-linked chain are usually associated with signaling processes, such as DNA-damage responses and activation of the transcription factor NF-κB (Finley, 2009; Smalle and Vierstra, 2004; Sun and Chen, 2004). Moreover, ubiquitination has been proved to modulate the subcellular dynamics of target proteins. The unanchored polyubiquitination chains also function as immune elicitors with the ability to activate innate immune signaling cascade (Xia et al., 2009). Protein ubiquitination is one of the key post-translational modifications that modulate the various actions of protein functions in diverse plant signaling pathways (Vierstra, 2009; Zhou et al., 2014).

There are more than 1300 genes in Arabidopsis genome encoding proteins that function in the ubiquitination pathway. These include two E1 activating enzyme genes, at least 45 E2 conjugating enzyme genes or E2-like genes. The remaining more than 1200 genes encode E3 ubiquitin ligase components. The large number of the E3 ubiquitin ligases are divided into different families depending on the mechanism of action, including RING, HECT, or U-box domains. The most recently discovered class of E3 ligases is U-box E3 ubiquitin ligase. This class of E3 ligases is categorized through a conserved U-box motif consisting of 70 amino acids originally identified in the yeast UFD2 protein. Interestingly, there is only one U-box E3 ligase in yeast genome, while plants possess a large number of this type of E3 ligases. Sequence and structural analyses have revealed that the U-box domain was actually a modified RING-finger domain. U-box proteins function as E3 ubiquitin ligases and mediate ubiquitin

ligation by simultaneously interacting with both E2 enzymes and the targeted proteins (Yee and Goring, 2009).

There are several PUBs that have been implicated in plant immunity and cell death control (Craig et al., 2009; Trujillo and Shirasu, 2010). Avr9/Cf9 rapidly elicited (ACRE) genes, ACRE74 (CMPG1) and ACRE276 (PUB17), have been shown to be required for plant defense and programmed cell death (PCD) in tomato, tobacco and *Arabidopsis* (Gonzalez-Lamothe et al., 2006; Yang et al., 2006). In contrast, Spotted leaf 11 (SPL11) in rice acts as a negative regulator of pathogen resistance and plant PCD (Zeng et al., 2004), and another three closely related *Arabidopsis* U-box E3 ubiquitin ligases, PUB22, PUB23 and PUB24, have been reported to negatively regulate PTI signaling (Trujillo et al., 2008). PUB22 protein interacts with and ubiquitinates its substrate protein Exo70B2. Exo70B2 is a subunit of the exocyst complex that regulates vesicle tethering during exocytosis (Stegmann et al., 2012) and is required for full activation of multiple PTI responses and resistance to different pathogen infections. Perception of flg22 by Arabidopsis stabilizes PUB22 protein and promotes PUB22-mediated degradation of Exo70B2 through the 26S proteasome system, thereby attenuating flg22-triggered immune signaling (Stegmann et al., 2012).

CHAPTER II

PROTEOLYTIC CLEAVAGE OF RECEPTOR-LIKE KINASE BAK1 CONTRIBUTES TO ARABIDOPSIS IMMUNITY AND DEVELOPMENT*

Introduction

As other organisms, plants use proteases to get rid of nonfunctional proteins by degrading them into amino acids. In addition, proteases have been shown to possess many more biological functions. Proteases are proved to be key regulators of diverse biological processes. Through irreversibly determining the fate of target proteins, proteases regulate different processes in response to environmental and developmental cues, indicating that proteases are substrate specific, and their activity is tightly controlled in time and space. Research on the existence and function of regulatory proteases in plants is quite recent and determining the targets of proteases is challenging.

In plants, one well-studied immune receptor is rice XA21 (Xanthomonas resistance 21). The rice XA21 receptor confers broad-spectrum immunity to the Gram-negative bacterial pathogen, *Xanthomonas oryzae pv. oryzae* upon recognition of an unknown ligand (Schwessinger and Ronald, 2012). XA21 is cleaved to release the intracellular kinase domain and exposes a functional nuclear localization sequence in the intracellular part. The XA21 intracellular domain interacts with the OsWRKY62

*The materials and methods part is reprinted with permission from Jinggeng Zhou, Dongping Lu, Guangyuan Xu, Scott A. Finlayson, Ping He and Libo Shan (2015), The dominant negative ARM domain uncovers multiple functions of PUB13 in Arabidopsis immunity, flowering, and senescence. Journal of Experimental Botany, 66(11): 3353–3366.

transcriptional factor exclusively in the rice nucleus. Proteolytic cleavage of XA21 and translocalization of the intracellular domain to the nucleus are essential for the XA21-mediated immune response (Park and Ronald, 2012). ETHYLENE INSENSITIVE2 (EIN2), an NRAMP-like integral membrane protein, plays an essential role in ethylene signaling. Phosphorylation-mediated proteolytic cleavage of EIN2 relocates it from endoplasmic reticulum (ER) to nucleus. Sensing ethylene signal induces dephosphorylation at multiple sites and proteolytic cleavage at one of these sites, leading to nuclear translocation of a carboxyl-terminal EIN2 fragment (EIN2-C') (Qiao et al., 2012). Rising evidence suggests that proteolytic cleavage of membrane-located proteins causes translocation.

We report the production of the BAK1 C-terminal fragments (BAK1-C') when *Arabidopsis* BAK1 was expressed in *Arabidopsis* protoplasts and transgenic plants, and very likely BAK1-C' fragments were derived from proteolytic cleavage of BAK1. We identified a D287A mutant of BAK1 with reduced protein level of BAK1-C' fragment through a site-specific mutagenesis screening. The D287A mutation did not affect BAK1 kinase activity, BAK1-FLS2 and BAK1-BRI1 interactions, whereas this mutation hampered BAK1 activity in immunity, growth and cell death control, indicating the importance of BAK1 proteolytic cleavage. Furthermore, plant hormone BR could reduce BAK1 cleavage. To our knowledge, this is a comprehensive characterization of BAK1 cleavage in *Arabidopsis*, and our studies may shed light on the research of RLK proteolytic cleavages in the near future.

Results

Detection of C-terminal BAK1 fragments

We transiently expressed BAK1 in *Arabidopsis* protoplasts, and detected one 70 KD band corresponding to the full-length BAK1 and one 47 KD band with a Western blot (WB) using an α-BAK1 antibody (Fig. 3A). The 47 KD band was not detected in the control protoplasts, suggesting it is derived from BAK1. The 47 KD product is the carboxyl-terminal BAK1 fragment (BAK1-C') as the α-BAK1 antibody targets the C-terminus of BAK1. The C-terminus of BAK1 is critical for its function and tags at the C-terminus may interfere with its activities in BR signaling and immune responses (Ntoukakis et al., 2011). We then tested BAK1 carrying a green fluorescent protein (GFP), two tandem hemagglutinin (HA) or two tandem FLAG tags at the C-terminus (BAK1-GFP, BAK1-HA and BAK1-FLAG) expressed in *Arabidopsis* protoplasts. One band corresponding to the BAK1-C' could be detected from WB of BAK1-GFP using α-GFP antibody, while three C-terminal BAK1 fragments, 49KD, 45 KD and 43 KD (including 2X HA or 2X FLAG tag with a molecular weight of ~2 KD), could be detected from WB of BAK1-HA and BAK1-FLAG using high-affinity α-HA and α-FLAG antibodies (Fig. 3A). To further characterize the C-terminal BAK1 fragments, we generated *Arabidopsis* transgenic plants stably expressing BAK1-HA under the control of CaMV 35S promoter (35S::BAK1-HA) and BAK1-GFP under the control of native BAK1 promoter (pBAK1::BAK1-GFP). Both the full length BAK1 and C-terminal BAK1 fragments could be detected from 35S::BAK1-HA and pBAK1::BAK1-GFP transgenic plants as shown by WB with respective α-HA and α-GFP antibodies (Fig.

3B). To test if the C-terminal BAK1 fragments were produced in other species, we expressed *Arabidopsis* BAK1-HA and C-terminal Myc-tagged *Arabidopsis* BAK1 (BAK1-Myc) in *Nicotiana benthamiana*, *Physcomitrella patens* and *Saccharomyces cerevisiae*. Both the full length BAK1 and C-terminal BAK1 fragments could be detected from all three tested species as shown by WB with an α-HA or an α-Myc antibody (Fig. 3C, D & E). To be noted, only one BAK1-C' in addition to the full length BAK1 could be detected from *P. patens* and *S. cerevisiae*, indicating the production of C-terminal BAK1 fragments may not be exactly the same as in *Arabidopsis* and *N. benthamiana.*

BAK1 is a member of the somatic embryogenesis receptor kinase (SERK) family (Hecht et al., 2001). We checked three other functional SERKs and found that C-terminal fragments could be detected in *Arabidopsis* protoplasts expressing SERK1, 2 or 4 with a FLAG-tag at the C-terminus. However the C-terminal fragments vary in the number and molecular weight among SERKs as shown by WB with an α-FLAG antibody. SERK1 has one (45 KD, including 2xFLAG tag) C-terminal fragment. SERK2 and SERK4 have three (48 KD, 44 KD and 43KD, including 2xFLAG tag) C-terminal fragments (Fig. 3E). Taken together, our data suggest there exists a common mechanism to produce the C-terminal fragment of SERKs.

We next investigated the cleavage of BAK1 in 35S::BAK1-HA transgenic plants at different growth stages and different organs using WB towards the HA tag. We found that the 49KD BAK1-C’ fragment was produced the most at the seedling stages (8 ~13

days post germination), and was continuously reduced at later growth stages (19 ~ 35 days post germination) (Fig. 3G). For the two-month old 35S::BAK1-HA transgenic

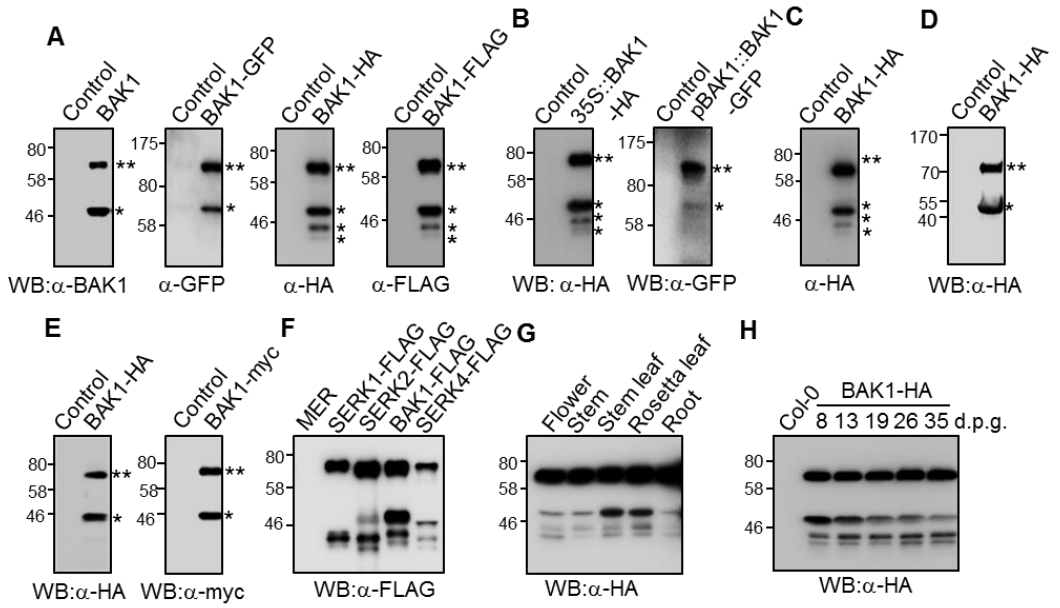

Figure 3. Production of C-terminal BAK1 fragments.

(A) C-terminal BAK1 fragments (BAK1-C') produced in *Arabidopsis* protoplasts. The upper band corresponding to the full-length BAK1 was indicated by **, and the lower bands corresponding to the C-terminal BAK1 fragments were indicated by *. (B) BAK1-C' produced in Arabidopsis transgenic plants. Protein extracts from 35S::BAK1-HA (left panel) and pBAK1::BAK1-GFP (right panel) transgenic plants were analyzed by WB with respective α-HA and α-GFP antibodies. (C) BAK1-C' produced in *Nicotiana benthamiana.* (D) BAK1-C' produced in *Physcomitrella patens.* (E) BAK1-C' produced in *Saccharomyces cerevisiae.* (F) SERKs. Protein extracts from *Arabidopsis* protoplasts expressing FLAG-tagged SERK1, 2, 3 and 4 were analyzed by WB with an α-HA antibody. (G) BAK1-C' produced more at early growth stage. Total proteins extracted from whole transgenic *Arabidopsis* 35S::BAK-HA at a series growth stages, ranging from 8 through 35 days post germination (d.p.g.) on ½ MS plates were analyzed by WB with an α-HA antibody. (H) BAK1-C' produced more at leaves. Total proteins extracted from different organs of two-months old 35S::BAK1-HA transgenic plants grown on soil were analyzed by WB with an α-HA antibody.

plants, the 47KD BAK1-C' fragment mainly existed in stem leaves and rosette leaves, with less in stems, flowers and roots (Fig. 3H). Therefore, the proteolytic cleavage of BAK1 may be regulated by plant growth and development.

C-terminal BAK1 fragments are produced from proteolytic cleavage

Mammalian Toll-like receptors (TLRs) sensing invasive pathogens were reported to undergo proteolytic cleavage (Ewald et al., 2011; Garcia-Cattaneo et al., 2012; Park et al., 2008). To determine if the C-terminal BAK1 fragments are also produced by the proteolytic cleavage, we tested a series of chemicals on the BAK1 cleavage in *Arabidopsis* protoplasts. As the 47 KD BAK1-C' fragment is much more abundant than the other two C-terminal BAK1 fragments, we focus on the 47 KD BAK1-C' in the following study. The commonly-used proteasome and protease inhibitor MG132 blocked the production of BAK1-C' fragment in the *Arabidopsis* protoplasts expressing BAK1, while the specific 26S proteasome inhibitor Lactacystin could not. The calcium (Ca^{2+}) chelating agents ethylenediaminetetraacetic acid (EDTA), ethylene glycol tetraacetic acid (EGTA) and the Ca^{2+} channel blocker Lanthanum(III) chloride ($LaCl_3$), Gadolinium(III) chloride ($GdCl_3$) could also block or reduce the production of BAK1-C' in protoplasts (Fig. 4A). These data suggest that a Ca^{2+}-activated protease may be responsible for producing BAK1-C'. MG132 was reported as an inhibitor of Calpain, a non-lysosomal cysteine proteases. We tested a series of Calpain inhibitors on BAK1 expressed in *Arabidopsis* protoplasts, and four of five could block production of BAK1-C' (Fig. 4B). We purified Calpain protein which actively cleaved substrate β-casein.

However, Calpain failed to cleave BAK1 protein (data not shown). We also found that γ-secretase inhibitor could reduce BAK1-C' production in *Arabidopsis* protoplasts (Fig. 4C). Nevertheless, Calpain and γ-secretase inhibitors are known to be nonspecific, making it hard to identify the exact protease responsible for cleavage of BAK1.

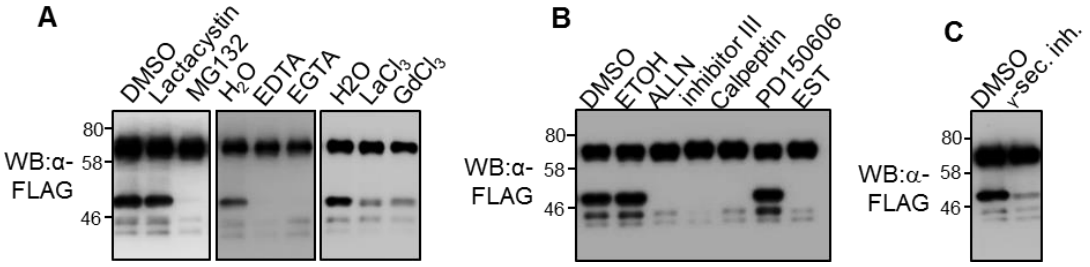

Figure 4. Protease inhibitors reduce the production of BAK1-C'.

(A, B&C) WB analysis of BAK1 expressed in *Arabidopsis* protoplasts with treatment of a variety of chemicals. 2 μM of Lactomysin, 2 μM of MG132, 1mM of EDTA, 1 mM of EGTA, 1mM of $LaCl_3$ and 0.5mM of $GdCl_3$ (A), 20 μM of Calpain inhibitors(B), 1 μM of γ-secretase inhibitor (C) were added to the protoplasts right after transformation with BAK1-FLAG. Total proteins were extracted from protoplasts and were analyzed by WB with an α-FLAG antibody.

BRI1 binding to BAK1 reduces BAK1 cleavage

The kinase activity of BAK1 is required for plant immune responses and BR signaling. We tested if the kinase activity of BAK1 could affect BAK1 cleavage. We first applied the kinase inhibitor K252a to *Arabidopsis* protoplasts expressing BAK1-HA, and K252a had no observable effect on BAK1 cleavage (Fig. 5A). Moreover, the BAK1-C' fragment could be detected from *Arabidopsis* protoplasts expressing HA-tagged BAK1 kinase mutant (BAK1km-HA) analyzed by WB with an α-HA antibody

(Fig. 5B). Nevertheless, we observed reduced proportion of the BAK1-C' fragment when co-expressing FLAG- or Myc-tagged BAK1 with BRI1-HA in *Arabidopsis* protoplasts and *S. cerevisiae* (Fig. 5C&D), whereas co-expression of other BAK1-interacting proteins, BIK1 and FLS2, in *Arabidopsis* protoplasts had no obvious effect on BAK1 cleavage (Fig. 5C). These results suggest that brassinosteroid (BR) signaling may regulate BAK1 cleavage. To test this possibility, we applied brassinolide (BL, most effective form of BR) to *Arabidopsis* protoplasts co-expressing BAK1-FLAG and BRI1-HA. The BAK1-C' fragment was significantly reduced in BL-treated *Arabidopsis* protoplasts (Fig. 5E). To confirm the role of BR in BAK1 cleavage, we also grew 35S::BAK1-HA transgenic plants on ½ MS plates without or with BL at two concentrations. BL at a lower concentration of 0.1 μM clearly reduced the production of the BAK1-C' fragment, and BL at a higher concentration of 1 μM further reduced the BAK1-C' fragment (Fig. 5F). Thus, BR signaling seems to be a negative regulator of BAK1 cleavage. Application of flg22 to 35S::BAK1-HA transgenic plants had no obvious effect on BAK1 cleavage (Fig. 5G). We next applied BL to *Arabidopsis* protoplasts co-expressing BAK1-FLAG and BRI1km-HA. BAK1-C' fragment was also significantly reduced in BL-treated *Arabidopsis* protoplasts co-expressing BAK1-FLAG and BRI1km-HA (Fig. 5H). Thus, BR-driven BRI1-BAK1 interaction may be sufficient to reduce BAK1 cleavage. To test this idea, we tested a BAK1 mutant that loses BRI1-BAK1 interaction. BAK1F60AF144A failed to interact with BRI1 in a co-IP assay (Fig. 5I). We co-expressed FLAG-tagged BAK1F60AF144A with BRI1-HA in *Arabidopsis*

Figure 5. BR-induced BRI1-BAK1 interaction reduces BAK1 cleavage.

(A) Kinase inhibitor does not affect BAK1 cleavage in Arabidopsis protoplasts. Protein extracts from *Arabidopsis* protoplasts expressing BAK1-HA were analyzed by WB with an α- HA antibody. K252a at a final concentration of 1 μM was added immediately after protoplasts transformation. (B) Kinase activity of BAK1 does not affect BAK1 cleavage in *Arabidopsis* protoplasts. HA-tagged wild type and kinase mutant (km) form of BAK1 (BAK1km) expressed in *Arabidopsis* protoplasts were analyzed by WB with an α-HA antibody. (C&D) Co-expression of BRI1 in *Arabidopsis* protoplasts and yeast reduces BAK1 cleavage. (C) Protein extracts from *Arabidopsis* protoplasts co-expressing FLAG-tagged BAK1 and HA-tagged BIK1, BRI1 or FLS2 were analyzed by WB with respective α-FLAG and α-HA antibodies. (D) Protein extracts form yeast *S. cerevisiae* co-expressing myc-tagged BAK1 and HA-tagged BRI1 were analyzed by WB with respective α-myc and α-HA antibodies. (E) BL reduces BAK1 cleavage in *Arabidopsis* protoplasts. Protein extracts from *Arabidopsis* protoplasts co-expressing FLAG-tagged BAK1 and HA-tagged BRI1 were analyzed by WB with respective α-FLAG and α-HA antibodies. BL at a final concentration of 1 μM was added immediately after protoplasts transformation. (F & G) BL while not flg22 reduces BAK1 cleavage in *Arabidopsis* plants. Total proteins extracted from 1-week old 35S::BAK1-HA transgenic plants on ½ MS plates with BL (F) or flg22 (G) as indicated concentration were analyzed by WB with α-HA antibody. (H) Co-expression of BRI1km in *Arabidopsis* protoplasts reduces BAK1 cleavage. Protein extracts from *Arabidopsis* protoplasts co-expressing BAK1-FLAG and HA-tagged BRI1 kinase mutant (BRI1km-HA) were analyzed by WB with respective α-FLAG and α-HA antibodies. BL at a final concentration of 1 μM was added immediately after protoplasts transformation. (I) F60A F144A mutations of BAK1 block BAK1-BRI1 interactions. *Arabidopsis* protoplasts were transfected with BRI1-HA and BAK1-FLAG or BAK1F60AF144A-FLAG, and incubated for 10 h before 1 μM BL treatment for 3 hr. The association of BAK1-BRI1 was detected by an α-HA WB after α-FLAG IP. The protein levels of BRI1, and BAK1 were detected by α-HA and α-FLAG WB, respectively. (J) BRI1F60AF144A does not reduce BAK1 cleavage. Protein extracts from *Arabidopsis* protoplasts co-expressing BAK1-FLAG and HA-tagged BRI1F60AF144A mutant were analyzed by WB with respective α-FLAG and α-HA antibodies. BL at a final concentration of 1 μM was added immediately after protoplasts transformation.

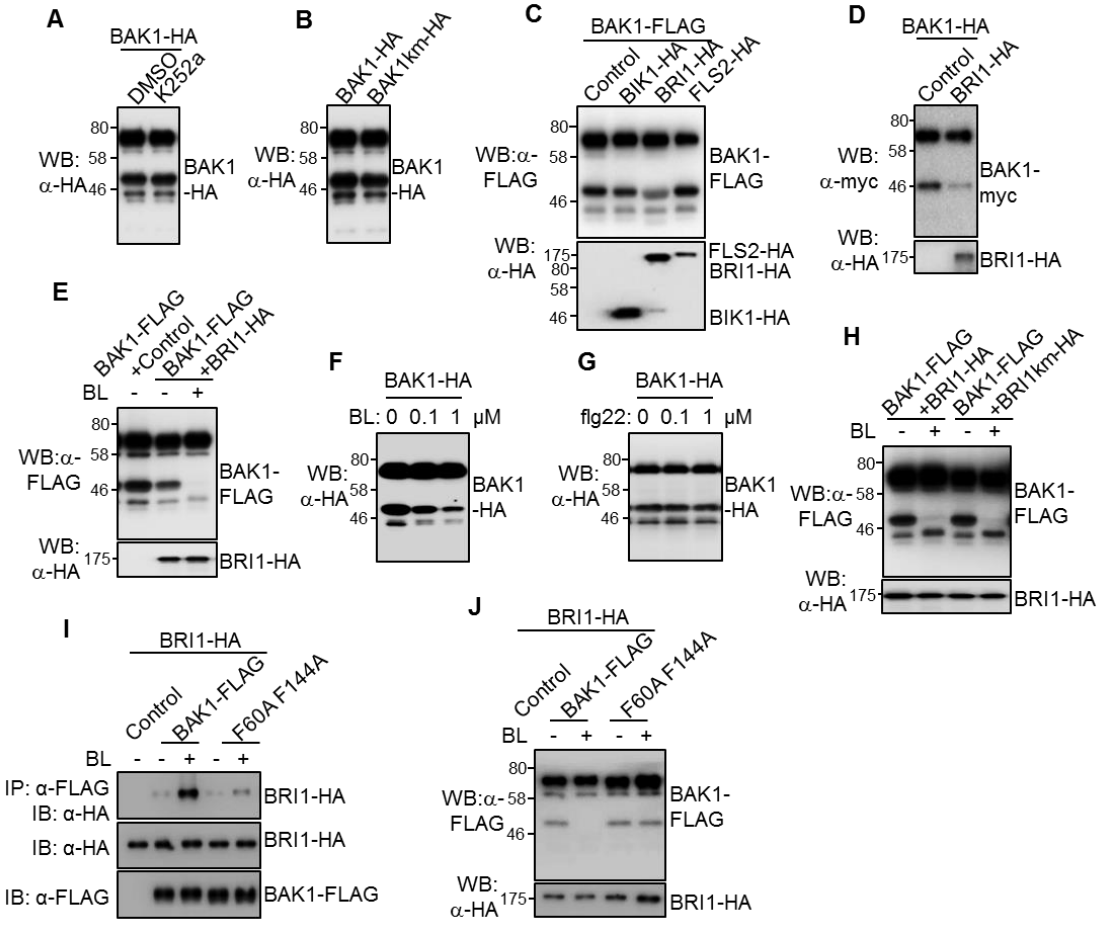

protoplasts and analyzed BAK1 cleavage by WB with respective α-FLAG and α-HA antibodies. Application of BL did not affect BAK1 cleavage in the protoplasts co-expressing BAK1F60AF144A and BRI1 (Fig. 5J). Taken together, BR-driven BRI1-BAK1 interaction could reduce BAK1 cleavage.

D287A mutation of BAK1 blocks BAK1 cleavage

To identify the cleavage site on BAK1, we expressed BAK1-GFP in *Arabidopsis* protoplasts. BAK1-GFP was immuno-precipitated (IP) with an α-GFP antibody and

analyzed on SDS-PAGE with silver staining and Coomassie Brilliant Blue (CBB) staining. The band corresponding to BAK1-C' was cut out and analyzed by Mass spectrometry (MS). A series of peptides covering the intracellular domain of BAK1 were identified. The coverage for BAK1 was only partial, we thus were not able to determine the precise sequence of BAK1-C' (Fig. 6). We generated a series of truncated BAK1 constructs, expressed these truncated BAK1 in *Arabidopsis* protoplasts, and compared BAK1-C' to these truncated constructs by WB with an α-BAK1 antibody (Fig. 7A). Truncated BAK1 consisting the whole transmembrane, juxtamembrane and kinase domains has slightly larger molecular weight than BAK1-C' (Fig. 7B), indicating the proteolytic cleavage mainly happens on BAK1 transmembrane domain close to the N-

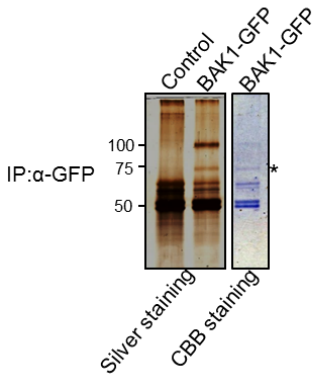


```
  1 MERRLMIPCF FWLILVLDLV LRVSGNAEGD ALSALKNSLA DPNKVLQSWD
 51 ATLVTPCTWF HVTCNSDNSV TRVDLGNANL SGQLVMQLGQ LPNLQYLELY
101 SNNITGTIPE QLGNLTELVS LDLYLNNLSG PIPSTLGRLK KLRFLRLNNN
151 SLSGEIPRSL TAVLTLQVLD LSNNPLTGDI PVNGSFSLFT PISFANTKLT
201 PLPASPPPPI SPTPPSPAGS NRITGAIAGG VAAGAALLFA VPAIALAWWR
251 RKKPQDHFFD VPAEEDPEVH LGQLKRFSLR ELQVASDNFS NKNILGRGGF
301 GKVYKGRLAD GTLVAVKRLK EERTQGGELQ FQTEVEMISM AVHRNLLRLR
351 GFCMTPTERL LVYPYMANGS VASCLRERPE SQPPLDWPKR QRIALGSARG
401 LAYLHDHCDP KIIHRDVKAA NILLDEEFEA VVGDFGLAKL MDYKDTHVTT
451 AVRGTIGHIA PEYLSTGKSS EKTDVFGYGV MLLELITGQR AFDLARLAND
501 DDVMLLDWVK GLLKEKKLEA LVDVDLQGNY KDEEVEQLIQ VALLCTQSSP
551 MERPKMSEVV RMLEGDGLAE RWEEWQKEEM FRQDFNYPTH HPAVSGWIIG
601 DSTSQIENEY PSGPR*
```

Figure 6. Mass spectrometry analysis of cleaved BAK1 band.

Protein extracts from *Arabidopsis* protoplasts expressing GFP-tagged BAK1 were immunoprecipitated (IP) with α-GFP antibody and agarose beads. Immunoprecipitates were separated on SDS-PAGE and stained with silver staining and CBB staining. The lower BAK1 band stained indicated with star (*) were cut out and subjected to a mass spectrometry (MS) analysis after trypsin digestion. BAK1 peptides identified by MS are shown in red.

terminus. To further identify the precise cleavage sites on BAK1, we did a series of mutations on the transmembrane domain of BAK1 (Fig. 7C). Each FLAG- or HA-tagged BAK1 mutant carrying three or four amino acids substitution with alanine was expressed in *Arabidopsis* protoplast and analyzed by WB with respective α-FLAG and α-HA antibodies. None of these mutations except PPPP (206-209)-to-AAAA mutation could largely reduce the production of 49 KD (MW of 2xFLAG is 2 KD) BAK1-C'. However, this mutation caused production of an additional 47 KD (MW of 2xHA is 2 KD) BAK1-C' fragment (Fig. 7D). We then checked several predicted cleavage sites by caspase, and found amino acids substitution with alanine at site 284-287 (VASD) could block the production of 49 KD (MW of 2xHA is 2 KD) BAK1-C' (Fig. 7E&F). Subsequent work showed that the aspartate-to-alanine or glutamate mutations at site 287 (BAK1D287A or D287E) were sufficient to block the production of 49 KD (MW of 2xFLAG is 2 KD) BAK1-C' (Fig. 7G&H). To further characterize the D287A mutation, we transiently expressed HA-tagged wild BAK1 and BAK1D287A mutant in *N. benthamiana*. D287A could also block the production of 49 KD (MW of 2xHA is 2 KD) BAK1-C' in *N. benthamiana* (Fig. 7I). We generated *Arabidopsis* transgenic plants stably expressing HA-tagged BAK1D287A under the control of CaMV 35S promoter (35S::BAK1D287A-HA) and GFP-tagged BAK1D287A under the control of native BAK1 promoter (pBAK1::BAK1D287A-GFP) (Fig. 7 J&K). 47 KD (MW of tags are not included) BAK1-C' was largely reduced in both the 35S::BAK1D287A-HA and pBAK1::BAK1D287A-GFP transgenic plants analyzed by WB with respective α-HA and α-GFP antibodies. The aspartate 287 residue is highly conserved among SERKs. To

Figure 7. D287A mutation blocks BAK1 cleavage.

(A) Truncated BAK1 constructs used in (B) are listed with expected molecular weights (MW). E: extra-cellular domain, T: trans-membrane domain, J: juxta-membrane domain, K: kinase domain. (B) Identification of cleavage site of BAK1. Protein extracts from *Arabidopsis* protoplasts expressing full-length and truncated BAK1 were analyzed by WB with an α-BAK1 antibody. The lower band corresponding to the C-terminal product of BAK1 is little smaller than the truncated BAK1 including transmembrane, juxtamembrane and kinase domains (TJK). (C) Every three or four amino acids on transmembrane domain (TM) of BAK1 were mutated to Alanine. (D) Protein extracts from *Arabidopsis* protoplasts expressing the FLAG- or HA- tagged BAK1 mutants listed in (C) were analyzed by WB with respective α-FLAG and α-HA antibodies. (E) Potential sites predicted to be targeted by caspase were mutated to Alanines. (F) Protein extracts from *Arabidopsis* protoplasts expressing HA-tagged BAK1 mutants listed in (E) were analyzed by WB with an α-HA antibody. (G &H) The Aspartic acid at 287aa of BAK1 is critical for BAK1 cleavage. Mutations of Aspartic acid at 287aa of BAK1 to Alanine (D287A) or Glutamic acid (D287E) block BAK1 cleavage. Protein extracts from *Arabidopsis* protoplasts expressing the FLAG-tagged BAK1 or mutants were analyzed by WB with an α-FLAG antibody. (I) D287A mutation blocks BAK1 cleavage in *N. benthamiana.* Protein extracts from *N. benthamiana* transiently expressing HA-tagged BAK1 or D287A mutant were analyzed by WB with α-HA antibody. (J & K) D287A blocks BAK1 cleavage in *Arabidopsis* transgenic plants. (J) Protein extracts from *Arabidopsis* transgenic plants expressing HA-tagged BAK1 or D287A mutant under the control of 35S promoter were analyzed by WB with α-HA antibody. (K) Protein extracts from *Arabidopsis* transgenic plants expressing GFP-tagged BAK1 or D287A mutant under the control of native BAK1 promoter were analyzed by WB with an α-GFP antibody. (L) D287 residue of BAK1 is conserved among SERKs. Protein extracts from *Arabidopsis* protoplasts expressing the FLAG-tagged SERKs WT or mutants were analyzed by WB with an α-FLAG antibody.

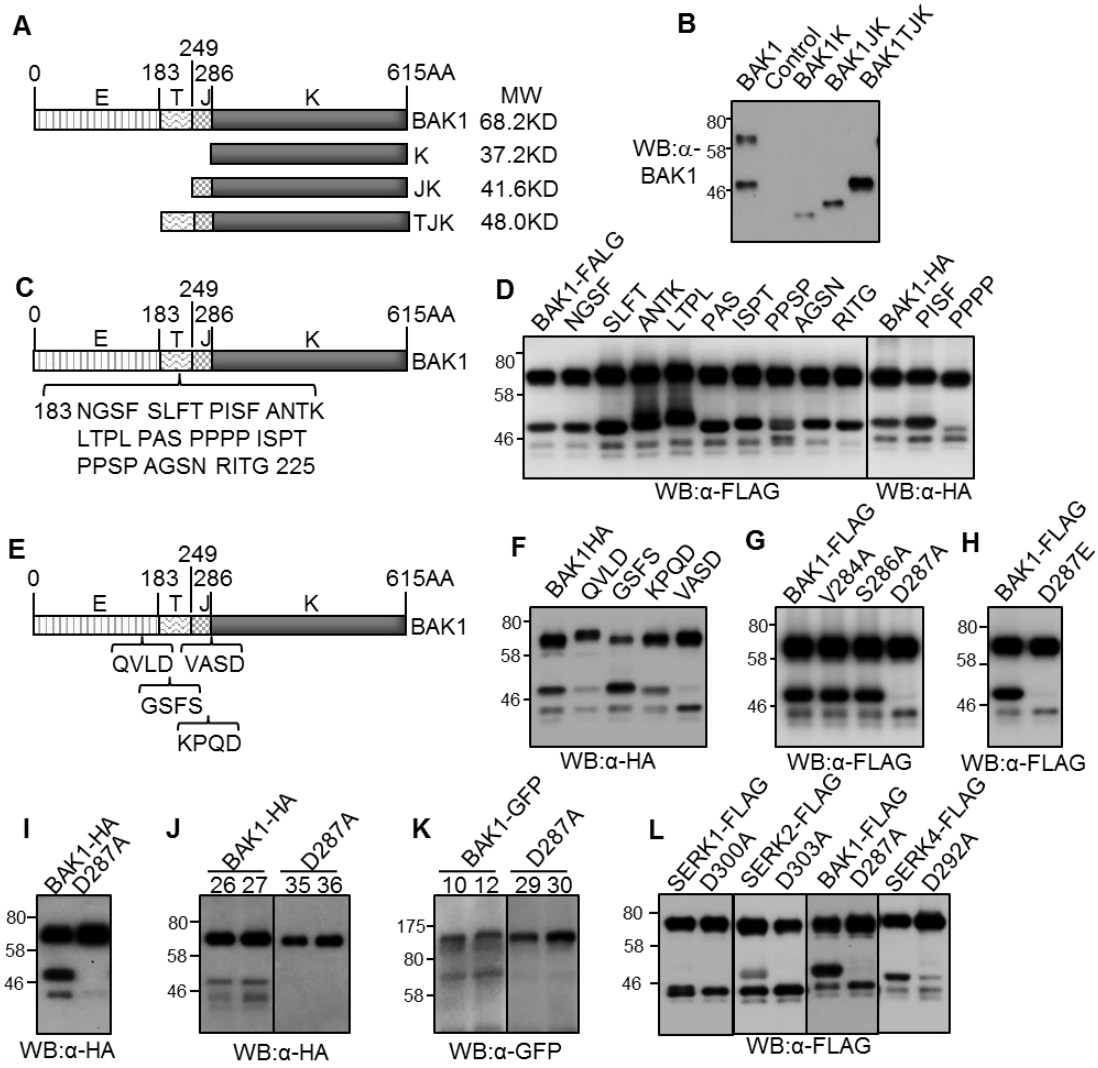

determine if this conserved site is required for proteolytic cleavage of other SERKs, we mutated the conserved aspartate of SERK1, 2 and 4 to alanine, and found that C-terminal fragments of SERK2 and SERK4 were reduced, indicating the conserved aspartate residue is required for proteolytic cleavage of SERKs (Fig. 7L).

BAK1D287A mutant loses activities in immune responses in Arabidopsis protoplasts

We next assessed if the D287 site is required for immune responses in *Arabidopsis* protoplasts. flg22-induced BIK1 phosphorylation is indicated by a mobility shift on SDS-PAGE and requires BAK1. We co-expressed HA-tagged BIK1 with BAK1, BAK1D287A or a control vector in *Arabidopsis* protoplasts isolated from the BAK1 null mutant *bak1-4*. flg22 induced mobility shift of BIK1-HA in *bak1-4* protoplasts co-expressing BAK1, whereas it failed to induce such mobility shift in *bak1-4* protoplasts co-expressing BAK1D287A (Fig. 8A). flg22-mediated activation of MAPKs was examined with an α-pERK antibody that cross-reacts with phosphorylated *Arabidopsis* MPK3 and MPK6. MPK3 and MPK6 were activated 15 min after flg22 treatment in *bak1-4* protoplasts expressing BAK1, whereas they were not activated in *bak1-4* protoplasts expressing BAK1D287A or a control gene (Fig. 8B). Moreover, we performed reporter assays in *bak1-4* protoplasts using FRK1 and WRKY29 promoters fused to the reporter luciferase (Fig. 8C). Both BAK1 and BAK1D287A could elevate FRK1 and WRKY29 promoter activities without flg22, whereas neither of these promoters could be activated by flg22 in protoplasts expressing BAK1D287A (Fig. 8C). Thus D287 site is required for BAK1 function in immune responses. Although we showed that the D287A mutation could block BAK1 cleavage, it is possible that this mutation can affect other properties of the BAK1 protein. We then tested protein-protein interactions for BAK1D287A-FLS2 and BAK1D287A-BRI1 in co-IP assays. BAK1-FLAG or BAK1D287A-FLAG was co-expressed with FLS2-HA in *Arabidopsis* protoplasts, and FLS2 was detected in the precipitates with an α-HA western blot upon

Figure 8 . BAK1D287A mutant is insensitive to flg22 in *Arabidopsis* protoplasts.

(A) flg22-induced BIK1 mobility shift. *Arabidopsis bak1-4* protoplasts were co-transformed with MER, BAK1 or D287A mutant and with HA-tagged BIK1 (BIK1-HA), and 12 hr after transformation protoplasts were treated with 1 μM of flg22 for 15 min. Equal loading was indicated by coomassie brilliant blue (CBB) staining towards Rubisco (Rub). (B) flg22-induced MAPK activation. *Arabidopsis bak1-4* protoplasts were transformed with MER, BAK1 WT or D287A mutant, and 12 hr after transformation protoplasts were treated with 1 μM of flg22 for 15 min. Protein extracts from protoplasts were analyzed by WB with an α-ERK1/2 antibody towards MPKs and WB with an α-BAK1 antibody towards BAK1. (C) flg22-induced activation of immunity-related genes. The pFRK1-LUC or pWRKY29-LUC was co-transfected with MER, BAK1 WT or D287A mutant in *Arabidopsis bak1-4* protoplasts to determine the activation of FKR1 or WRKY29 promoters triggered by 100nM of flg22. The data are shown as the mean ± SE (n = 3). (D) BAK1-FLS2 interactions in *Arabidopsis* protoplasts. *Arabidopsis* protoplasts were transfected with FLS2-HA and BAK1-FLAG or BAK1D287A-FLAG, and incubated for 10 h before 1 μM flg22 treatment for 10 min. The association of BAK1-FLS2 was detected by an α-HA WB after α-FLAG immunoprecipitation (IP). The protein levels of FLS2, and BAK1 were detected by α-HA and α-FLAG WB, respectively. (E) BAK1-BRI1 interactions in *Arabidopsis* protoplasts. *Arabidopsis* protoplasts were transfected with BRI1-HA and BAK1-FLAG or BAK1D287A-FLAG, and incubated for 10 h before 1 μM BL treatment for 3 hr. The association of BAK1-BRI1 was detected by an α-HA WB after α-FLAG IP. (F) D287A mutation does not affect kinase activity of BKA1. GST–BIK1km proteins (10 μg) were used as substrates and MBP–BAK1JK (1 μg) as the kinase in an *in vitro* kinase assay. Phosphorylation was detected by autoradiography (top panel), and the protein loading is shown by CBB staining (bottom panel). (G) BAK1TJK interacts with BIK1. *Arabidopsis* protoplasts were transfected with BIK1-HA and BAK1TJK-FLAG or FLS2-FLAG, and incubated for 10 h before 1 μM flg22 treatment for 10 min. The association of BAK1TJK-BIK1 was detected by an α-HA WB after α-FLAG immunoprecipitation. (H) BAK1TJK does not interact with FKS2. *Arabidopsis* protoplasts were transfected with FLS2-HA and BAK1TJK-FLAG or BAK-FLAG, and incubated for 10 h before 1 μM flg22 treatment for 10 min. The association of BAK1TJK-FLS2 was detected by an α-HA WB after α-FLAG immunoprecipitation.

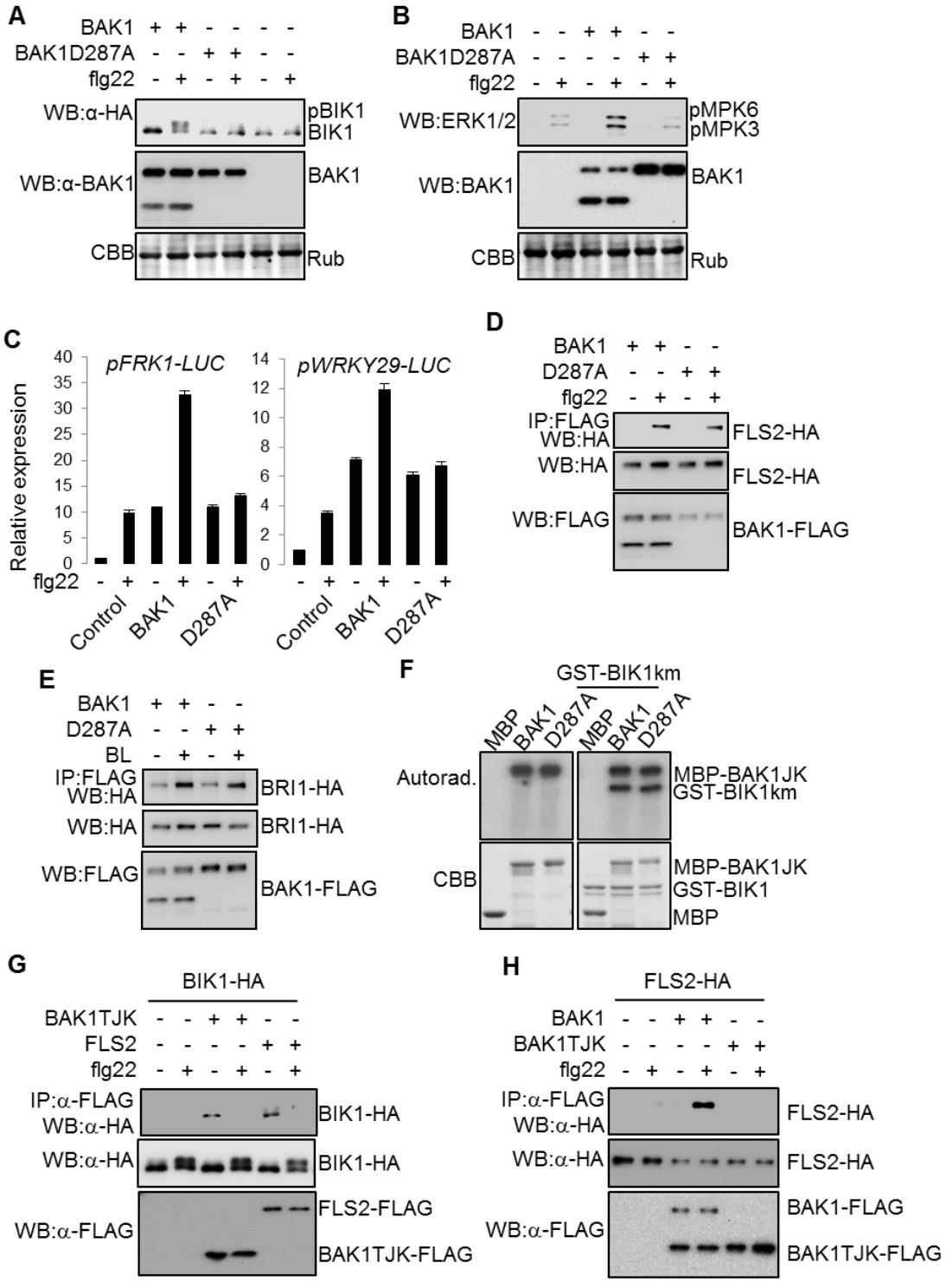
A
BAK1
BAK1D287A
flg22
WB:α-HA
pBIK1
BIK1
WB:α-BAK1
BAK1
CBB
Rub
B
BAK1
BAK1D287A
flg22
WB:ERK1/2
pMPK6
pMPK3
WB:BAK1
BAK1
CBB
Rub
C
pFRK1-LUC
pWRKY29-LUC
Relative expression
flg22
Control
BAK1
D287A
D
BAK1
D287A
flg22
IP:FLAG
WB:HA
FLS2-HA
WB:HA
FLS2-HA
WB:FLAG
BAK1-FLAG
E
BAK1
D287A
BL
IP:FLAG
WB:HA
BRI1-HA
WB:HA
BRI1-HA
WB:FLAG
BAK1-FLAG
F
GST-BIK1km
MBP
BAK1
D287A
MBP
BAK1
D287A
Autorad.
MBP-BAK1JK
GST-BIK1km
CBB
MBP-BAK1JK
GST-BIK1
MBP
G
BIK1-HA
BAK1TJK
FLS2
flg22
IP:α-FLAG
WB:α-HA
BIK1-HA
WB:α-HA
BIK1-HA
WB:α-FLAG
FLS2-FLAG
BAK1TJK-FLAG
H
FLS2-HA
BAK1
BAK1TJK
flg22
IP:α-FLAG
WB:α-HA
FLS2-HA
WB:α-HA
FLS2-HA
WB:α-FLAG
BAK1-FLAG
BAK1TJK-FLAG

immunoprecipitation with α-FLAG antibody. The D287A mutation did not affect flg22-triggered BAK1-FLS2 interaction (Fig. 8D). A similar co-IP assay was performed to assess BAK-BRI1 interactions, and the D287A mutation did not affect BL-triggered BRI1-BAK1 interaction either (Fig. 8E). To investigate the effect of D287A mutation on kinase activity of BAK1, we purified MBP-fused BAK1 and BAK1D287A harboring juxtamembrane and kinase domains, and tested their auto-phosphorylation and trans-phosphorylation activities using BIK1km as substrate. D287A did not affect auto-phosphorylation and trans-phosphorylation activities of BAK1 in *in-vitro* kinase assays (Fig. 8F). The dynamic interactions of FLS2/BAK1/BIK1 are modulated by perception of flg22, while the role of BAK1-C' in FLS2/BAK1/BIK1 complex is unknown. We performed a co-IP assay for BAK1TJK containing transmembrane, juxta-membrane and kinase domains that mimics BAK1-C'. FLAG-tagged BAK1TJK associated with HA-tagged BIK1 at steady state and dissociated from BIK1-HA after 15 minutes treatment of 1 μM of flg22 (Fig. 8G). We also found that BAK1TJK did not interact with FLS2 in a co-IP assay (Fig. 8H). In summary, proteolytic cleavage of BAK1 may be required for immune responses.

BAK1D287A mutant loses activities in immune responses in Arabidopsis plants

We further tested the activity of BAK1 D287A mutant in *Arabidopsis* plants by transforming *bak1-4* mutant plants with wild type BAK1 or BAK1D287A mutant genes under the control of native BAK1 promoter. Four transgenic lines, BAK1#2, 5 and BAK1 D287A #2, 3, with similar BAK1 expression level confirmed by RT-PCR and

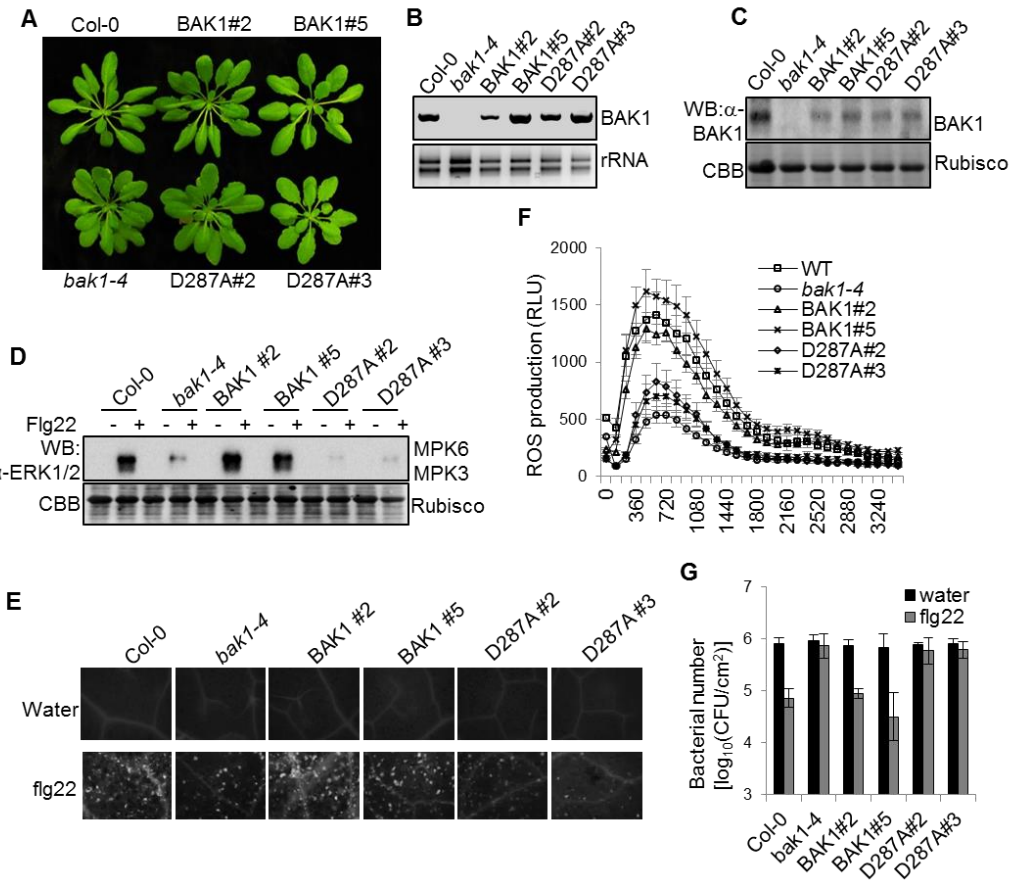

Figure 9. pBAK1::BAK1D287A/*bak1* transgenic plants are insensitive to flg22.

(A) Transgenic plants pBAK1::BAK1/*bak1* and pBAK1::BAK1D287A/*bak*. Two lines of transgenic plants with similar RNA and protein levels identified by RT-PCR of BAK1 (B) and WB with α-BAK1 antibody (C) were used for consequent assays. (D) flg22-induced MAPK activation in pBAK1::BAK1D287A/*bak1* transgenic plants. Two-week-old seedlings were treated with 100 nM flg22 for 15 min. (E) Callose deposition in pBAK1::BAK1D287A/*bak1* transgenic plants. Leaves of four-week-old plants were collected for aniline blue staining 12 h after inoculation with 100 nM flg22. (F) ROS production in pBAK1::BAK1D287A/*bak1* transgenic plants. Leaf discs from 5-week-old plants were treated with 100 nM flg22, and ROS production was detected at the indicated time points. The data are shown as the mean ±SE from 24 leaf discs. (G) flg22-mediated resistance of pBAK1::BAK1D287A/*bak1* transgenic plants to bacterial infection. Four-week old plants were pretreated with or without 200 nM of flg22 and then infected with *P. syringae pv. tomato* DC3000 strain at 5 × 105 cfu/ml. The bacterial growth assays were performed 2 days after infection.

WB analysis were used to test immune responses (Fig. 9A, B&C). BAK1::BAK1/*bak1-4* transgenic plants respond effectively to flg22 treatment in ROS production, MAPK activation and callose deposition. In contrast, both lines of BAK1::BAK1 D287A/*bak1-4* transgenic plants behave like *bak1-4* mutant plants in flg22-induced immune responses with reduced ROS production, MAPK activation and callose deposition (Fig. 9D, E&F). Flg22 was reported to protect *Arabidopsis* plants from bacterial infection, and *bak1-4* mutant plants lose such protection (Chinchilla et al., 2007; Zipfel et al., 2004). We infiltrated *Arabidopsis* plants with 200nM of flg22 12 hours before *Pseudomonas syringae* pv. *tomato* DC3000 challenge. Bacterial growth on BAK1::BAK1/*bak1-4* transgenic plants was reduced after flg22 protection, while bacterial growth on BAK1::BAK1 D287A/*bak1-4* transgenic plants was not affected by flg22 treatment (Fig. 9G).

D287 site of BAK1 is required for its activities in BR signaling

The homozygous *bak1* knockout mutant resembles the weak *bri1* knockout mutant, showing a compact rosette with round leaves and short petioles. Expression of BAK1 in *bak1-4* (pBAK1::BAK1/*bak1*) restored *bak1-4* to wild type-looking, whereas expression of BAK1D287A (pBAK1::BAK1D287A/*bak1*) could not restore *bak1-4* growth phenotype (Fig. 10A), indicating the D287 residue may be required for BAK1 function in BR signaling. To test the requirement of the D287 residue in BR signaling, we first grew these transgenic plants in the dark. After 5 days, pBAK1::BAK1/*bak1* is

similar to Col-0 with about 19 mm-long hypocotyl, whereas pBAK1::BAK1D287A/*bak1* is similar to *bak1-4* with about 16 mm-long hypocotyl (Fig. 10A&B). When growing on the ½ MS plates containing 0.5 μM BRZ (BR biosynthesis inhibitor), pBAK1::BAK1D287A/*bak1* also displayed shorter hypocotyl length than pBAK1::BAK1/*bak1* (Fig. 10C&D). To further investigate the requirement of the D287 site of BAK1 in BR signaling, we generated Arabidopsis transgenic plants expressing BAK1 and BAK1D287A under the control of the CaMV 35S promoter in a *bri1-5* background (35S::BAK1/*bri1* and 35S::BAK1D287A/*bri1*). Two lines of each transgenic plant with comparable BAK1 protein level were selected for further study (Fig.10E). Overexpression of BAK1 in bri1-5 could partially rescue the dwarf phenotype of bri1-5, and the 35S::BAK1/*bri1* transgenic plants displayed bigger leaves, longer stems and set larger and more siliques, consistent with the previous report (Nam and Li, 2002). In contrast, overexpression of BAK1D287A in *bri1-5* did not recover the dwarf phenotype of bri1-5, but deteriorated the dwarf phenotype and 35S::BAK1D287A/*bri1* transgenic plants were sterile (Fig. 10F). Thus, the D287 site of BAK1 is required for its function in BR signaling.

D287 site of BAK1 is required for BAK1 -controlled cell death

To assess the requirement of the D287 site of BAK1 in cell death control, we first performed virus-induced gene silence (VIGS) towards BKK1, the closest homolog of BAK1. Knock-down of BKK1 in Col-0 and pBAK1::BAK1/*bak1* backgrounds via VIGS did not show significant growth defect or cell death, whereas knock-down of

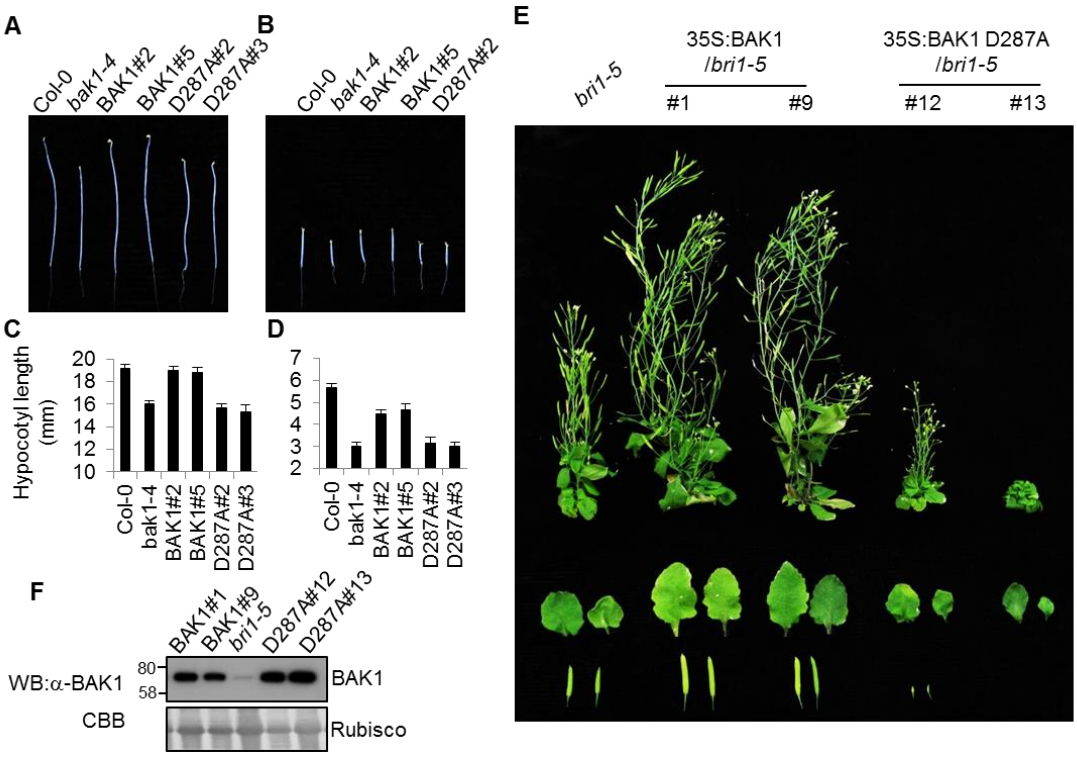

Figure 10. pBAK1::BAK1D287A/*bak1* plants are compromised in BR signaling.

A, B, C & D) pBAK1::BAK1D287A/*bak1* transgenic plants are less sensitive to BRZ. The seedlings of WT, *bak1-4* and transgenic plants were grown in the dark for 8 days on ½ MS plates without (A) or with (B) 1 μM of BRZ. Quantification of the hypocotyl length shown in (C & D) . (E) BAK1D287A mutant can not complement bri1 dwarf defect. Transgenic plants expressing BAK1 WT or D287A mutant under the control of 35S promoter in *bri1-5* background at two months old. Detached leaves and siliques were placed at the bottom. Transgenic plants in (E) were identified by WB with an α-BAK1 antibody (F). Protein loading is shown by CBB for Rubisco.

BKK1 in the bak1-4 mutant mimics the bak1bkk1 double mutant with severe growth defect and cell death stained by trypan blue. Knock-down of BKK1 in pBAK1::BAK1D287A/bak1 background also shows growth defects with small architecture, yellowing leaves and strong cell death (Fig. 11A&B). Plant defense and

senescence related genes were reported to be up-regulated in the *bak1bkk1* double mutant (He et al., 2007a). RT-PCR analysis indicated that transcripts of PR1 and PR2 in pBAK1::BAK1D287A/bak1 were significantly increased in pBAK1::BAK1/bak1 with BKK1 knocked down by VIGS (Fig. 11C). To confirm the involvement of the D287 site of BAK1 in cell death control, we transformed pBAK1::BAK1 and pBAK1::BAK1D287A into the Arabidopsis $BAK1^{+/-}BKK1^{-/-}$ mutant and genotyped the BAK1 background in the T1 generation of transgenic plants. Among T1 generation lines, transgenic plants in neither $BAK1^{+/+}BKK1^{-/-}$ nor $BAK1^{+/+}BKK1^{-/-}$ genetic backgrounds displayed a growth defect. However in the $BAK1^{-/-}BKK1^{-/-}$ genetic background, pBAK1::BAK1D287A transgenic plants showed severe growth defects, with much shorter petioles and smaller round leaves, whereas pBAK1::BAK1 transgenic plants did not show any obvious growth defect. To be noted, the growth defect of pBAK1::BAK1D287A transgenic plants in the $BAK1^{-/-}BKK1^{-/-}$ genetic background is not as severe as the $BAK1^{-/-}BKK1^{-/-}$ double mutant (Fig. 11D). Thus, the D287 site of BAK1 is at least partially required for BAK1/BKK1-mediated cell death.

D287A mutation of BAK1 enhances cell death caused by over-expression of BAK1

It was recently reported that over-expression of BAK1 in Arabidopsis caused severely dwarfed growth with extensive cell death (Dominguez-Ferreras et al., 2015). We first tested the transient expression of BAK1 in *N. benthamiana*. Expression of BAK1 under the control of double 35S promoter (2x35S::BAK1) triggered clear cell

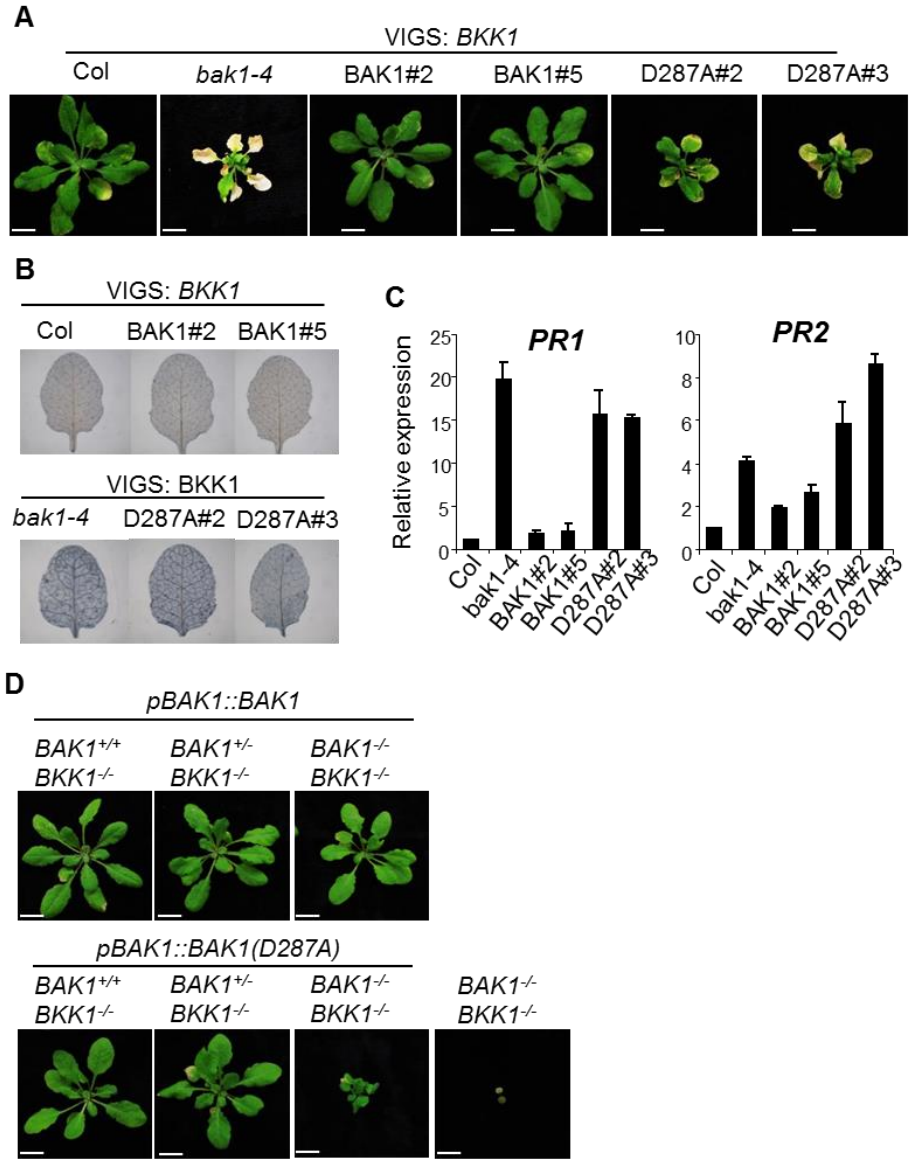

Figure 11. The D287 site is critical for BAK1/BKK1-mediated cell death.

(A) VIGS of BKK1 in Col-0, *bak1-4*, transgenic plants. Cell death was indicated by trypan blue staining (B), and PR genes expression levels were determined by qRT-PCR (C). (D) BAK1 transgenic plants on different backgrounds. BAK1+/-BKK1-/ heterozygous mutant plants were transformed with pBAK1::BAK1 or pBAK1::BAK1D287A. Plants of T1 generation with transgene were screened by basta selection and then subjected to genotyping towards BAK1. Four-week old transgenic plants were genotyped and BAK1 background genotypes are labeled on the top of pictures.

death, and the whole leaf of *N. benthamiana* was imaged under a UV light, while expression of BAK1 D287A under the control of double 35S promoters (2x35S::BAK1 D287A) triggered even more severe cell death (Fig. 12A). We checked the protein level of BAK1 and BAK1 D287A expressed in *N. benthamiana* by WB with an α-BAK1 antibody, showing that the D287A mutation largely reduced the portion of BAK1-C' (D287A) (Fig. 12B). The cell death was quantified by fluorescence signal under the UV light, showing signal intensities of both 2x35S::BAK1 and 2x35S::BAK1 D287A were much higher than the control (35S::GFP), and the signal intensity of 2x35S::BAK1 D287A was even higher than 2x35S::BAK1 (Fig. 12C). Furthermore, the electrolyte and leakage of 2x35S::BAK1 is more than the control, and the electrolyte leakage of2x35S::BAK1 D287A was two times more than 2x35S::BAK1, indicating 2x35S::BAK1 D287A caused much more severe cell death than 2x35S::BAK1 (Fig. 12D). Expression of BAK1 and BAK1 D287A under single 35S promoter (35S::BAK1 and 35S::BAK1 D287A) were much lower than the 2x35S promoter, analyzed by WB with α-BAK1 antibody (Fig. 12B). 35S::BAK1 D287A but not 35S::BAK1 induced obvious cell death, quantified by fluorescence signal and measured with electrolyte leakage (Fig. 12 A, C&D). To confirm the role of the D287 residue in BAK1-triggeredcell death, we generated *Arabidopsis* transgenic plants over-expressing BAK1 BAK1 D287A under single 35S promoter in Col-0 (WT) and BAK1 null-mutant (*bak1-4*) backgrounds, and checked protein expression by WB with α-BAK1 antibody (Fig. 12E&F). Only *Arabidopsis* expressing BAK1D287A but not BAK1 displayed an

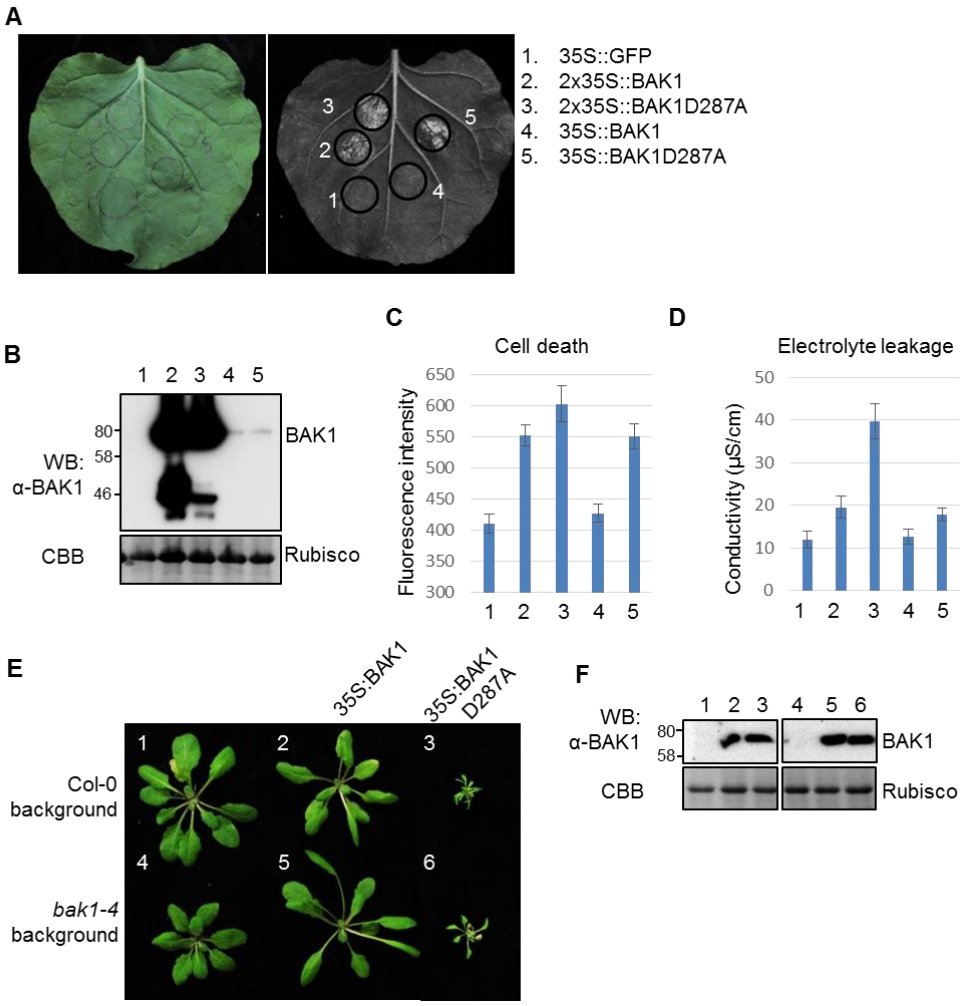

Figure 12. D287 site is critical for over-expression of BAK1-induced cell death.

(A) Overexpression of BAK1 D287A in *N. benthamiana*. Four-week old *N. benthamiana* were hand-inoculated with Agrobacteria carrying 35S::GFP, 2x35S::BAK1, 2x35S::BAK1D287A, 35S::BAK1 or 35S::BAK1D287A, and photos were taken 3 days after inoculation. (B) Protein extracts from *N. benthamiana* transiently expressing BAK1 shown in (A) were analyzed by WB with an α-BAK1 antibody after two days of inoculation. (C) Fluorescence signal from leaf cell death of (A) were obtained under the UV light and were quantified (n=10). (D) Electrolyte leakage of leaf discs from (A) were measured (n=3). (E) Overexpression of BAK1 D287A in *Arabidopsis*. Photos of *Arabidopsis* overexpressing BAK1 or BAK1 D287 were taken at four-week old stage. (F) Protein extracts from *Arabidopsis* shown in (E) were analyzed by WB with an α-BAK1 antibody.

obvious growth defect (Fig. 12E). Taken together, our data suggests that D287A mutation enhances over-expression of BAK1-triggered cell death.

Materials and methods

Plant materials and growth conditions

The *bak1-4, bri1-5* single mutant plants have been described previously (Lin et al., 2013; Lu et al., 2010). The *bri1-301* mutant was obtained from Yanhai Yin (Ames, IA). The *ps1ps2* double mutant was obtained from Dr. Przemysław Wojtaszek (Poznań, Poland). *Arabidopsis* plants were grown in soil (Metro Mix 360) in a growth chamber with 23°C, 65% relative humidity, 75 μE m^{-2} s^{-1} light and a photoperiod of 12 hr of light /12 hr of dark for 4 weeks before protoplast isolation and disease assays. To grow *Arabidopsis* seedlings on medium, the seeds were surface-sterilized with 50% bleach for 15 min, washed with sterilized ddH_2O and then placed on the plates with half-strength Murashige and Skoog medium (½ MS) containing 0.5% sucrose, 0.8% agar and 2.5 mm MES at pH 5.7. The plates were first stored at 4°C for 3 days in the dark for seed stratification, and then moved to the growth chamber set to the same parameters as the soil-grown plants.

Plasmid construction and generation of transgenic plants

The constructs of *BAK1, BIK1, FLS2* and *BRI1* in the plant expression vector (pHBT) or protein expression vector (pMAL or pGST) were reported previously (Lin et al., 2013; Lu et al., 2011; Lu et al., 2010). The *Arabidopsis SERKs, P. patens SERKs*

and different *BAK1* domain truncations were cloned into the pHBT vector with PCR amplification using the primers listed in Table 1. The constructs of Calpain in pHBT and pMAL vectors were generated with PCR amplification using the primers listed in Table 1. The construct BAK1-myc in the yeast expression vector pESC, the construct BRI1-HA in the yeast expression vector pYES2, and the construct pBAK1::BAK1-GFP in a binary cloning vector pPZP212 were obtained from Dr. Jianmin Li (Ann Arbor, MI). The construct of 2x35S::BAK1 was obtained from Dr. Delphine Chinchilla (Switzerland). The constructs 35S::BAK1-HA, 35S::BAK1 and pBAK1::BAK1 in a binary vector pCB302 were created by sub-cloning the BAK1 gene from pHBT vector with BamHI + StuI enzymes digestion. The *BAK1* promoter was amplified from genomic DNA of Col-0 with primers listed in Table 1. Point mutations were generated by a site-directed mutagenesis kit (Stratagene) using the primers listed in Table 1.The *BAK1* transgenic plants in Col-0 and *bak1-4, bri1-5, bak1/bkk1* mutants were generated by Agrobacterium (strain GV3101) -mediated transformation with constructs of *BAK1* in binary vectors. The pBAK1::BAK1-GFP transgenic plants were screened with Kanamycin (resistance conferred by the binary vector) and confirmed with an α-GFP antibody. The 35S::BAK1-HA, 35S::BAK1 and pBAK1::BAK1 transgenic plants were screened with the herbicide BASTA (resistance conferred by the binary vector) and confirmed by either PCR of WB with an α-HA or α-BAK1 antibody. The homozygous lines were selected based on the survival ratio of T2 and T3 generation plants after BASTA spray.

Table 1. Primers for cloning and point mutations.

BAK1-F	CATGCC*ATG*GAACGAA GATTAATGAT C
BAK1 TJK-F	CATGCC*ATG*GGTTCCTTTTC ACTTTTCACT
BAK1 JK-F	CGGGATCC*ATG*CGA AGGAAAAAGC CGCAGGAC
BAK1 K-F	CATGCC*ATG*GA TAATTTTAGC AACAAG
BAK1-R	GAAGGCCTTCTTGGACCCGAGGGGTATTC
pBAK1-F	CCGCTCGAGTCTAGAGTAGTAGTAAATAAGAAAATTGG
pBAK1-R	CGGGATCCTTTATCCTCAAGAGATTAAAAAC
BAK1 D287A-F	GTGAACTACAAGTTGCTTCGGCTAATTTTAGCAAC
BAK1 D287A-R	GTTGCTAAAATTAGCCGAAGCAACTTGTAGTTCAC
SERK1 D300A-F	CTACAAGTGGCGAGTGCTGGGTTTAGTAACAAG
SERK1 D300A-R	CTTGTTACTAAACCCAGCACTCGCCACTTGTAG
SERK2 D303A-F	CTTCAAGTAGCAACTGCTAGCTTCAGCAACAAG
SERK2 D303A-R	CTTGTTGCTGAAGCTAGCAGTTGCTACTTGAAG
SERK4 D292A-F	CTGTTAGTTGCTACTGCTAACTTTAGCAATAAAAATG
SERK4 D292A-R	CATTTTTATTGCTAAAGTTAGCAGTAGCAACTAACAG
PR1-F	5’-ACACGTGCAATGGAGTTTGTGG-3’
PR1-R	5’-TTGGCACATCCGAGTCTCACTG-3’
PDF1.2-F	5’-TGTTTGGCTCCTTCAAGGTT-3’
PDF1.2-R	5’-TTCTCTTTGCTGCTTTCGAC-3’
UBQ10-F	5’-AGATCCAGGACAAGGAAGGTATTC-3’
UBQ10-R	5’-CGCAGGACCAAGTGAAGAGTAG-3’

qRT-PCR analysis

Total RNA was isolated from leaves or seedlings after treatment with TRIzol Reagent (Invitrogen). Complementary DNA (cDNA) was synthesized from 1 ug of total RNA with oligo (dT) primer and reverse transcriptase (New England BioLabs). Real-time RT-PCR analysis was carried out using iTaq SYBR green Supermix (Bio-Rad) supplemented with ROX in an ABI GeneAmp PCR System 9700. The expression of

immunity-related genes was normalized to the expression of UBQ10. The primer sequences for RT-PCR are listed in Table 1.

Arabidopsis protoplast transient expression and reporter assays

Protoplast isolation and transfection were performed as described (He et al., 2007b). The promoter of FRK1 or WRKY29 fused to a luciferase gene (FRK1-LUC or WRKY29-LUC) was co-transfected with UBQ10-GUS (an internal control) and BAK1 into *bak1-4* protoplasts, and the promoter activity was presented as the ratio of LUC/GUS.

Co-immunoprecipitation assays

The total proteins from 2 x 10^5 transfected protoplasts were isolated with 0.5 ml of extraction buffer (10 mM HEPES, pH 7.5, 100 mM NaCl, 1 mM EDTA, 10% glycerol, 0.5% Triton X-100, and 1 x protease inhibitor cocktail from Roche). The samples were vortexed vigorously for 30 s, and then centrifuged at 13,000 rpm for 10 min at 4 °C. The supernatant was inoculated with α-FLAG agarose beads for 2 hr at 4 °C with gentle shaking. The beads were collected and washed three times with washing buffer (10 mM HEPES, pH 7.5, 100 mM NaCl, 1 mM EDTA, 10% glycerol, 0.1% Triton X-100, and 1 x protease inhibitor cocktail) and once more with 50 mM Tris-HCl, pH 7.5. Bound proteins were released from beads by boiling in SDS-PAGE sample loading buffer and analyzed by Western blot with an α-HA antibody.

In vitro *phosphorylation, immunocomplex kinase and* in vivo *MAP kinase assays*

For *in vitro* kinase assay, reactions were performed in 30 μl of kinase buffer (20 mM Tris-HCl, pH 7.5, 10 mM $MgCl_2$, 5 mM EGTA, 100 mM NaCl, and 1 mM DTT) containing 1 μg of kinase protein and 10 μg of fusion protein with 0.1 mM cold ATP and 5 μCi [^{32}P]-γ-ATP at room temperature for 3 hr with gentle shaking. The reactions were stopped by adding 4 x SDS loading buffer. The phosphorylation of fusion proteins was analyzed by autoradiography after separation with 12% SDS-PAGE.

For immunocomplex kinase assay, the total proteins from 2 x 10^5 transfected protoplasts were isolated with 1 ml of IP buffer (50 mM Tris-HCl, pH 7.5, 150 mM NaCl, 5 mM EDTA, 1 mM DTT, 2 mM NaF, 2 mM Na_3VO_3, 1% Triton, and protease inhibitor cocktail). The samples were vortexed vigorously for 30 s, and then centrifuged at 13,000 rpm for 10 min at 4°C. The supernatant was incubated with α-HA antibody for 2 hr and then with protein-G-agarose beads for another 2 hr at 4°C with gentle shaking. The beads were harvested and washed once with IP buffer and once with kinase buffer. The kinase reactions were performed in 20 μl of kinase buffer with 2 μg of myelin basic protein (MBP) as substrate, 0.1 mM cold ATP, and 5 μCi of [^{32}P]-γ-ATP at room temperature for 1 hr with gentle shaking. The phosphorylation of MBP proteins was analyzed by autoradiography after separation with 15% SDS-PAGE.

For detecting MAP kinase activity *in vivo*, two-week-old seedlings grown on ½ MS medium were transferred to water overnight and then treated with 100 nM flg22 or H_2O for the times indicated and frozen in liquid nitrogen. The seedlings were homogenized in IP buffer and equal amount of total protein was electrophoresed on 10%

SDS–PAGE. An α-pERK antibody (1:2,000) (Cell Signaling) was used to detect phosphorylation status of MPK3 and MPK6 with an immunoblot.

Expression of BAK1 in N. benthamiana, P. patens and S. cerevisiae

For expression of BAK1 in *N. benthamiana*, Agrobacteria (strain GV3101) harboring the derivatives of pCB302 vector were grown overnight in LB medium containing 50 μg/ml of kanamycin, collected by centrifugation, and resuspended in solution containing 10 mM $MgCl_2$, 150 μM acetosyringone to an OD_{600} of 1.0. After 3 h incubation at room temperature, Agrobacteria were pressure infiltrated to 4- week- old *N. benthamiana* plants grown in a growth chamber with 23°C, 65% relative humidity, 75 μE m^{-2} s^{-1} light and a photoperiod of 12 hr of light /12 hr of dark. Infiltrated leaves were then harvested after 2 d and subjected to WB analysis.

For expression of BAK1 in S. cerevisiae, the plasmids derived from pESC and pYES2 were introduced into the yeast strain W303. The yeast colonies containing pESC- and pYES2-derived plasmids were selected on the SD medium without leucine and uracil (SD-L-U). Transformed yeast cells were inoculated into 2 ml synthetic dropout medium containing 2% galactose and grown overnight at 28°C. After centrifugation, yeast cells were re-suspended in 30 μl lysis buffer (0.1M NaOH, 2% β-ME, 2% SDS and 0.05M EDTA) and boiled at 95°C for 10 min. Add 0.75 μl of 4M acetic acid to each sample and boil at 95˚C for 10 mins. Finally, add 7.5 μl of loading buffer (0.25M Tris-HCl pH 6.8, 50% glycerol, 0.25% bromophenol blue) to each sample, boil again at 95˚C for 5 min and keep at -20°C for future WB analysis.

Measurement of ROS production

Four leaves of each of six five-week-old *Arabidopsis* plants were excised into leaf discs of 0.25 cm^2, following an overnight incubation in 96-well plate with 100 µl of H_2O to eliminate the wounding effect. H_2O was replaced by 100 µl of reaction solution containing 50 µM luminol and 10 µg/ml horseradish peroxidase (Sigma) supplemented with 100 nM flg22. The luminescence was measured with a luminometer (Perkin Elmer, 2030 Multilabel Reader, Victor X3) immediately after adding the solution, with a 2 min interval reading time for a period of 60 min. The measurement value of ROS production from 24 leaf discs per treatment was indicated as the mean of RLU (Relative Light Units).

Callose deposition

Three leaves from four-week-old *Arabidopsis* were inoculated with 100 nM of flg22 for 12 hr at room temperature. leaves were immediately cleared in alcoholic lactophenol [95% ethanol: lactophenol (phenol: glycerol: lactic acid: H_2O=1:1:1:1) = 2:1] overnight. Samples were subsequently rinsed with 50% ethanol and H_2O. Cleared leaves were stained with 0.01% aniline blue in 0.15 M phosphate buffer (pH = 9.5) and the callose deposits were visualized under a UV filter using a fluorescence microscope. Callose deposits were counted using ImageJ 1.43U software (http://rsb.info.nih.gov/ij/). The number of deposits was expressed as the mean of six different leaf areas with standard error.

Pathogen infection assays

P. syringae pv. *tomato* DC3000 strain was cultured overnight at 28°C in KB medium with 50 µg/ml rifampicin. Bacteria were collected, washed and diluted to the desired density with H_2O. Four-week-old *Arabidopsis* leaves were infiltrated with 200 nM flg22 or an H_2O control for 24 h and then infiltrated with bacteria at a concentration of 5 x 10^5 cfu/ml using a needleless syringe. To measure bacterial growth, two leaf discs were ground in 100 µl of H_2O and serial dilutions were plated on KB medium with appropriate antibiotic. Bacterial colony forming units (cfu) were counted 2 days after incubation at 28°C. Each data point is shown as triplicates.

VIGS assay

BKK1 were sub-cloned into the pYL156 (pTRV-RNA2) vector. The binary TRV vectors pTRV-RNA1, pTRV-RNA2 (pYL156) and pYL156 derivatives were transformed into Agrobacterium tumefaciens GV3101 strain by electroporation. Agrobacterium culture was grown for overnight at 28 °C in LB medium containing the antibiotics 25 µg/ml of gentamicin and 50 µg/ml of kanamycin, as well as 10 mM of MES and 20 µM of acetosyringone. The cells were pelleted by centrifugation at 1200 g at room temperature for 10 min, and re-suspended in infiltration culture containing 10 mM of $MgCl_2$,10mM of MES and 200 µM of acetosyringone. Cell suspensions were incubated at room temperature for 3 h. Agrobacterium cultures containing pTRV-RNA1 and pTRV-RNA2 or its derivatives were mixed at a 1:1 ratio and infiltrated into first pair of true leaves of six 2-week-old plants using a needle-less syringe.

Plant cell death assays

For trypan blue staining, the leaves of four-week-old plants were excised and subsequently immersed in boiled lactophenol (lactic acid: glycerol: liquid phenol: distilled water=1:1:1:1) solution with 0.25 mg/ml trypan blue for 1 min. The stained leaves were destained with 95% ethanol/lactophenol solution, and washed with 50% ethanol. The destained leaves were subjected to microscope observation.

For electrolyte leakage assays, three leaf discs (0.5 cm diameter) were excised from the *N. benthamiana* infiltrated with agrobacteria for 3 days and pre-floated in 5 ml of ddH_2O for 5-10 min to eliminate wounding effect. The ddH_2O was then exchanged and electrolyte leakage from leaf disc was measured using a conductivity meter (VWR; Traceable Conductivity Meter) with three replicates per time point per sample (n= 3).

Summary

Similar with plant RLKs, animal Toll-like receptors (TLRs) are essential sensors of pathogenic infections. TLR family consists of 13 members in mice and 10 in humans (Kawai and Akira, 2006; Takeda and Akira, 2005). TLR3, TLR7 and TLR9 localize in intracellular compartments and sense pathogen-derived RNA or DNA. TLR9 needs to be cleaved by the main thiol protease cathepsin L, which belongs to the papain-like lysosomal cysteine protease family to produce a functional C-terminal fragment including a partial TLR9 ectodomain, as well as the transmembrane and cytoplasmic domains. The C-terminal cleavage fragment of TLR9 bound CpG DNA more strongly

than full-length TLR9 and is sufficient to activate CpG DNA-induced cytokine production (Park et al., 2008). Compared with the TLR9, the double strand RNA receptor TLR3 is cleaved by cathepsins B and H in endosome. A truncated form of TLR3 lacking the N-terminal 345 aa responds to ligand activation (Garcia-Cattaneo et al., 2012). We tested the activities of truncated BAK1 consisting the transmembrane, juxtamembrane and kinase domains (BAK1TJK), and found that BAK1TJK can not complement *bak1-4* mutant in immune responses (data not shown). The molecular weight of BAK1TJK is similar as BAK1-C'. Therefore, BAK1-C' itself may not be enough to complement *bak1-4* mutant in immune responses.

BAK1-C' did not interact with FLS2 after flg22 treatment in a co-IP assay, indicating BAK1-C' may not involve in perception of flg22 directly. Our data indicate that BAK1-C' are required for flg22-induced immune response, we thus infer that BAK1-C' may either negatively regulate suppressers of FLS2/BAK1 complex, or positively regulate enhancers of FLS2/BAK1. BAK1-interacting receptor-like kinase 2 (BIR2) and Protein Ser/Thr Phosphatase type 2A (PP2A), BR Signaling Kinase 1 (BSK1), Stomatal Cytokinesis-Defective 1 (SCD1) and kinase-associated protein phosphatase (KAPP) are considered as negative regulators of BAK1/FLS2 complex, while BIK1 is a positive regulator of this complex (Gomez-Gomez et al., 2001; Halter et al., 2014; Korasick et al., 2010; Lu et al., 2010; Segonzac et al., 2014; Shi et al., 2013). Our data suggests that BAK1-C' interacts with BIK1, so we hypothesize that BAK1-C' may promote the activities of BIK1 in immune responses, which needs to be further tested.

Arabidopsis genomes encode hundreds of proteases, which are divided into dozens of unrelated families. The functions and target proteins of these proteases in plant is largely unknown, but gene silencing, mutant alleles, and overexpression studies provided different phenotypes for a growing number of proteases. It has been reported that diverse biological processes are regulated by proteases, although the underlying molecular mechanisms are unknown. The regulated biological processes include gametophyte survival, meiosis, seed coat formation, embryogenesis, stomata development, cuticle deposition, chloroplast biogenesis, epidermal cell fate, and defense responses. Plant proteases are expressed in time and space specifically and accumulate in distinct subcellular compartments. The substrates and activation mechanisms of proteases are elusive. We show in this dissertation that BAK1 undergoes proteolytic cleavage, and identifying the protease responsible for such cleavage process will help researchers understand the mechanism of how proteases function in plant immunity.

CHAPTER III

CHARACTERIZATION OF BAK1-INTERACTING E3 UBIQUITIN LIGASE PUB13 IN ARABIDOPSIS IMMUNITY, FLOWERING AND SENESCENCE*

Introduction

PRR activation and attenuation are also regulated by protein ubiquitination, endocytosis and degradation (Geldner and Robatzek, 2008; Li et al., 2014a). FLS2 has been shown to translocate into intracellular vesicles within 30 min of flg22 treatment (Beck et al., 2012; Robatzek et al., 2006). The non-activated FLS2 constitutively recycles between plasma membrane and early endosome likely regulating the abundance of receptor at plasma membrane and maintaining a constant pool of signaling receptor (Beck et al., 2012). Upon flg22 perception, FLS2 enters a distinct endocytic trafficking pathway followed by sorting into the vacuole for degradation (Beck et al., 2012; Choi et al., 2013). As an important posttranslational modification process, protein ubiquitination often marks target proteins for degradation through vacuole or proteasome, or regulates endosomal sorting of plasma membrane-localized proteins (Vierstra, 2009). The ubiquitination pathway directs covalent conjugation of conserved ubiquitin molecules to specific protein substrates through a stepwise reaction mediated by three distinct classes of enzymes, ubiquitin-activating enzyme (E1), ubiquitin-conjugating enzyme (E2) and

*This chapter is reprinted with permission from Jinggeng Zhou, Dongping Lu, Guangyuan Xu, Scott A. Finlayson, Ping He and Libo Shan (2015), The dominant negative ARM domain uncovers multiple functions of PUB13 in Arabidopsis immunity, flowering, and senescence. Journal of Experimental Botany, 66(11): 3353–3366.

ubiquitin-protein ligase (E3) (Dreher and Callis, 2007; Vierstra, 2009). The substrate specificity is dictated by ubiquitin E3 ligases, which are broadly classified into three groups: HECT (homologous to E6-AP C terminus), RING finger, and U-box (Yee and Goring, 2009). Two closely related plant U-box (PUB) E3 ubiquitin ligases PUB12 and PUB13 interact with BAK1, and are recruited to FLS2 upon flg22 perception. BAK1 directly phosphorylates PUB12 and PUB13, and is indispensable for FLS2 and PUB12/13 association. PUB12 and PUB13 polyubiquitinate FLS2 and lead to flg22-induced FLS2 degradation, thereby negatively regulating flg22 signaling (Lu et al., 2011). Interestingly, the *pub13* mutant displays certain auto-immune responses, such as spontaneous cell death and accumulation of hydrogen peroxide and plant defense hormone salicylic acid (SA) when grown under long day (LD, 16 hr of light/8 hr of dark) and high light (250 $\mu E\ m^{-2}\ s^{-1}$) conditions with high humidity (95% RH) treatment (Li et al., 2012). PUB13 also negatively regulates flowering time, suggesting a broad role of PUB13 in controlling plant immunity and growth (Li et al., 2012) (Fig. 13).

The largest class of PUBs in *Arabidopsis* is the ARMADILLO (ARM) repeat domain-containing PUB proteins (Azevedo et al., 2001; Yee and Goring, 2009). The ARM repeat domain is composed of multiple 42-amino-acid ARM repeats with significant sequence divergence but highly conserved right-handed super helix of α-helices that is predicted to form a specific protein interaction domain (Samuel et al., 2006). In this study, we have performed a series of domain deletion and truncation studies of PUB12 and PUB13. We show that the ARM domain of PUB13 interacts with BAK1 and is phosphorylated by BAK1. Ectopic expression of the PUB13 ARM domain

inhibits flg22-induced FLS2-PUB13 association and PUB12/13-mediated FLS2 ubiquitination and degradation in *Arabidopsis*. Similar to the *pub12pub13* double mutant, transgenic plants expressing the PUB13 ARM domain display enhanced immune responses compared to wild type (WT) plants. Apparently, ectopic expression of the protein-protein interacting ARM domain creates a dominant negative effect and interferes with the endogenous PUB functions, implying a potential alternative to dissect the overlapping functions of multiple closely related *PUB* genes. Interestingly, similarly to the *pub12pub13* double mutant, PUB13 ARM transgenic plants showed enhanced dark-induced senescence accompanied with elevated expression of the stress-induced senescence marker genes, senescence-associated gene 13 (*SAG13)* and *SAG14*.

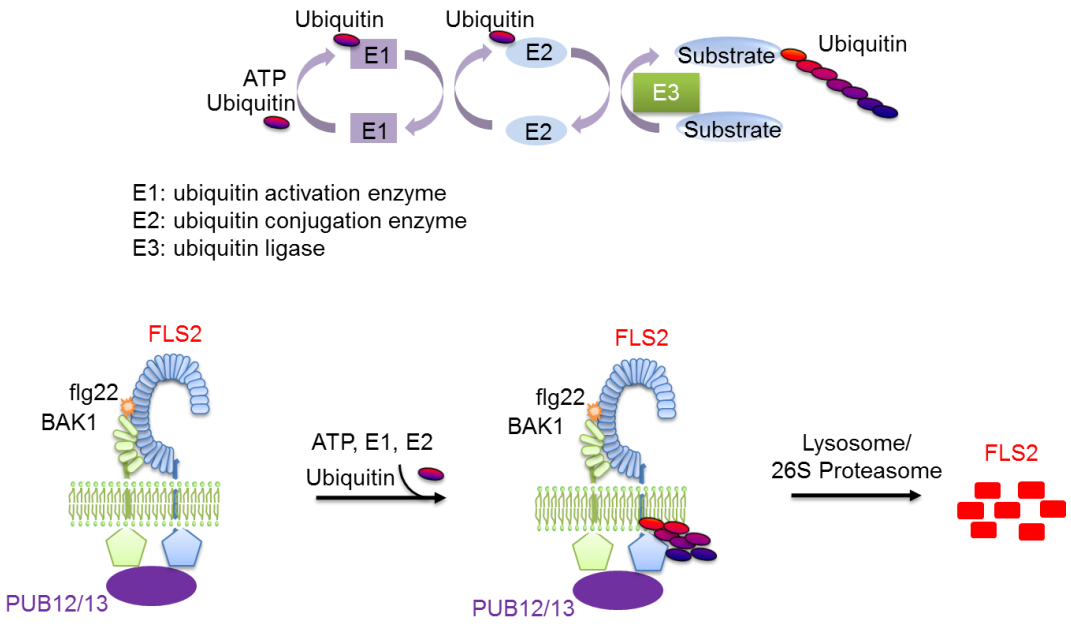

Figure 13. PUB12/13-mediated FLS2 ubiquitination and degradation.

Results

PUB13 ARM domain interacts with and is phosphorylated by BAK1

PUB13 contains a U-box N-terminal domain (UND), a U-box domain and a C-terminal ARM repeat domain (Fig. 14A). PUB13 co-immunoprecipitated with BAK1 and FLS2 in *Arabidopsis* (Lu et al., 2011). To test whether PUB13 directly interacts with BAK1 and/or FLS2, we performed an *in vitro* pull-down assay with the cytoplasmic domain of BAK1 (BAK1CD) or FLS2 (FLS2CD) fused to maltose binding protein (MBP) immobilized on amylose-agarose beads as the bait against glutathione S-transferase (GST)-PUB13 fusion proteins. As shown in Fig. 14B, GST-PUB13 was able to be pulled down by MBP-BAK1CD, but not MBP-FLS2CD or MBP itself, suggesting a physical interaction between PUB13 and BAK1 but not between PUB13 and FLS2. This is consistent with our previous report that PUB13 constitutively associates with BAK1, whereas flg22 induces BAK1-dependent PUB13 and FLS2 association (Lu et al., 2011). It has been suggested that the ARM domain mediates protein-protein interaction whereas the U-box domain confers E3 ubiquitin ligase activity (Samuel et al., 2006). We further examined whether the ARM domain is sufficient to mediate the PUB13 interaction with BAK1. As shown in Fig. 14B, the ARM domain of PUB13 (GST-ARM) was pulled down by MBP-BAK1CD, indicating that the ARM domain mediates a direct interaction with BAK1. Notably, the ARM domain interaction with BAK1 appears to be much stronger than full-length PUB13 (Fig. 14B). We further performed pull-down assays using different truncations of PUB13 with MBP-BAK1CD. The BAK1 interaction with the U-box-ARM domain is similar to that with the ARM domain, and

stronger than that with PUB13, but no interaction was detected with the UND domain (Fig. 14C). These results suggest that the UND domain may negatively regulate PUB13-BAK1 interaction. To test the *in vivo* interaction of PUB13ARM and BAK1, we performed bimolecular fluorescence complementation (BiFC) assay. A strong fluorescence signal was detected in the cell periphery with co-transfection of BAK1 fused to the C-terminal half of YFP (yellow fluorescence protein) (BAK1-cYFP) and PUB13ARM fused to the N-terminal half of YFP (ARM-nYFP) in protoplasts, suggesting that PUB13ARM interacts with BAK1 *in vivo* (Fig. 14D). Neither of the individual constructs nor co-transfection of UND-nYFP or U-box-nYFP with BAK1-cYFP emitted YFP signals in protoplasts. PUB13 is a phosphorylation substrate of BAK1 (Lu et al., 2011). The interaction between the ARM domain of PUB12 or PUB13 and BAK1 was confirmed in a coimmunoprecipitation (Co-IP) assay (data not shown). We determined which domain(s) of PUB13 mediates the phosphorylation by BAK1 with an *in vitro* kinase assay using MBP-BAK1CD as a kinase and different truncated versions of PUB13 as substrates in the presence of [^{32}P]-γ-ATP. Consistent with our previous report (Lu et al., 2011), BAK1CD possesses autophosphorylation activity and could phosphorylate the full length PUB13 (data not shown). Apparently, BAK1CD strongly phosphorylated the ARM domain or U-box-ARM domain yet exhibited little phosphorylation activity towards the UND, UND-U-box or U-box domain (Fig. 14E). The data indicate that BAK1 phosphorylation mainly occurs on the ARM domain of PUB13. Notably, the BAK1CD kinase inactive mutant (BAK1CDKm), in which lysine 317 was mutated to methionine (K317M), was no longer able to interact with

Figure 14. The PUB13 ARM domain interacts with and phosphorylates BAK1.

(A) A schematic protein domain structure of PUB13. PUB13 contains a U-box N-terminal domain (UND), a U-box domain and a C-terminal ARMADILLO (ARM) repeat domain. The amino acid position is labeled on the top. The PUB13 truncations used for the following experiments are listed. (B) & (C) The ARM domain interacts with BAK1 cytosolic domain (CD) in *in vitro* pull-down (PD) assays. (B) GST fused PUB13 or ARM proteins were incubated with MBP, MBP-BAK1CD or MBP-FLS2CD amylose beads, and the beads were collected and washed for Western blot (WB) of immunoprecipitated proteins with an α-GST antibody (top gel). (C) MBP-BAK1CD was incubated with GST, GST-PUB13 or various truncated forms of PUB13 proteins with glutathione beads, and the beads were collected and washed for WB of immunoprecipitated proteins with an α-HA antibody (top gel).The protein inputs are indicated by Coomassie Brilliant Blue (CBB) staining. (D) The ARM domain interacts with BAK1 with BiFC assay in *Arabidopsis* protoplasts. Protoplasts were transfected with various BiFC constructs, and the fluorescence was visualized under a confocal microscope. YFP: yellow fluorescence signal; Chlorophyll: auto-fluorescence signal; BF: bright field. Scale bars = 50 μm. (E) The ARM domain is phosphorylated by BAK1. GST-PUB13 or various truncated forms of PUB13 proteins (10 μg) were used as substrates and MBP-BAK1CD (1 μg) as the kinase in an *in vitro* kinase assay. Phosphorylation was detected by autoradiography (top panel), and the protein loading is shown by CBB staining (bottom panel). (F) Interaction of PUB13 ARM with BAK1 requires BAK1 kinase activity. GST-ARM proteins were incubated with MBP, MBP-BAK1CD or MBP-BAK1CDKm amylose beads for *in vitro* pull-down assay. The pull-down precipitates were examined with α-GST antibody in WB (top panel). The protein inputs are shown by CBB staining (middle and bottom panels).

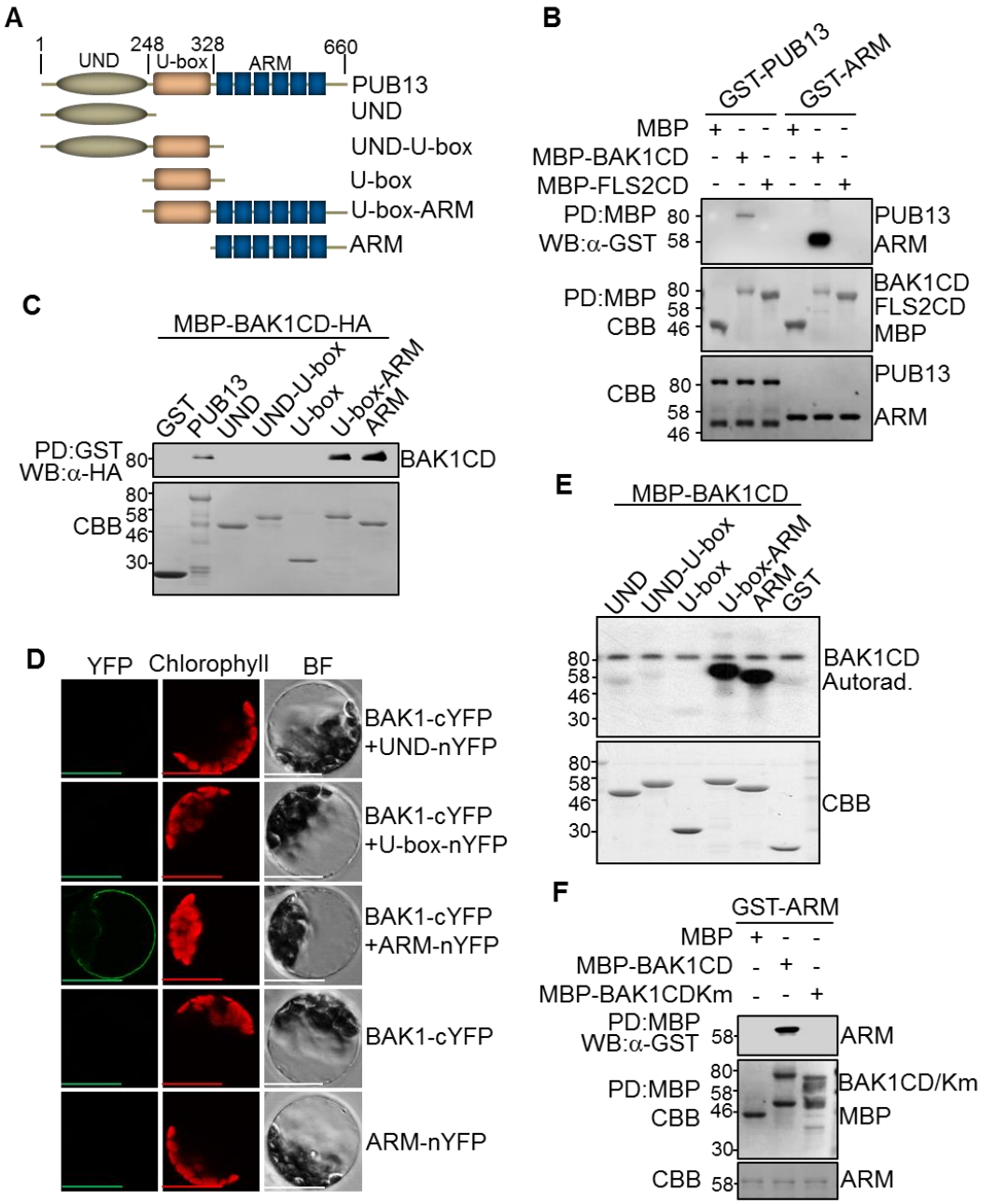

PUB13ARM in an *in vitro* pull-down assay (Fig. 14F), indicating that BAK1 kinase activity is essential in mediating its interaction with PUB13.

Ectopic expression of PUB13ARM blocks PUB13-mediated FLS2 ubiquitination and degradation

We further tested whether ectopic expression of the ARM domain *in planta* will generate a dominant negative effect on the function of endogenous PUB13 and its closest homologs, such as PUB12. We first determined whether the excess ARM domain protein could interfere with PUB13 ubiquitination activity towards FLS2CD in an *in vitro* ubiquitination assay. The addition of PUB13ARM proteins into the reactions resulted in a gradually shortened ladder formation of FLS2CD in a dosage-dependent manner (Fig. 15A). Notably, the overall ubiquitination reaction was not affected by PUB13ARM protein as detected with an α-ubiquitin (α-Ub) antibody (Fig. 15A). We further tested the effect of ARM protein on FLS2 ubiquitination with an *in vivo* ubiquitination assay. We co-expressed HA epitope-tagged full-length FLS2 and FLAG epitope-tagged Ub in the presence or absence of GFP-tagged PUB13ARM in *Arabidopsis* protoplasts. The ubiquitinated FLS2 protein was detected with an α-HA Western blot upon immunoprecipitation with α-FLAG antibody. As reported, flg22 treatment induced FLS2 ubiquitination as shown by the enhanced ladder-like smear formation (Fig. 15B). Ectopic expression of PUB13ARM-GFP largely diminished flg22-induced ladder formation suggesting compromised flg22-induced FLS2 ubiquitination (Fig. 15B). Thus, the PUB13 ARM domain is able to interfere with the ubiquitination activity of full length PUB13 towards FLS2 in both *in vitro* and *in vivo* ubiquitination assays.

Next, we tested whether PUB13ARM interferes with flg22-induced FLS2-PUB13 association by co-immunoprecipitation (Co-IP) assay (Fig. 15C). FLAG-tagged PUB13 was co-expressed with HA-tagged FLS2, and FLS2 was detected in the precipitates with an α-HA Western blot upon immunoprecipitation with α-FLAG antibody. Apparently, ectopic expression of PUB13ARM-GFP reduced flg22-induced PUB13-FLS2 association (Fig. 15C). The prolonged flg22 treatment induces FLS2 degradation (Lu et al., 2011). To quantify the FLS2 degradation rate, we fused firefly luciferase gene (*LUC*) to the C-terminus of full length *FLS2* gene under the control of the constitutive cauliflower mosaic virus (CaMV) *35S* promoter. The resulting construct *35S::FLS2-LUC* was transfected into *Arabidopsis* protoplasts and the luciferase activity was monitored upon flg22 treatment (Fig. 15D). We observed a reduction of luciferase activity 2 hr and 4 hr after flg22 treatment in the vector control transfection, indicating the occurrence of flg22-induced FLS2-LUC degradation (Fig. 15D). However, ectopic expression of PUB13ARM ameliorated flg22-induced degradation of FLS2-LUC luciferase activity, suggesting that PUB13ARM blocks flg22-induced FLS2 degradation (Fig. 15D). We further generated transgenic plants carrying HA-tagged PUB13ARM under the control of the CaMV *35S* promoter in the WT *Arabidopsis* Col-0 ecotype. Two independent transgenic lines, 7-2 and 15-1, with moderate protein expression levels of PUB13ARM, were selected for phenotypic and molecular analyses. The polymerase chain reaction (PCR) analysis indicated that the transgenes did not disrupt the endogenous *PUB13* gene (data not shown). To examine flg22-induced endogenous FLS2 protein degradation, we monitored FLS2 protein level in these transgenic plants with α-

Figure 15. PUB13ARM blocks flg22-induced FLS2 ubiquitination and degradation. (A) PUB13ARM blocks PUB13-mediated FLS2 ubiquitination. MBP-FLS2CD-HA was incubated with GST-PUB13 in an *in vitro* ubiquitination reaction in the presence of different amount of proteins of GST (Control) or GST-ARM. The ubiquitination of FLS2CD was detected by α-HA antibody (top panel). The overall ubiquitination was detected by α-ubiquitin (Ub) antibody (middle panel). GST protein loading is shown by CBB staining (bottom panel). (B) Ectopic expression of PUB13ARM blocks flg22-induced FLS2 ubiquitination. *Arabidopsis* protoplasts were transfected with FLAG-Ub, FLS2-HA, and PUB13ARM-GFP or a control vector, and incubated for 10 hr before 1 μM flg22 treatment for 30 min. The ubiquitinated FLS2 was detected with an α-HA antibody WB after immunoprecipitation with α-FLAG antibody. Equal protein loading is shown by CBB staining for RuBisCo (RBC). (C) Ectopic expression of PUB13ARM suppresses flg22-induced FLS2-PUB13 association. *Arabidopsis* protoplasts were transfected with FLS2-HA, PUB13-FLAG, and PUB13ARM-GFP or a control vector, and incubated for 10 hr before 1 μM flg22 treatment for 10 min. The association of FLS2-PUB13 was detected by an α-HA WB after α-FLAG immunoprecipitation. The protein levels of FLS2, PUB13 and ARM were detected by α-HA, α-FLAG or α-GFP WB respectively. (D) Ectopic expression of PUB13ARM inhibits flg22-induced FLS2-LUC degradation in protoplasts. The 35S::FLS2-LUC was co-transfected with ARM or a control vector in *Arabidopsis* protoplasts. The transfected protoplasts were incubated for 12 hr before 10 μM cycloheximide treatment for 1 hr, and then treated with 1 μM flg22 for the indicated times (hpt: hr post flg22 treatment). The UBQ-GUS was included as an internal transfection control. The LUC activity was normalized to GUS activity to reflect the relative protein level of FLS2. (E) & (F) Stable expression of PUB13ARM in transgenic plants blocks flg22-induced FLS2 degradation. ARM7 and ARM15 are two independent PUB13ARM transgenic lines (ARM7-2 and ARM15-1). Two-week-old seedlings were treated with 1 μM flg22 for 0.5 or 1 hr. The endogenous FLS2 proteins were detected by α-FLS2 WB (E) and were quantified by the band intensity (F). Equal protein loading is shown by CBB staining for RBC. The data are shown as the mean ± standard error (n = 3) and the asterisk (*) indicates a significant difference before and after flg22 treatment ($p < 0.05$).

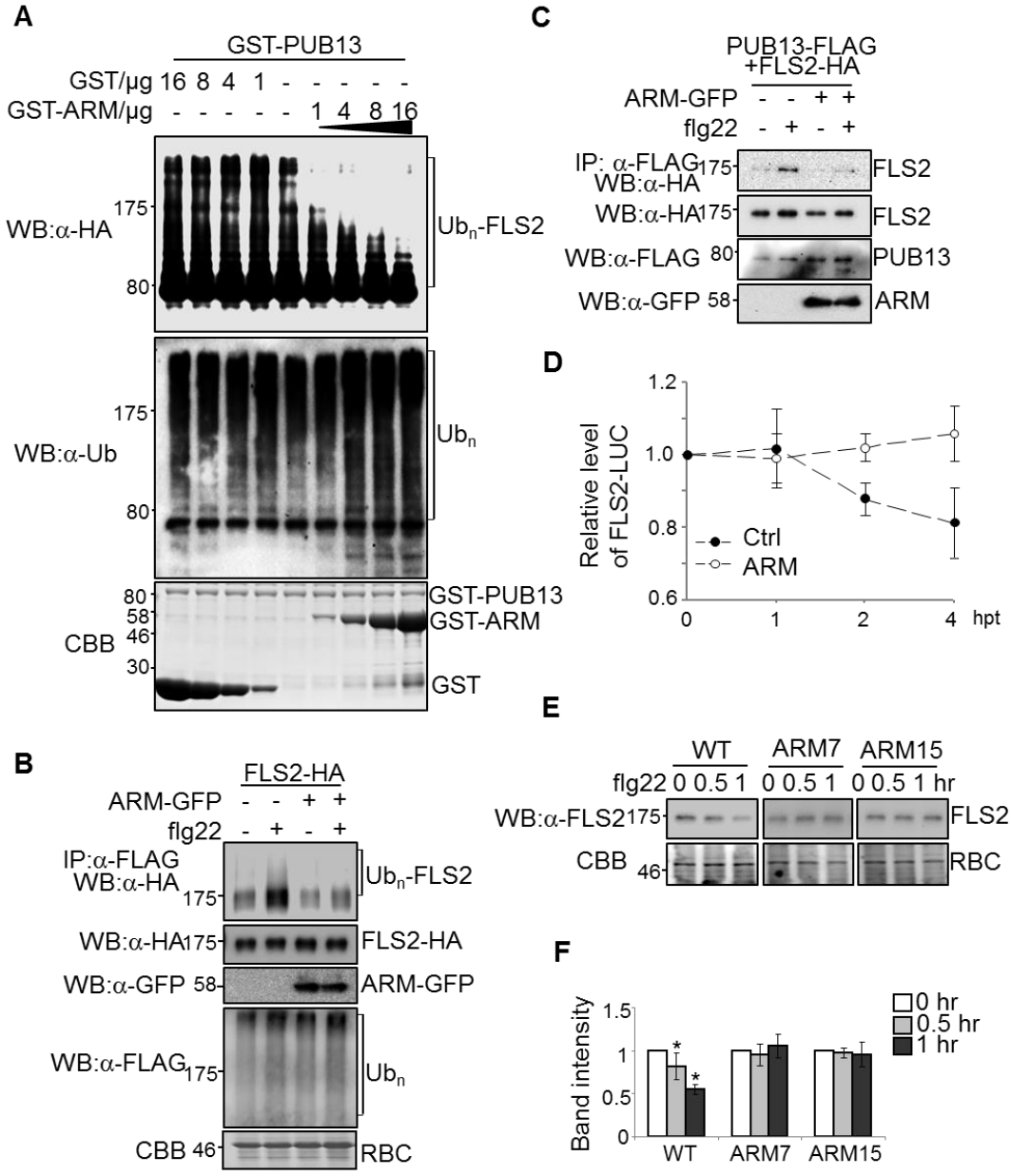

FLS2 antibody (Fig. 15E & 2F). In WT plants, the protein level of FLS2 was reduced by about 20% and 50% 30 min and 60 min after flg22 treatment respectively. However, no significant change of FLS2 protein level was detected in the two lines of PUB13ARM

transgenic plants upon flg22 treatment (Fig. 15E & 2F), which is consistent with the result of FLS2-LUC reporter assays in protoplasts (Fig. 15D). Notably, it appears that the degradation rate of FLS2-LUC in protoplast-based assay was slower than that of endogenous FLS2 in seedling assay, likely due to the different protein expression level of FLS2. Taken together, ectopic expression of PUB13ARM blocked flg22-induced FLS2 ubiquitination and degradation in *Arabidopsis*.

The PUB13ARM transgenic plants display elevated flg22-mediated immunity

The *pub12pub13* (*pub12/13*) double mutant showed the elevated flg22-mediated defense gene activation, callose deposition and ROS production (Lu et al., 2011). We examined these immune responses in PUB13ARM transgenic plants. Quantitative reverse transcriptase-PCR (qRT-PCR) analysis showed that flg22-mediated induction of defense genes *WRKY30* (*At5g24110*), *AP2* (*At3g23230*) and *FRK1* (*At2g19190*) was increased to about twofold in PUB13ARM transgenic plants compared to that in WT plants (Fig. 16A). Similar to the *pub12/13* mutant plants, PUB13ARM transgenic plants accumulated greater than three times more callose deposits than WT plants 12 hr after flg22 treatment (Fig. 16B). In addition, the peak of flg22-induced ROS production in PUB13ARM transgenic plants was about 50% higher than that in WT plants (Fig. 16C). Taken together, the data indicate that flg22-induced immune responses were elevated in PUB13ARM transgenic plants compared to WT plants.

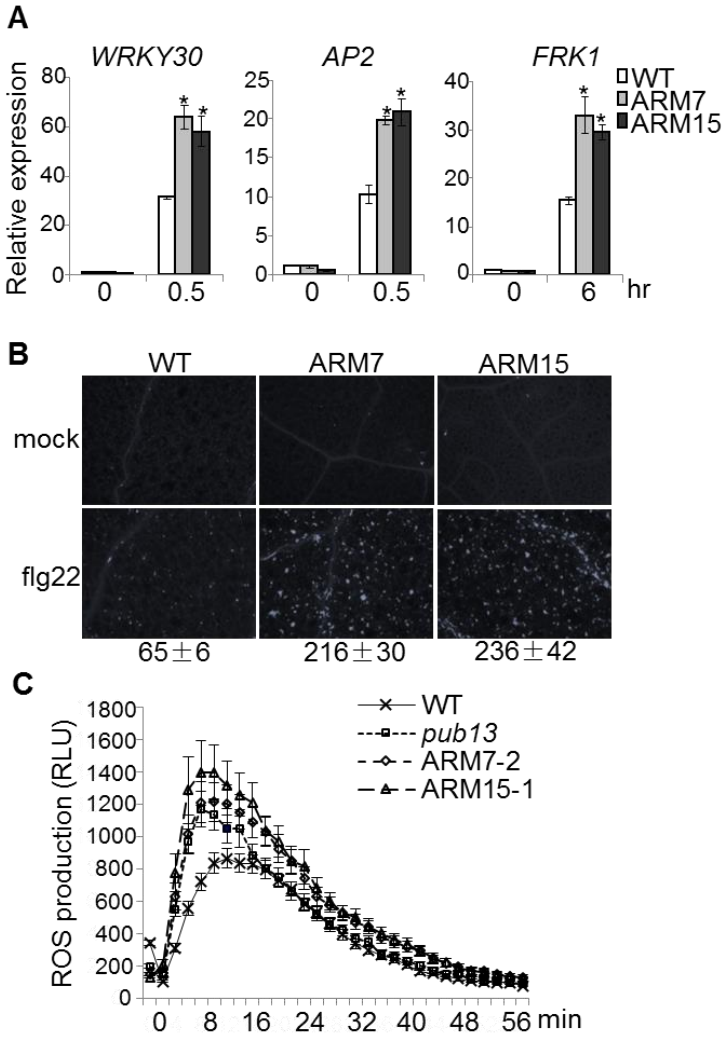

Figure 16. Elevated immune responses in PUB13ARM transgenic plants.

(A) Expression of flg22-induced genes in PUB13ARM transgenic plants. Real-time RT-PCR analysis of two-week-old seedlings after 0.5 or 6 hr treatment of 100 nM flg22. The expression of *WRKY30*, *AP2* and *FRK1* was normalized to the expression of *UBQ10*. The data are shown as the mean ± standard error (n = 3) and asterisks (*) indicate a significant difference between WT and PUB13ARM transgenic plants ($p < 0.05$). (B) Callose deposition in PUB13ARM transgenic plants. Two-week-old seedlings were collected for aniline blue staining 12 hr after treatment with 500 nM flg22. The data are shown as the mean ± standard error (n = 6). (C) ROS production in PUB13ARM transgenic plants. Leaf discs from five-week-old plants were treated with 100 nM flg22 and ROS production was detected at indicated time points. The data are shown as the mean ± standard error from 24 leaf discs.

PUB13ARM transgenic plants display elevated flg22-induced MAPK activation

Activation of MAPKs is one of the earliest signaling events following MAMP recognition (Meng and Zhang, 2013). It remains unknown whether PUB13 and its closest homolog PUB12 also regulate flg22-induced MAPK activation. We first examined flg22-mediated activation of MAPKs with α-pERK antibody that cross-reacts with phosphorylated *Arabidopsis* MPK3 and MPK6. MPK3 and MPK6 were activated 15 min after flg22 treatment in WT plants, whereas the activation was enhanced in *pub12*, *pub13* and *pub12/13* mutants seedlings compared with WT plants (Fig. 17A). Importantly, two independent lines of PUB13ARM transgenic plants also exhibited enhanced flg22-mediated MPK3 and MPK6 activation compared to WT plants (Fig. 17B). We further carried out an immunocomplex kinase assay to determine the activation of endogenous MPK3 and MPK4. The MPK3 and MPK4 proteins were immunoprecipitated with α-MPK3 or α-MPK4 antibody from WT or *pub12/13* mutant seedlings treated with or without flg22, and subjected to an *in vitro* kinase assay using myelin basic protein as a substrate in the presence of [^{32}P]-γ-ATP. Consistent with the detection by α-pERK antibody, flg22 treatment elicited a stronger activation of MPK3 and MPK4 in *pub12/13* mutants compared to WT plants (Fig. 17C & 17D). Notably, the elevated MAPK activation in PUB13ARM transgenic plants resembled that detected in *pub12/13* double mutant and was more pronounced than that in *pub12* or *pub13* single mutants, suggesting that ectopic expression of PUB13ARM may interfere with both *PUB12* and *PUB13* functions.

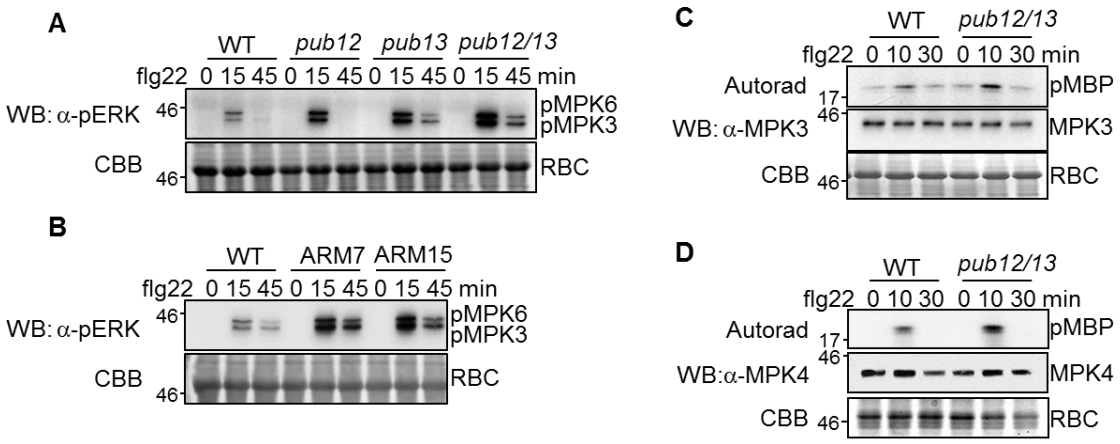

Figure 17. PUB12/13 negatively regulate MAPK activation.

(A) & (B) Enhanced MAPK activity in *pub12/13* mutant and PUB13ARM transgenic plants as detected by α-pERK antibody. Two-week-old seedlings were treated with 100 nM flg22 for 15 or 45 min. Phosphorylated MPK3 (pMPK3) and MPK6 (pMPK6) were detected by α-pERK WB. Protein loading is shown by CBB for RBC. (C) & (D) Enhanced MAPK activity in the *pub12/13* mutant as detected by immunocomplex kinase assay. Two-week-old seedlings were treated with 1 μM flg22 for 10 or 30 min. MPK3 (A) and MPK4 (B) proteins were immunoprecipitated with α-MPK3 or α-MPK4 antibody respectively and subjected to an *in vitro* kinase assay using MBP as the substrate. The protein loading of MPK3 or MPK4 is shown by α-MPK3 or α-MPK4 Western blot.

PUB13ARM transgenic plants show enhanced disease resistance

The *pub12/13* mutant is more resistant to infections by *Pseudomonas syringae* pv. *maculicola* ES4326 and *P. syringae* pv. *tomato* DC3000 compared to WT plants (Lu et al., 2011). We tested whether PUB13ARM transgenic plants were also more resistant to bacterial infections. Two days or four days after inoculation, *in planta* bacterial population of *Psm* ES4326 in two independent lines of PUB13ARM transgenic plants or *pub12/13* mutant was about fivefold to tenfold lower than that in WT plants (Fig. 18A).

Figure 18. Enhanced disease resistance in PUB13ARM transgenic plants.

(A) & (B) Growth of bacteria *Pseudomonas syringae* in PUB13ARM transgenic plants. Four-week-old *Arabidopsis* leaves were hand-inoculated with *P. syringae* pv. *maculicola* ES4326 or *P. syringae* pv. *tomato* DC3000 strain at 5×10^5 CFU/ml. Bacterial counting was performed 2 and 4 days post inoculation (dpi). An asterisk (*) indicates a significant difference ($p < 0.05$) between WT plants and PUB13ARM transgenic plants. (C) Lesion development of *Botrytis cinerea* in PUB13ARM transgenic plants. Five-week-old plants were infected with *B. cinerea* BO5 at the concentration of 10^5 spores/ml. Disease symptoms were recorded and area of infection was measured 3 dpi. An asterisk (*) indicates a significant difference with $p < 0.05$ between WT and PUB13ARM transgenic plants. (D) Cell death and (E) H_2O_2 accumulation in the leaves of four-week-old plants were examined by trypan blue and DAB staining respectively. (F) Measurement of SA levels in WT plants and PUB13ARM transgenic plants. Four-week-old *Arabidopsis* leaves were hand-inoculated with *Pst* DC3000 strain at 5×10^5 CFU/ml. SA was analyzed by GC-3 dpi. The data are shown as the mean ± standard error (n = 4). (G) The expression of *PR1* and *PDF1.2* genes in four-week-old plants was normalized to the expression of *UBQ10*. The data were shown as the mean ± standard error (n = 3). The plants were grown under 23°C, 65% relative humidity, 75 μE m^{-2} s^{-1} light and a photoperiod of 12 hr of light/12 hr of dark.

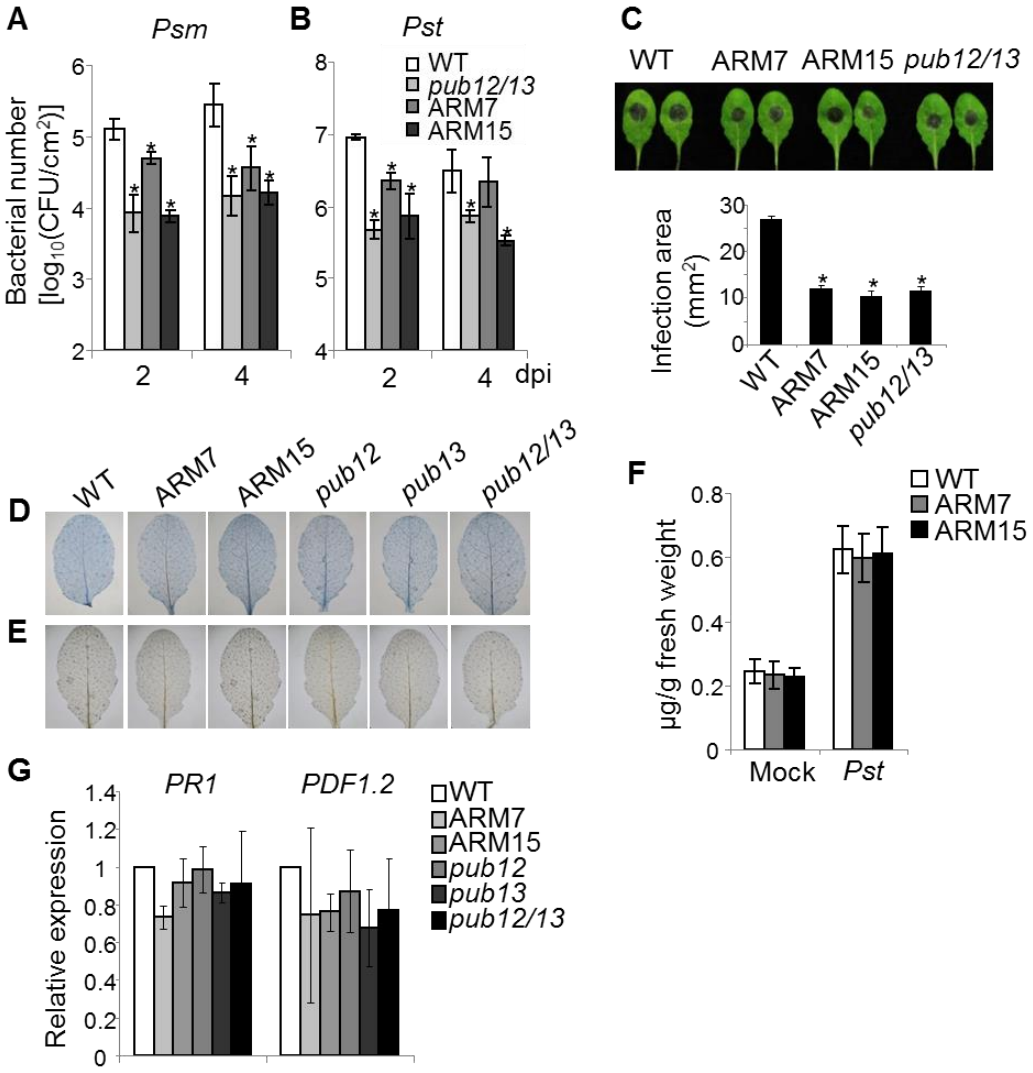

A similar result was observed with *Pst* DC3000 infection (Fig. 18B). Thus, similar to the *pub12/13* double mutant, PUB13ARM transgenic plants are more resistant to bacteria *Psm* and *Pst* infections than WT plants. In addition, we also examined the infection of the necrotrophic pathogen *Botrytis cinerea* BO5 in *pub12/13* mutant and PUB13ARM transgenic plants. Three days after infection, leaves detached from WT plants formed large lesion at the infection sites. By contrast, the lesion area on the leaves of *pub12/13*

mutant and PUB13ARM transgenic plants was about 50% smaller than that on WT leaves (Fig. 18C), suggesting that both *pub12/13* mutant and PUB13ARM transgenic plants were more resistant to necrotrophic *Botrytis* infection than WT plants in our growth conditions. It was reported that *pub13* mutant exhibited spontaneous cell death and H_2O_2 accumulation under the growth condition of 22°C, 70% relative humidity and 250 μE m^{-2} s^{-1} light with a photoperiod of 16 hr of light/8 hr of dark. High humidity treatment (95% relative humidity for 48 hr) further aggravated these phenotypes (Li et al., 2012). Notably, 250 μE m^{-2} s^{-1} light is a relatively high intensity for *Arabidopsis* growth. When grown under the condition of 23°C, 65% relative humidity, 75 μE m^{-2} s^{-1} light with a photoperiod of 12 hr of light/12 hr of dark, neither *pub13* nor *pub12/13* mutant plants exhibited detectable cell death and H_2O_2 accumulation (Fig. 18D & 18E). The plant defense hormone salicylic acid (SA) was indicated to be involved in PUB13-reguated defense (Li et al., 2012). We measured endogenous SA levels in WT and PUB13ARM transgenic plants without and with *Pst* DC3000 infection, and did not detect statistically significant difference between WT and PUB13ARM transgenic plants (Fig. 18F). In addition, the transcript level of *PR1*, a marker gene in SA signaling pathway, and *PDF1.2*, a marker gene in the ethylene (ET) and jasmonic acid (JA) signaling pathways remained similar among WT, *pub12/13* mutant and PUB13ARM transgenic plants under our growth condition (Fig. 18G). In addition, the flg22-induced FLS2 degradation was comparable in WT and *sid2* mutant deficient in SA biosynthesis (Fig. 19A), suggesting that flg22-induced FLS2 degradation is largely SA-independent. This is further substantiated by the early observations that *eds1*, *npr1*, and *pad4* mutants

deficient in SA signaling and plants expressing *NahG* (a salicylate hydroxylase) show normal flg22-mediated resistance (Zipfel et al., 2004). Furthermore, the flg22-induced MAPK activation and ROS production were also elevated in the *sid2pub13* mutant compared to the *sid2* mutant (Fig. 19B & 19C). Taken together, the data indicate that flg22-induced PUB13-mediated early defense responses are not completely due to the elevated SA level in the *pub13* mutant.

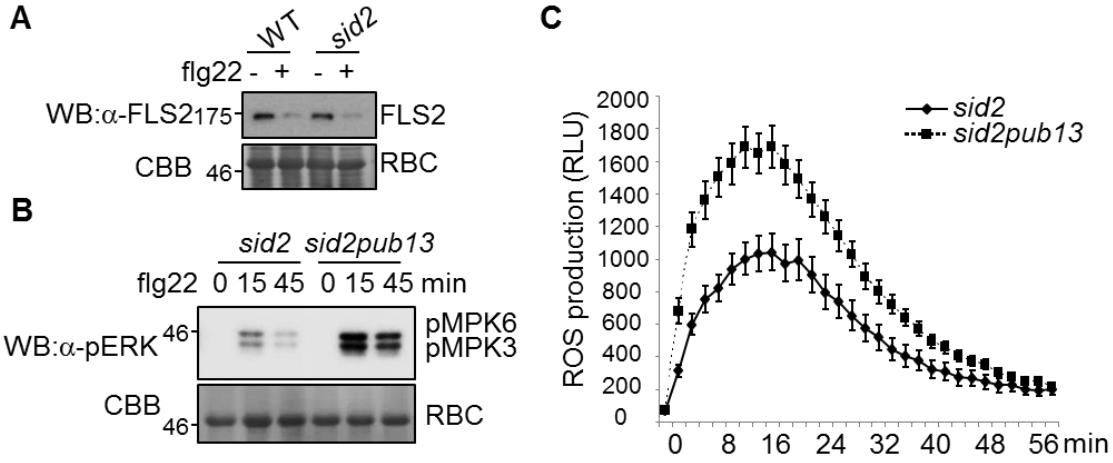

Figure 19. Flg22-induced immune responses in WT, *pub13*, *sid2* and *sid2pub13* mutants.

(A) Flg22-induced FLS2 degradation in WT and *sid2* mutant plants. Two-week-old seedlings were treated with 1 μM flg22 for1 hr. The endogenous FLS2 proteins were detected by α-FLS2 Western blot and the equal protein loading is shown by CBB staining for RuBisCo (RBC). (B) MAPK activity in *sid2* and *sid2pub13* mutants as detected by α-pERK antibody. Two-week-old seedlings were treated with 100 nM flg22 for 15 or 45 min. Phosphorylated MPK3 (pMPK3) and MPK6 (pMPK6) were detected by α-pERK Western blot. The protein loading is shown by CBB for RBC. (C) ROS production in *sid2* and *sid2pub13* mutants. Leaf discs from five-week-old plants were treated with 100 nM flg22 and ROS production was detected at indicated time points. The data are shown as the mean ± standard error from 24 leaf discs.

PUB12 and PUB13 negatively regulate stress-induced leaf senescence

The phenotypes of *pub12/13* mutant and PUB13ARM transgenic plants were not obviously different from WT plants at four-week-old stage in our growth conditions (Fig. 20A). However, we noticed that mutant and transgenic plants were prone to be stressed. After a four-day period of dark treatment, *pub12* and *pub13* single mutant or *pub12/13* double mutant plants senescenced earlier with more yellowing leaves than WT plants (Fig. 20A). Thus, it appears that stresses, including increased light intensity, high humidity and dark treatment, likely induce cell death and/or H_2O_2 accumulation in *pub13* and *pub12* mutant plants. These observations indicate that PUB12 and PUB13 may play a role in stress-induced senescence and cell death regulation. To test this, we measured the transcript levels of several senescence-associated genes (SAGs), among which *SAG12* is a commonly used marker for age-dependent leaf senescence whereas *SAG13* and *SAG14* are stress-induced senescence markers (Du et al., 2013). Importantly, *pub12*, *pub13* and *pub12/13* mutant exhibited a WT level of *SAG12* expression whereas they showed dramatically enhanced transcript levels of *SAG13* and *SAG14* upon dark treatment (Fig. 20B). The data suggest that PUB12 and PUB13 are involved in stress-induced leaf senescence regulation. Similar to the *pub12/13* double mutant, PUB13ARM transgenic plants also showed early senescence with elevated transcript levels of *SAG13* and *SAG14* after dark treatment (Fig. 20A & 20B). To determine the role of SA in PUB13-regulated leaf senescence, we performed dark treatment to *sid2* and *sid2pub13* mutants. Similar to *pub13*, *sid2pub13* mutant, but not *sid2*, showed yellowing leaves

after 4 days dark treatment (data not shown), indicating that PUB13-mediated senescence is SA-independent.

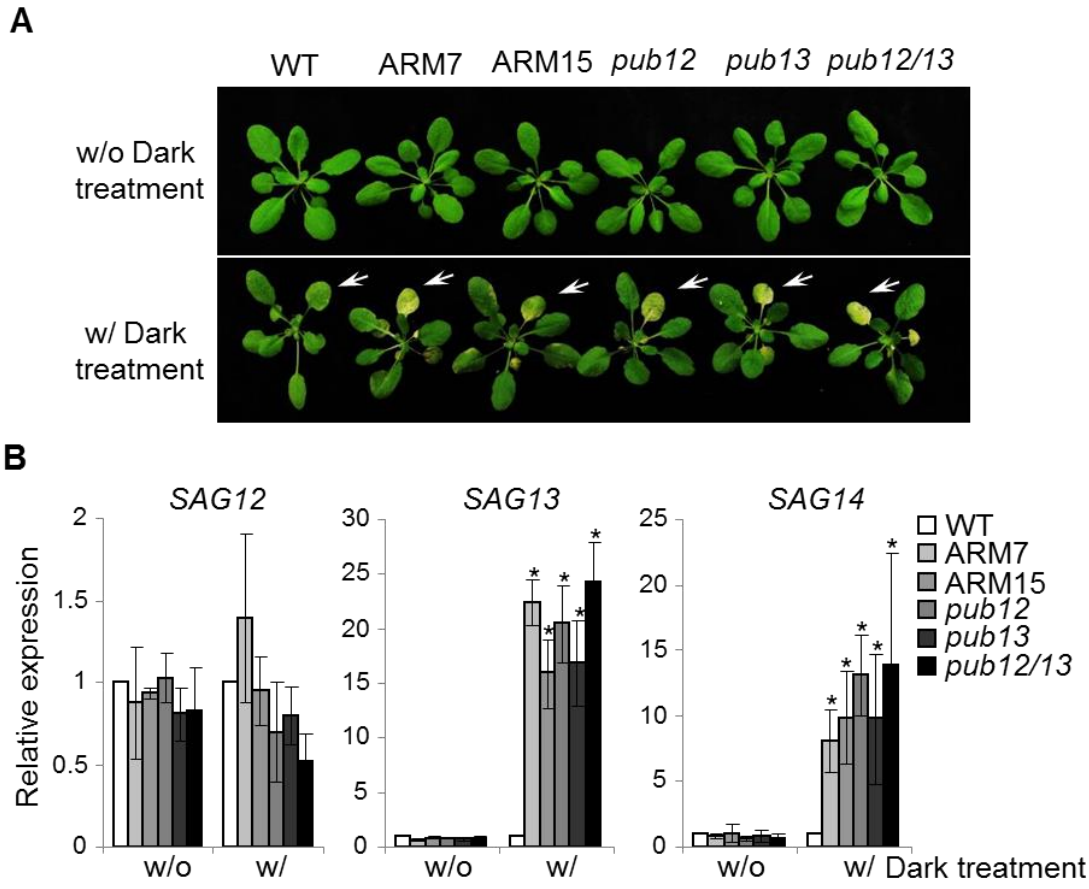

Figure 20. PUB12/13 negatively regulate leaf senescence.

(A) Dark-induced senescence in *pub* mutant and ARM transgenic plants. Four-week-old WT, *pub* mutants and PUB13ARM transgenic plants were subjected to a four-day dark treatment. Yellowing leaves at the same positions are indicated by the white-colored arrows. (B) Expression of *senescence-associated genes* (*SAG*) in WT, *pub* mutants and PUB13ARM transgenic plants. The expression of *SAG12*, *SAG13* and *SAG14* was normalized to the expression of *UBQ10*. The data are shown as the mean ± standard error (n = 3) and the asterisks (*) indicate a significant difference compared to WT plants ($p < 0.05$).

PUB13ARM transgenic plants show early flowering

The *pub13* mutant displayed early flowering compared to WT plants under 12 hr of light /12 hr of dark (medium-day, MD) or 16 hr of light /8 hr of dark (long-day, LD) photoperiods (Li et al., 2012). Similar to the *pub13* mutant, *pub12* and *pub12/13* mutant plants and PUB13ARM transgenic plants flowered about three days earlier than WT (Fig. 21A). The rosette leaf number at flowering of two lines of PUB13ARM transgenic plants was three to four less than that of WT plants (Fig. 21B). Signal transduction pathways regulating flowering time converge at the integrators including flowering locus T (FT), suppressor of overexpression of constans 1 (SOC1) and LEAFY (LFY), and the expression level of these integrators determines the exact flowering time (Seo et al., 2009). qRT-PCR analysis indicated that the transcript levels were elevated by about fourfold for *FT* and twofold for *SOC1* in PUB13ARM transgenic plants and *pub12/13* mutant compared to WT plants (Fig. 21C). We further compared flowering time of WT, *pub13*, *sid2* and *sid2pub13* mutants. Although *pub13* mutant plants flowered at eight weeks post-germination, earlier than WT plants, the *sid2* mutant flowered later than WT plants (data not shown) as reported (Martinez et al., 2004). However, both WT and the *sid2pub13* mutant flowered at about nine weeks post-germination, which was earlier than the *sid2* mutant (data not shown). Therefore, early flowering was still observed in the *sid2pub13* mutant compared to *sid2* mutant.

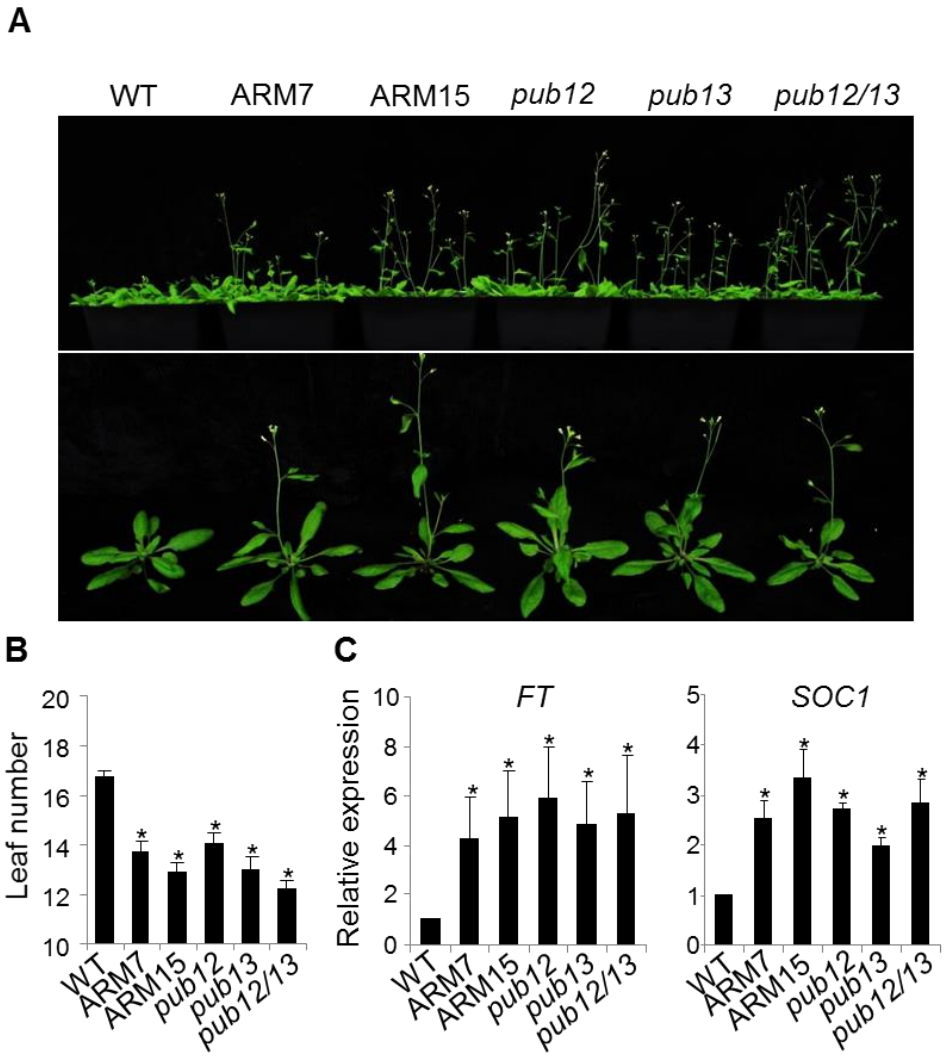

Figure 21. PUB12/13 negatively regulate plant flowering time.

(A) Flowering phenotype. Photos were taken of eight-week-old WT, *pub* mutants and PUB13ARM transgenic plants grown under 23°C, 65% relative humidity, 75 μE m^{-2} s^{-1} light and photoperiod of 16 hr of light /8 hr of dark. (B) Leaf number of WT, *pub* mutants and PUB13ARM transgenic plants. The leaf number of tested plants was counted when the first flower bud appeared. An asterisk (*) indicates a significant difference ($p < 0.05$) compared to the leaf number of WT plants. (C) Expression of flowering marker genes in WT, *pub* mutants and PUB13ARM transgenic plants. The expression of *FT* and *SOC1* was normalized to the expression of *UBQ10*. The data are shown as the mean ± standard error (n = 3) and the asterisks (*) indicate a significant difference compared to WT plants ($p < 0.05$).

Materials and methods

Plant materials and growth conditions

The *pub12* and *pub13* single mutant and *pub12/13* double mutant plants were reported previously (Lu et al., 2011). *Arabidopsis* plants were grown in soil (Metro Mix 360) in a growth chamber with 23°C, 65% relative humidity, 75 μE m^{-2} s^{-1} light and a photoperiod of 12 hr of light /12 hr of dark for 4 weeks before protoplast isolation and disease assays. For flowering time, plants were grown under 23°C, 65% relative humidity, 75 μE m^{-2} s^{-1} light and a photoperiod of 16 hr of light /8 hr of dark. To grow *Arabidopsis* seedlings on medium, the seeds were surface-sterilized with 50% bleach for 15 min, washed with sterilized ddH_2O and then placed on the plates with half-strength Murashige and Skoog medium (½ MS) containing 0.5% sucrose, 0.8% agar and 2.5 mm MES at pH 5.7. The plates were first stored at 4°C for 3 days in the dark for seed stratification, and then moved to the growth chamber set to the same parameters as the soil-grown plants.

Plasmid construction and generation of transgenic plants

The constructs of *BAK1, FLS2* and *PUB13* in the plant expression vector (pHBT) or protein expression vector (pMAL or pGST) were reported previously (Lu et al., 2011; Lu et al., 2010). The different *PUB13* domain truncations were cloned into the plant expression vector, protein expression vector or modified bimolecular fluorescence complementation (BiFC) vector with PCR amplification using the primers listed in the Table 2. The *35S::FLS2-LUC* construct was made by sub-cloning the full length *FLS2*

gene into the plant expression vector pHBT fused with a *Luciferase* gene. The *PUB13ARM* was sub-cloned into a modified plant transformation binary vector *pCB302* derivative under the control of the *35S* promoter with an HA epitope tag. The transgenic plants were generated by *Agrobacterium tumefaciens*-mediated transformation in *Arabidopsis* accession Col-0 plants. The transgenic plants were screened with the herbicide BASTA (resistance conferred by the binary vector) and confirmed by Western blotting with an α-HA antibody. The homozygous lines were selected based on the survival ratio of T2 and T3 generation plants after BASTA spray.

In vitro *pull-down assay*

Maltose binding protein (MBP), MBP-BAK1CD, MBP-BAK1CDKm, MBP-FLS2CD, GST, GST-PUB13 and GST-PUB13ARM proteins were individually expressed in *E. coli* BL21 strain and purified with standard amylose or glutathione agarose-based procedure. About 10 μg of MBP, MBP-BAK1CD or MBP-FLS2CD proteins were incubated with 5 μl of pre-washed amylose beads in 1 ml of pull-down buffer (20 mM Tris-HCl, pH 7.5, 1 mM β-mercaptoethanol, 3 mM EDTA, 150 mM NaCl and 1% NP40) for 30 min at 4°C with gentle shaking. The beads were harvested by centrifugation at 2,000 rpm for 1 min and then inoculated with 10 μg of GST or GST-tagged proteins in 1 ml of pull-down buffer for 1 hr at 4°C with gentle shaking. The beads were harvested and washed 3 times with 1 ml of pull-down buffer and once with 1 ml of 50 mM Tris-HCl, pH 7.5. Bound proteins were released from beads by boiling in

Table 2. Primers for cloning and PCR analysis.

PUB13 UND-F	5’-CATGCC*ATGG*AGGAAGAGAAAGCTTC-3’
PUB13 UND-R	5’-GAAGGCCTTATCTTCTGACTCGCTGCC-3’
PUB13 U-box-F	5’-CATGCC*ATGG*CGAGTCAGAAGATACCTGTG-3’
PUB13 U-box-R	5’-GAAGGCCTCTCAATATCGTTGGCCTCGC-3’
PUB13 ARM-F	5’-CATGCC*ATGG*AGCCTCCAAAGCCTCCGAG-3’
PUB13 ARM-R	5’-GAAGGCCTAGTATCTGCAGCTTCTGTGG-3’
PUB12 ARM-F	5’-CATGCC*ATGG*AGCCTCCAAAGCGTCCCAAC-3’
PUB12 ARM-R	5’-TCCCCCGGGGATTAGGGAGATTTGATCTTCC-3’
BAK1-F	5’-CATGCC*ATGG*AACGAA GATTAATGATC-3’
WRKY30-F	5’-GCAGCTTGAGAGCAAGAATG-3’
WRKY30-R	5’-AGCCAAATTTCCAAGAGGAT-3’
AP2-F	5’-CTCAGCGGTCTCAAATGTCC-3’
AP2-R	5’-AGGAGCAGCAACAACCAATC-3’
FRK1-F	5’-ATCTTCGCTTGGAGCTTCTC-3’
FRK1-R	5’-TGCAGCGCAAGGACTAGAG-3’
SAG12-F	5’-CTGCGAAGGCGGTTTAATGG-3’
SAG12-R	5’-CGGGACATCCTCATAACCTGT-3’
SAG13-F	5’-CTTACGTGAATGGCAAGCAA-3’
SAG13-R	5’-CCACATTGTTGACGAGGATG-3’
SAG14-F	5’-CCCAAGTACTGGAGGAACCA-3’
SAG14-R	5’-TAATGAGGAAGCGGCATTTC-3’
PR1-F	5’-ACACGTGCAATGGAGTTTGTGG-3’
PR1-R	5’-TTGGCACATCCGAGTCTCACTG-3’
PDF1.2-F	5’-TGTTTGGCTCCTTCAAGGTT-3’
PDF1.2-R	5’-TTCTCTTTGCTGCTTTCGAC-3’
UBQ10-F	5’-AGATCCAGGACAAGGAAGGTATTC-3’
UBQ10-R	5’-CGCAGGACCAAGTGAAGAGTAG-3’

20 μl of 2 x SDS-PAGE sample loading buffer and analyzed by Western blot with an α-GST antibody.

qRT-PCR analysis

Total RNA was isolated from leaves or seedlings after treatment with TRIzol Reagent (Invitrogen). Complementary DNA (cDNA) was synthesized from 1 ug of total RNA with oligo (dT) primer and reverse transcriptase (New England BioLabs). Real-time RT-PCR analysis was carried out using iTaq SYBR green Supermix (Bio-Rad) supplemented with ROX in an ABI GeneAmp PCR System 9700. The expression of immunity-related genes was normalized to the expression of UBQ10. The primer sequences for RT-PCR are listed in Table 2.

BiFC assay

Protoplast isolation and transfection were performed as described (He et al., 2007b). *Arabidopsis* protoplasts were co-transfected with various BiFC constructs as indicated in the figures. Fluorescence signals in protoplasts were visualized under a confocal microscope (Olympus FV1000 Confocal Microscope) 18 hr after transfection. Following are the filter sets used for excitation (Ex) and emission (Em): YFP, 515 nm (Ex)/520 nm to 550 nm (Em); chlorophyll, 488 nm (Ex)/560 nm to650 nm (Em); bright

field, 633 nm. Images were captured in a multichannel mode, analyzed and processed with OLYMPUS FLUOVIEW Version 3.0 Viewer.

Co-immunoprecipitation and in vivo *ubiquitination assays*

The total proteins from 2 x 10^5 transfected protoplasts were isolated with 0.5 ml of extraction buffer (10 mM HEPES, pH 7.5, 100 mM NaCl, 1 mM EDTA, 10% glycerol, 0.5% Triton X-100, and 1 x protease inhibitor cocktail from Roche). The samples were vortexed vigorously for 30 s, and then centrifuged at 13,000 rpm for 10 min at 4 °C. The supernatant was inoculated with α-FLAG agarose beads for 2 hr at 4 °C with gentle shaking. The beads were collected and washed three times with washing buffer (10 mM HEPES, pH 7.5, 100 mM NaCl, 1 mM EDTA, 10% glycerol, 0.1% Triton X-100, and 1 x protease inhibitor cocktail) and once more with 50 mM Tris-HCl, pH 7.5. Bound proteins were released from beads by boiling in SDS-PAGE sample loading buffer and analyzed by Western blot with an α-HA antibody.

In vitro *phosphorylation, immunocomplex kinase and* in vivo *MAP kinase assays*

For *in vitro* kinase assay, reactions were performed in 30 μl of kinase buffer (20 mM Tris-HCl, pH 7.5, 10 mM $MgCl_2$, 5 mM EGTA, 100 mM NaCl, and 1 mM DTT) containing 10 μg of fusion proteins with 0.1 mM cold ATP and 5 μCi [^{32}P]-γ-ATP at room temperature for 3 hr with gentle shaking. The reactions were stopped by adding 4 x SDS loading buffer. The phosphorylation of fusion proteins was analyzed by autoradiography after separation with 12% SDS-PAGE.

For immunocomplex kinase assay, two-week-old seedlings (10) were ground with 1 ml of IP buffer (50 mM Tris-HCl, pH 7.5, 150 mM NaCl, 5 mM EDTA, 1 mM DTT, 2 mM NaF, 2 mM Na_3VO_3, 1% Triton, and protease inhibitor cocktail). The samples were vortexed vigorously for 30 s, and then centrifuged at 13,000 rpm for 10 min at 4°C. The supernatant was incubated with α-MPK antibody for 2 hr and then with protein-G-agarose beads for another 2 hr at 4°C with gentle shaking. The beads were harvested and washed once with IP buffer and once with kinase buffer. The kinase reactions were performed in 20 μl of kinase buffer with 2 μg of myelin basic protein (MBP) as substrate, 0.1 mM cold ATP, and 5 μCi of [^{32}P]-γ-ATP at room temperature for 1 hr with gentle shaking. The phosphorylation of MBP proteins was analyzed by autoradiography after separation with 15% SDS-PAGE.

For detecting MAP kinase activity *in vivo*, two-week-old seedlings grown on ½ MS medium were transferred to water overnight and then treated with 100 nM flg22 or H_2O for the times indicated and frozen in liquid nitrogen. The seedlings were homogenized in IP buffer and equal amount of total protein was electrophoresed on 10% SDS–PAGE. An α-pERK antibody (1:2,000) (Cell Signaling) was used to detect phosphorylation status of MPK3 and MPK6 with an immunoblot.

In vitro *ubiquitination assay*

The *in vitro* ubiquitination assay was performed as described with some modifications (Lu et al., 2011). The reactions contain 1 μg of purified MBP-FLS2CD, 1 μg of purified His_6-E1 (AtUBA1), 1 μg of purified His_6-E2 (AtUBC8), 1 μg of His_6-

ubiquitin (Boston Biochem), 1 μg of purified GST-PUB and 1~16 μg of purified GST or GST-ARM in the ubiquitination buffer (0.1 M Tris-HCl, pH 7.5, 25 mM $MgCl_2$, 2.5 mM dithiothreitol, 10 mM ATP) to a final volume of 30 μl. The reactions were incubated at 30°C for 2 hr, and then stopped by adding SDS sample buffer and boiled at 100°C for 5 min. The samples were then separated by 7.5% SDS–PAGE and the ubiquitinated substrates were detected by Western blot analysis.

Measurement of ROS production

Four leaves of each of six five-week-old *Arabidopsis* plants were excised into leaf discs of 0.25 cm^2, following an overnight incubation in 96-well plate with 100 μl of H_2O to eliminate the wounding effect. H_2O was replaced by 100 μl of reaction solution containing 50 μM luminol and 10 μg/ml horseradish peroxidase (Sigma) supplemented with 100 nM flg22. The luminescence was measured with a luminometer (Perkin Elmer, 2030 Multilabel Reader, Victor X3) immediately after adding the solution, with a 2 min interval reading time for a period of 60 min. The measurement value of ROS production from 24 leaf discs per treatment was indicated as the mean of RLU (Relative Light Units).

Callose deposition

Three two-week-old seedlings were incubated with 500 nM flg22 for 12 hr at room temperature. Seedlings were immediately cleared in alcoholic lactophenol [95% ethanol: lactophenol (phenol: glycerol: lactic acid: H_2O=1:1:1:1) = 2:1] overnight.

Samples were subsequently rinsed with 50% ethanol and H_2O. Cleared leaves were stained with 0.01% aniline blue in 0.15 M phosphate buffer (pH = 9.5) and the callose

deposits were visualized under a UV filter using a fluorescence microscope. Callose deposits were counted using ImageJ 1.43U software (http://rsb.info.nih.gov/ij/). The number of deposits was expressed as the mean of six different leaf areas with standard error.

Pathogen infection assays

P. syringae pv. *tomato* DC3000 and *P. syringae* pv. *maculicola* ES4326 strains were cultured overnight at 28°C in KB medium with 50 μg/ml rifampicin for DC3000 and 50 μg/ml streptomycin for ES4326. Bacteria were collected, washed and diluted to the desired density with H_2O. Four-week-old *Arabidopsis* leaves were infiltrated with bacteria at a concentration of 5 x 10^5 cfu/ml using a needleless syringe. To measure bacterial growth, two leaf discs were ground in 100 μl of H_2O and serial dilutions were plated on KB medium with appropriate antibiotic. Bacterial colony forming units (cfu) were counted 2 days after incubation at 28°C. Each data point is shown as triplicates.

Botrytis cinerea BO5 was grown on potato dextrose agar (Difco, USA) and was incubated at room temperature. Conidia were re-suspended in distilled water and the spore concentration was adjusted to 10^5 spores/ml. Gelatin (0.5%) was added to conidial suspension before inoculation. The detached *Arabidopsis* leaves were laid on a plastic tray with wet paper at the bottom and 10 μl of spores were dropped onto the center of

each leaf. The tray was covered with a dome to keep high humidity, and disease development was monitored over a period of 3 days.

SA measurement

For SA measurements, four-week-old plants were infested with *P. syringae* pv. *tomato* DC3000 at a concentration of 5 x 10^5 cfu/ml, or water as a mock control. Three days later, leaves were harvested and ground in liquid nitrogen. SA was quantified using the method described previously (Lei et al., 2014) with the following modifications. During solvent partitioning, the pH of the aqueous solution was first adjusted to pH 8.0 and then to pH 6.0, and the Mass Spectrometer was operated in SIM mode only.

Trypan blue and DAB staining

For trypan blue staining, the leaves of four-week-old plants were excised and subsequently immersed in boiled lactophenol (lactic acid: glycerol: liquid phenol: distilled water=1:1:1:1) solution with 0.25 mg/ml trypan blue for 1 min. The stained leaves were destained with 95% ethanol/lactophenol solution, and washed with 50% ethanol. For DAB staining, the leaves of four-week-old plants were immersed in 1 mg/ml DAB (3, 3'-diaminobenzidine) (pH 3.8) solution with low vacuum pressure for 30 min, followed by an overnight incubation at room temperature in the dark. The stained leaves were fixed and cleared in alcoholic lacto-phenol (95% ethanol: lactic acid: phenol = 2: 1: 1) at 65°C, rinsed once with 50% ethanol, and twice with H_2O. The destained leaves were subjected to microscope observation.

Summary

The ARMADILLO (ARM) repeat domain composed of multiple tandem repeats of approximately 40-amino-acid motif was first discovered in *Drosophila* β-catenin, and later was found in all eukaryotic organisms (Samuel et al., 2006). The *Arabidopsis* genome encodes ~94 ARM repeat containing proteins, 41 of which belong to the PUB family (Samuel et al., 2006). Although the ARM repeat domain is predicted to be involved in protein-protein interactions, few interacting proteins have been identified for plant ARM repeat proteins. In this study, we show that the kinase domain of receptor-like kinase BAK1 physically interacts with the ARM domain of PUB13 *in vivo* and *in vitro*. This interaction is specific since the PUB13 ARM domain does not directly interact with the FLS2 kinase domain. Interestingly, the interaction with BAK1 for the ARM domain of PUB13 is much stronger than that for the full length PUB13, suggesting that other region(s) of PUB13 may negatively regulate ARM-BAK1 interaction. PUB13 and some other PUBs have a plant specific N-terminal UND domain with unknown functions. It is possible that the UND domain regulates ARM-BAK1 interaction. BAK1 interacts and phosphorylates the PUB13 ARM domain. We attempted to define BAK1 phosphorylation motif/residues in the ARM domain with truncations of individual ARM repeats. It appears that BAK1 likely phosphorylates PUB13 ARM domain at multiple sites and could strongly phosphorylate each individual ARM repeat (data not shown). Consistently, mass spectrometry analysis identified many phosphorylation sites scattered in the ARM domain by BAK1 (data not shown). Thus, it is challenging to address the consequence of BAK1 phosphorylation on PUB13 with mutational analysis. We have

shown previously that BAK1 is required for flg22-induced FLS2-PUB13 association and FLS2 degradation, and kinase inhibitor could block flg22-induced FLS2-PUB13 association (Lu et al., 2011). It is likely that PUB13 phosphorylation by BAK1 leads to its association with FLS2 for receptor ubiquitination and degradation.

Among 64 *Arabidopsis* PUB proteins, 41 of them contain the ARM repeat domain. The functions of the majority of ARM domain containing PUB proteins have not been elucidated (Yee and Goring, 2009). This might be in part due to the functional redundancy of closely related PUB protein family members. For example, three ARM containing *Arabidopsis* PUBs, PUB22, PUB23 and PUB24, play redundant role in PTI signaling (Trujillo et al., 2008), and PUB22 and PUB23 also have combinatory function in response to drought stress (Cho et al., 2008). PUB12 and PUB13 with 65% amino acid identity and 79% similarity possess functional redundancy in fine-tuning flg22-mediated immune responses (Lu et al., 2011). Notably, PUB12/13 and PUB22/23/24 target different components in FLS2 signaling, suggesting ubiquitination regulates multiple steps in plant innate immunity. Nevertheless, there is a pressing need for the generation of PUB mutants with the possibility to block the functions of multiple closely related members. In this study, we showed that ectopic expression of the ARM domain of PUB13 acts as a dominant negative mutant that interferes with activities of endogenous PUB12 and PUB13 proteins. The PUB13 ARM domain strongly interacts with BAK1, thereby blocking BAK1 interaction and phosphorylation of endogenous PUB12 and PUB13. Alternatively, the PUB13 ARM domain may directly interfere with the function of endogenous PUB12 and PUB13. This leads to the attenuation of

PUB12/13-FLS2 association and PUB12/13-mediated FLS2 ubiquitination and degradation. Consistent with this hypothesis, stable transgenic plants overexpressing the PUB13 ARM domain resemble *pub12/13* double mutant with elevated immunity-related gene expression, ROS production and callose deposition upon flg22 treatment and enhanced resistance to bacterial infections compared to WT plants. We further demonstrated that both PUB13ARM transgenic plants and *pub12/13* mutant plants showed enhanced MAPK activation upon flg22 treatment, consistent with the regulation of the upstream FLS2 receptor by PUB12 and PUB13. Thus, ectopic expression of the ARM domain could provide an alternative approach to study the complex function of PUBs and other ARM domain containing proteins (Fig. 22).

The phenotypic resemblance between PUB13ARM transgenic plants and *pub12/13* mutant plants extends to the regulation of flowering. Both plants showed early flowering and elevated expression of flowering marker genes compared to WT plants. It has been shown that SPL11, the rice ortholog of *Arabidopsis* PUB13, regulates flowering via interaction with SPIN1, a K homology domain protein involved in RNA binding (Vega-Sanchez et al., 2008). SPIN1 represses flowering since overexpression of SPIN1 caused late flowering independently of day length (Vega-Sanchez et al., 2008). In contrast to *Arabidopsis pub13* mutant with an early flowering phenotype (Li et al., 2012), the rice *spl11* mutant showed delayed flowering under long-day conditions (Vega-Sanchez et al., 2008). SPL11 monoubiquitinated SPIN1. However, rather than controlling SPIN1 protein stability, SPL11 regulates SPIN1 mainly at the transcriptional level (Vega-Sanchez et al., 2008). The results indicate that a different mechanism may

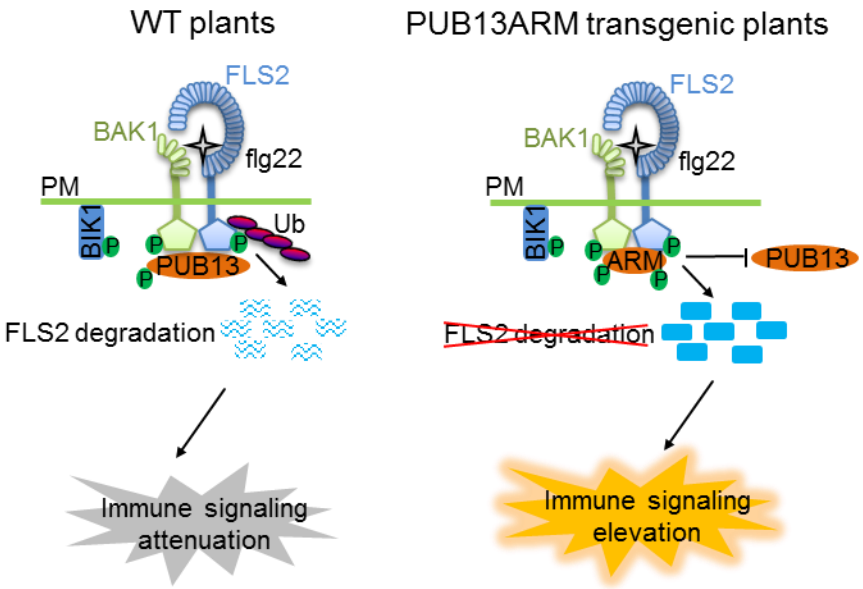

Figure 22. A model of dominant negative function of ARM domain.
n WT plants, perception of flg22 by FLS2 induces formation of the FLS2-BAK1 complex, release of BIK1 and activation of downstream immune responses. The ARM domain of PUB13 interacts with BAK1 and is phosphorylated by BAK1. PUB13 associates with FLS2 during flagellin-induced formation of the FLS2-BAK1 complex, mediates the ubiquitination of FLS2 and directs FLS2 for degradation, resulting in the attenuation of immune signaling. In the PUB13ARM transgenic plants, the overexpressed PUB13ARM proteins strongly interact with BAK1 and prevent BAK1 interaction with endogenous PUB13 and likely PUB12, or alternatively interfere with the function of endogenous PUB13 and PUB12. Therefore, the ectopically expressed PUB13ARM proteins block PUB12/13-mediated FLS2 ubiquitination and degradation, resulting in elevated immune responses. P: phosphate; Ub: ubiquitin; PM: plasma membrane.

exist for PUB13 regulation of *Arabidopsis* flowering time. Ubiquitination has been reported to modulate flowering time by regulating the stability and accumulation of CONSTANS (CO, a photoperiodic protein), GIGANTEA (GI, a circadian-associated protein), and FLOWERING LOCUS C (FLC, a negative regulator of the autonomous

and vernalization pathways) (Liu et al., 2012). PUB13 positively regulates the flowering suppressor FLC to delay flowering under LD conditions (Liu et al., 2012). However, the detailed mechanism how PUB13 regulates FLC is unknown. Although immunity and flowering are two seemingly independent pathways in plants, emerging evidence suggests that two pathways are likely interconnected. Similar to the dual functions of PUB13 in immunity and flowering, the *Arabidopsis* small ubiquitin-like modifier (SUMO) E3 ligase SIZ1 is a negative regulator of both immunity and flowering time (Jin et al., 2008; Lee et al., 2007). HopW1-1-interacting 3 (WIN3) was reported to promote plant innate immunity and delay flowering time in *Arabidopsis* (Wang et al., 2011). These findings suggest that tightly controlled flowering time may associate with plant fitness to defend pathogen attacks.

PUB13ARM transgenic plants and *pub12/13* mutant plants are also more sensitive to dark-induced senescence with elevated transcript levels of stress-induced senescence marker genes. Leaf senescence is a type of programmed cell death that allows plants to mobilize nutrients from senescing cells to actively growing tissues (Zhang et al., 2013). Another ARM domain containing PUB protein, PUB44, also regulates leaf senescence. The *Arabidopsis pub44* mutant, also termed *senescence-associated ubiquitin ligase1 (saul1)*, showed early senescence when challenged with low light (20 μE m^{-2} s^{-1}) (Vogelmann et al., 2012). Interestingly, *saul1/pub44* mutation-mediated senescence depends on PAD4-dependent and NPR1-independent SA pathway. Accumulating evidence has suggested that plant defense and leaf senescence share some components in SA signaling and regulation. An SA catabolic enzyme SA 3-hydroxylase regulates onset

and progression of leaf senescence (Zhang et al., 2013). Several SAGs have been identified as defense-related genes, such as *SAG26*, *SAG29*, *elicitor-activated gene 3-2* (*ELI3-2)*, *nitrilase 2 (NIT2)*, *osmotin* 34 (*AtOSM34), sucrose-induced receptor kinase 1 (SIRK1)* and *WRKY6* (Quirino et al., 1999; Robatzek and Somssich, 2002). It has been shown that mutation of a LRR-RLK, RPK1, resulted in significant delay in age- and stress hormone ABA-induced senescence (Lee et al., 2011). It will be interesting to test whether PUB13 and/or PUB44 control leaf senescence through regulating RPK1 or other above-mentioned proteins by ubiquitination-mediated degradation.

CHAPTER IV

CONCLUSIONS

In the dissertation we show that BAK1, a co-receptor of multiple plant receptors, undergoes proteolytic cleavage. We have identified the D287 residue of BAK1 that is required for its proteolytic cleavage. In comparison of the molecular weight of BAK1 C-terminal fragment to a series of truncated BAK1, the proteolytic cleavage primarily happens in the transmembrane domain, whereas the D287 residue locates between juxtamembrane and kinase domains. Thus D287 residue is not located at the cleavage site, but is a crucial site for regulation of BAK1 proteolytic cleavage either through direct or indirect interaction with an unknown protease. Our data show that the D287 residue of BAK1 is critical for its functions in BR signaling, immune responses and cell death control, indicating proteolytic cleavage of BAK1 may be involved in these events. We could detect the C-terminal fragment of BAK1 in *Arabidopsis* protoplast and transgenic plants, which were consistent with the report from Dr. Delphine Chinchilla's group (Dominguez-Ferreras et al., 2015), while we were unable to detect the existence of the N-terminal fragment of BAK1 (data not shown). These findings suggest that the C-terminal fragment of BAK1 were functional in multiple events regulated by BAK1.

In the second part of this dissertation, we focus on BAK1-interacting E3 ubiquitin ligases PUB12/13. Our results indicate that the ARM domain of PUB12/13 interacts with FLS2/BAK1 complex and is phosphorylated by BAK1 whereas the U-box domain directly ubiquitinates FLS2. Ectopic expression of PUB13 ARM domain

inhibited flg22-triggered FLS2-PUB13 interaction and PUB12/13-regulated FLS2 ubiquitination and degradation in *Arabidopsis*. Similar with the *pub12pub13* double mutant, the stable transgenic plants expressing PUB13 ARM domain displayed enhanced multiple immune responses. In addition, the PUB13 ARM transgenic plants showed elevated resistance to infections by bacterium *P. syringae* and fungus *B. cinerea*. Moreover, the PUB13 ARM transgenic plants exhibited early flowering and senescence phenotype accompanied with altered marker gene expression compared to WT plants. Thus, generation of ARM overexpressing lines represents a unique opportunity for functional genomic analysis of PUB and other ARM-containing gene families in plants.

REFERENCES

Azevedo, C., Santos-Rosa, M.J., and Shirasu, K. (2001). The U-box protein family in plants. Trends in Plant Science *6*, 354-358.

Beck, M., Zhou, J., Faulkner, C., MacLean, D., and Robatzek, S. (2012). Spatio-temporal cellular dynamics of the Arabidopsis flagellin receptor reveal activation status-dependent endosomal sorting. The Plant Cell *24*, 4205-4219.

Boller, T., and Felix, G. (2009). A renaissance of elicitors: perception of microbe-associated molecular patterns and danger signals by pattern-recognition receptors. Annu Rev Plant Biol *60*, 379-406.

Chinchilla, D., Shan, L., He, P., de Vries, S., and Kemmerling, B. (2009). One for all: the receptor-associated kinase BAK1. Trends in Plant Science *14*, 535-541.

Chinchilla, D., Zipfel, C., Robatzek, S., Kemmerling, B., Nurnberger, T., Jones, J.D., Felix, G., and Boller, T. (2007). A flagellin-induced complex of the receptor FLS2 and BAK1 initiates plant defence. Nature *448*, 497-500.

Cho, S.K., Ryu, M.Y., Song, C., Kwak, J.M., and Kim, W.T. (2008). Arabidopsis PUB22 and PUB23 are homologous U-Box E3 ubiquitin ligases that play combinatory roles in response to drought stress. The Plant Cell *20*, 1899-1914.

Choi, S.W., Tamaki, T., Ebine, K., Uemura, T., Ueda, T., and Nakano, A. (2013). RABA members act in distinct steps of subcellular trafficking of the Flagellin Sensing2 receptor. The Plant Cell *25*, 1174-1187.

Craig, A., Ewan, R., Mesmar, J., Gudipati, V., and Sadanandom, A. (2009). E3 ubiquitin ligases and plant innate immunity. Journal of Experimental Botany *60*, 1123-1132.

Dominguez-Ferreras, A., Kiss-Papp, M., Jehle, A.K., Felix, G., and Chinchilla, D. (2015). An overdose of the Arabidopsis coreceptor brassinosteroid insensitive1-associated receptor kinase1 or its ectodomain causes autoimmunity in a suppressor of BIR1-1-dependent manner. Plant Physiology *168*, 1106-1121.

Dreher, K., and Callis, J. (2007). Ubiquitin, hormones and biotic stress in plants. Annals of Botany *99*, 787-822.

Du, J., Li, M., Kong, D., Wang, L., Lv, Q., Wang, J., Bao, F., Gong, Q., Xia, J., and He, Y. (2013). Nitric oxide induces cotyledon senescence involving co-operation of the NES1/MAD1 and EIN2-associated ORE1 signalling pathways in Arabidopsis. Journal of Experimental Botany *65*, 4051-4063.

Ewald, S.E., Engel, A., Lee, J., Wang, M., Bogyo, M., and Barton, G.M. (2011). Nucleic acid recognition by Toll-like receptors is coupled to stepwise processing by cathepsins and asparagine endopeptidase. The Journal of Experimental Medicine *208*, 643-651.

Finley, D. (2009). Recognition and processing of ubiquitin-protein conjugates by the proteasome. Annu Rev Biochem *78*, 477-513.

Gao, M., Wang, X., Wang, D., Xu, F., Ding, X., Zhang, Z., Bi, D., Cheng, Y.T., Chen, S., Li, X., *et al.* (2009). Regulation of cell death and innate immunity by two receptor-like kinases in Arabidopsis. Cell Host & Microbe *6*, 34-44.

Garcia-Cattaneo, A., Gobert, F.X., Muller, M., Toscano, F., Flores, M., Lescure, A., Del Nery, E., and Benaroch, P. (2012). Cleavage of Toll-like receptor 3 by cathepsins B and H is essential for signaling. Proceedings of the National Academy of Sciences of the United States of America *109*, 9053-9058.

Geldner, N., and Robatzek, S. (2008). Plant receptors go endosomal: a moving view on signal transduction. Plant Physiology *147*, 1565-1574.

Gish, L.A., and Clark, S.E. (2011). The RLK/Pelle family of kinases. The Plant Journal : for cell and molecular biology *66*, 117-127.

Gomez-Gomez, L., Bauer, Z., and Boller, T. (2001). Both the extracellular leucine-rich repeat domain and the kinase activity of FSL2 are required for flagellin binding and signaling in Arabidopsis. The Plant Cell *13*, 1155-1163.

Gomez-Gomez, L., and Boller, T. (2000). FLS2: an LRR receptor-like kinase involved in the perception of the bacterial elicitor flagellin in Arabidopsis. Mol Cell *5*, 1003-1011.

Gonzalez-Lamothe, R., Tsitsigiannis, D.I., Ludwig, A.A., Panicot, M., Shirasu, K., and Jones, J.D. (2006). The U-box protein CMPG1 is required for efficient activation of defense mechanisms triggered by multiple resistance genes in tobacco and tomato. The Plant Cell *18*, 1067-1083.

Greeff, C., Roux, M., Mundy, J., and Petersen, M. (2012). Receptor-like kinase complexes in plant innate immunity. Front Plant Sci *3*, 209.

Halter, T., Imkampe, J., Mazzotta, S., Wierzba, M., Postel, S., Bucherl, C., Kiefer, C., Stahl, M., Chinchilla, D., Wang, X., *et al.* (2014). The leucine-rich repeat receptor kinase BIR2 is a negative regulator of BAK1 in plant immunity. Current Biology : CB *24*, 134-143.

He, K., Gou, X., Yuan, T., Lin, H., Asami, T., Yoshida, S., Russell, S.D., and Li, J. (2007a). BAK1 and BKK1 regulate brassinosteroid-dependent growth and brassinosteroid-independent cell-death pathways. Current Biology : CB *17*, 1109-1115.

He, P., Shan, L., and Sheen, J. (2007b). The use of protoplasts to study innate immune responses. Methods Mol Biol *354*, 1-9.

Hecht, V., Vielle-Calzada, J.P., Hartog, M.V., Schmidt, E.D., Boutilier, K., Grossniklaus, U., and de Vries, S.C. (2001). The Arabidopsis Somatic Embryogenesis Receptor Kinase 1 gene is expressed in developing ovules and embryos and enhances embryogenic competence in culture. Plant Physiology *127*, 803-816.

Heese, A., Hann, D.R., Gimenez-Ibanez, S., Jones, A.M., He, K., Li, J., Schroeder, J.I., Peck, S.C., and Rathjen, J.P. (2007). The receptor-like kinase SERK3/BAK1 is a central regulator of innate immunity in plants. Proceedings of the National Academy of Sciences of the United States of America *104*, 12217-12222.

Jin, J.B., Jin, Y.H., Lee, J., Miura, K., Yoo, C.Y., Kim, W.Y., Van Oosten, M., Hyun, Y., Somers, D.E., Lee, I., *et al.* (2008). The SUMO E3 ligase, AtSIZ1, regulates flowering by controlling a salicylic acid-mediated floral promotion pathway and through affects on FLC chromatin structure. The Plant Journal : for cell and molecular biology *53*, 530-540.

Kadota, Y., Sklenar, J., Derbyshire, P., Stransfeld, L., Asai, S., Ntoukakis, V., Jones, J.D., Shirasu, K., Menke, F., Jones, A., *et al.* (2014). Direct Regulation of the NADPH Oxidase RBOHD by the PRR-Associated Kinase BIK1 during Plant Immunity. Mol Cell *54*, 43-55

Kawai, T., and Akira, S. (2006). TLR signaling. Cell Death and Differentiation *13*, 816-825.

Korasick, D.A., McMichael, C., Walker, K.A., Anderson, J.C., Bednarek, S.Y., and Heese, A. (2010). Novel functions of Stomatal Cytokinesis-Defective 1 (SCD1) in innate immune responses against bacteria. The Journal of Biological Chemistry *285*, 23342-23350.

Ladwig, F., Dahlke, R.I., Stuhrwohldt, N., Hartmann, J., Harter, K., and Sauter, M. (2015). Phytosulfokine Regulates Growth in Arabidopsis through a Response Module at the Plasma Membrane That Includes cyclic nucleotide-gated channel17, H+-ATPase, and BAK1. The Plant Cell *27*, 1718-1729.

Lee, I.C., Hong, S.W., Whang, S.S., Lim, P.O., Nam, H.G., and Koo, J.C. (2011). Age-dependent action of an ABA-inducible receptor kinase, RPK1, as a positive regulator of senescence in Arabidopsis leaves. Plant & Cell Physiology *52*, 651-662.

Lee, J., Nam, J., Park, H.C., Na, G., Miura, K., Jin, J.B., Yoo, C.Y., Baek, D., Kim, D.H., Jeong, J.C., *et al.* (2007). Salicylic acid-mediated innate immunity in Arabidopsis is regulated by SIZ1 SUMO E3 ligase. The Plant Journal : for cell and molecular biology *49*, 79-90.

Lei, J., S, A.F., Salzman, R.A., Shan, L., and Zhu-Salzman, K. (2014). Botrytis-induced kinase1 modulates Arabidopsis resistance to green peach aphids via phytoalexin deficient4. Plant Physiology *165*, 1657-1670.

Li, B., Lu, D., and Shan, L. (2014a). Ubiquitination of pattern recognition receptors in plant innate immunity. Molecular Plant Pathology *15*, 737-746.

Li, J., Wen, J., Lease, K.A., Doke, J.T., Tax, F.E., and Walker, J.C. (2002). BAK1, an Arabidopsis LRR receptor-like protein kinase, interacts with BRI1 and modulates brassinosteroid signaling. Cell *110*, 213-222.

Li, L., Li, M., Yu, L., Zhou, Z., Liang, X., Liu, Z., Cai, G., Gao, L., Zhang, X., Wang, Y., *et al.* (2014b). The FLS2-Associated Kinase BIK1 Directly Phosphorylates the NADPH Oxidase RbohD to Control Plant Immunity. Cell Host Microbe *15*, 329-338.

Li, W., Ahn, I.P., Ning, Y., Park, C.H., Zeng, L., Whitehill, J.G., Lu, H., Zhao, Q., Ding, B., Xie, Q., *et al.* (2012). The U-Box/ARM E3 ligase PUB13 regulates cell death, defense, and flowering time in Arabidopsis. Plant Physiology *159*, 239-250.

Lin, W., Li, B., Lu, D., Chen, S., Zhu, N., He, P., and Shan, L. (2014). Tyrosine phosphorylation of protein kinase complex BAK1/BIK1 mediates Arabidopsis

innate immunity. Proceedings of the National Academy of Sciences of the United States of America *111*, 3632-3637.

Lin, W., Lu, D., Gao, X., Jiang, S., Ma, X., Wang, Z., Mengiste, T., He, P., and Shan, L. (2013). Inverse modulation of plant immune and brassinosteroid signaling pathways by the receptor-like cytoplasmic kinase BIK1. Proceedings of the National Academy of Sciences of the United States of America *110*, 12114-12119.

Liu, J., Li, W., Ning, Y., Shirsekar, G., Cai, Y., Wang, X., Dai, L., Wang, Z., Liu, W., and Wang, G.L. (2012). The U-Box E3 ligase SPL11/PUB13 is a convergence point of defense and flowering signaling in plants. Plant Physiology *160*, 28-37.

Lu, D., Lin, W., Gao, X., Wu, S., Cheng, C., Avila, J., Heese, A., Devarenne, T.P., He, P., and Shan, L. (2011). Direct ubiquitination of pattern recognition receptor FLS2 attenuates plant innate immunity. Science *332*, 1439-1442.

Lu, D., Wu, S., Gao, X., Zhang, Y., Shan, L., and He, P. (2010). A receptor-like cytoplasmic kinase, BIK1, associates with a flagellin receptor complex to initiate plant innate immunity. Proceedings of the National Academy of Sciences of the United States of America *107*, 496-501.

Macho, A.P., and Zipfel, C. (2014). Plant PRRs and the activation of innate immune signaling. Mol Cell *54*, 263-272.

Martinez, C., Pons, E., Prats, G., and Leon, J. (2004). Salicylic acid regulates flowering time and links defence responses and reproductive development. The Plant Journal : for cell and molecular biology *37*, 209-217.

Meng, X., and Zhang, S. (2013). MAPK cascades in plant disease resistance signaling. Annual Review of Phytopathology *51*, 245-266.

Nam, K.H., and Li, J. (2002). BRI1/BAK1, a receptor kinase pair mediating brassinosteroid signaling. Cell *110*, 203-212.

Ntoukakis, V., Schwessinger, B., Segonzac, C., and Zipfel, C. (2011). Cautionary notes on the use of C-terminal BAK1 fusion proteins for functional studies. The Plant Cell *23*, 3871-3878.

Park, B., Brinkmann, M.M., Spooner, E., Lee, C.C., Kim, Y.M., and Ploegh, H.L. (2008). Proteolytic cleavage in an endolysosomal compartment is required for activation of Toll-like receptor 9. Nature Immunology *9*, 1407-1414.

Park, C.J., and Ronald, P.C. (2012). Cleavage and nuclear localization of the rice XA21 immune receptor. Nature Communications *3*, 920.

Postel, S., Kufner, I., Beuter, C., Mazzotta, S., Schwedt, A., Borlotti, A., Halter, T., Kemmerling, B., and Nurnberger, T. (2010). The multifunctional leucine-rich repeat receptor kinase BAK1 is implicated in Arabidopsis development and immunity. Eur J Cell Biol *89*, 169-174.

Qiao, H., Shen, Z., Huang, S.S., Schmitz, R.J., Urich, M.A., Briggs, S.P., and Ecker, J.R. (2012). Processing and subcellular trafficking of ER-tethered EIN2 control response to ethylene gas. Science *338*, 390-393.

Quirino, B.F., Normanly, J., and Amasino, R.M. (1999). Diverse range of gene activity during Arabidopsis thaliana leaf senescence includes pathogen-independent induction of defense-related genes. Plant Molecular Biology *40*, 267-278.

Robatzek, S., Chinchilla, D., and Boller, T. (2006). Ligand-induced endocytosis of the pattern recognition receptor FLS2 in Arabidopsis. Genes & Development *20*, 537-542.

Robatzek, S., and Somssich, I.E. (2002). Targets of AtWRKY6 regulation during plant senescence and pathogen defense. Genes & Development *16*, 1139-1149.

Roux, M., Schwessinger, B., Albrecht, C., Chinchilla, D., Jones, A., Holton, N., Malinovsky, F.G., Tor, M., de Vries, S., and Zipfel, C. (2011). The Arabidopsis leucine-rich repeat receptor-like kinases BAK1/SERK3 and BKK1/SERK4 are required for innate immunity to hemibiotrophic and biotrophic pathogens. The Plant Cell *23*, 2440-2455.

Samuel, M.A., Salt, J.N., Shiu, S.H., and Goring, D.R. (2006). Multifunctional arm repeat domains in plants. International Review of Cytology *253*, 1-26.

Schwessinger, B., and Ronald, P.C. (2012). Plant innate immunity: perception of conserved microbial signatures. Annual Review of Plant Biology *63*, 451-482.

Segonzac, C., Macho, A.P., Sanmartin, M., Ntoukakis, V., Sanchez-Serrano, J.J., and Zipfel, C. (2014). Negative control of BAK1 by protein phosphatase 2A during plant innate immunity. The EMBO Journal *33*, 2069-2079.

Seo, E., Lee, H., Jeon, J., Park, H., Kim, J., Noh, Y.S., and Lee, I. (2009). Crosstalk between cold response and flowering in Arabidopsis is mediated through the

flowering-time gene SOC1 and its upstream negative regulator FLC. The Plant Cell *21*, 3185-3197.

Shi, H., Shen, Q., Qi, Y., Yan, H., Nie, H., Chen, Y., Zhao, T., Katagiri, F., and Tang, D. (2013). BR-SIGNALING KINASE1 physically associates with FLAGELLIN SENSING2 and regulates plant innate immunity in Arabidopsis. The Plant Cell *25*, 1143-1157.

Smalle, J., and Vierstra, R.D. (2004). The ubiquitin 26S proteasome proteolytic pathway. Annual Review of Plant Biology *55*, 555-590.

Stegmann, M., Anderson, R.G., Ichimura, K., Pecenkova, T., Reuter, P., Zarsky, V., McDowell, J.M., Shirasu, K., and Trujillo, M. (2012). The ubiquitin ligase PUB22 targets a subunit of the exocyst complex required for PAMP-triggered responses in Arabidopsis. The Plant Cell *24*, 4703-4716.

Sun, L., and Chen, Z.J. (2004). The novel functions of ubiquitination in signaling. Curr Opin Cell Biol *16*, 119-126.

Takeda, K., and Akira, S. (2005). Toll-like receptors in innate immunity. International Immunology *17*, 1-14.

Trujillo, M., Ichimura, K., Casais, C., and Shirasu, K. (2008). Negative regulation of PAMP-triggered immunity by an E3 ubiquitin ligase triplet in Arabidopsis. Current Biology : CB *18*, 1396-1401.

Trujillo, M., and Shirasu, K. (2010). Ubiquitination in plant immunity. Current Opinion in Plant Biology *13*, 402-408.

Vega-Sanchez, M.E., Zeng, L., Chen, S., Leung, H., and Wang, G.L. (2008). SPIN1, a K homology domain protein negatively regulated and ubiquitinated by the E3 ubiquitin ligase SPL11, is involved in flowering time control in rice. The Plant Cell *20*, 1456-1469.

Vierstra, R.D. (2009). The ubiquitin-26S proteasome system at the nexus of plant biology. Nat Rev Mol Cell Biol *10*, 385-397.

Vogelmann, K., Drechsel, G., Bergler, J., Subert, C., Philippar, K., Soll, J., Engelmann, J.C., Engelsdorf, T., Voll, L.M., and Hoth, S. (2012). Early senescence and cell death in Arabidopsis saul1 mutants involves the PAD4-dependent salicylic acid pathway. Plant Physiology *159*, 1477-1487.

Wang, G.F., Seabolt, S., Hamdoun, S., Ng, G., Park, J., and Lu, H. (2011). Multiple roles of WIN3 in regulating disease resistance, cell death, and flowering time in Arabidopsis. Plant Physiology *156*, 1508-1519.

Wang, X., and Chory, J. (2006). Brassinosteroids regulate dissociation of BKI1, a negative regulator of BRI1 signaling, from the plasma membrane. Science *313*, 1118-1122.

Xia, Z.P., Sun, L., Chen, X., Pineda, G., Jiang, X., Adhikari, A., Zeng, W., and Chen, Z.J. (2009). Direct activation of protein kinases by unanchored polyubiquitin chains. Nature *461*, 114-119.

Xu, J.H., Wei, X.C., Yan, L.M., Liu, D., Ma, Y.Y., Guo, Y., Peng, C.N., Zhou, H.G., Yang, C., Lou, Z.Y., *et al.* (2013). Identification and functional analysis of phosphorylation residues of the Arabidopsis botrytis induced kinase1. Protein Cell *4*, 771-781.

Yang, C.W., Gonzalez-Lamothe, R., Ewan, R.A., Rowland, O., Yoshioka, H., Shenton, M., Ye, H., O'Donnell, E., Jones, J.D., and Sadanandom, A. (2006). The E3 ubiquitin ligase activity of arabidopsis plant U-box17 and its functional tobacco homolog ACRE276 are required for cell death and defense. The Plant Cell *18*, 1084-1098.

Yee, D., and Goring, D.R. (2009). The diversity of plant U-box E3 ubiquitin ligases: from upstream activators to downstream target substrates. Journal of Experimental Botany *60*, 1109-1121.

Zeng, L.R., Qu, S., Bordeos, A., Yang, C., Baraoidan, M., Yan, H., Xie, Q., Nahm, B.H., Leung, H., and Wang, G.L. (2004). Spotted leaf11, a negative regulator of plant cell death and defense, encodes a U-box/armadillo repeat protein endowed with E3 ubiquitin ligase activity. The Plant Cell *16*, 2795-2808.

Zhang, J., Li, W., Xiang, T., Liu, Z., Laluk, K., Ding, X., Zou, Y., Gao, M., Zhang, X., Chen, S., *et al.* (2010). Receptor-like cytoplasmic kinases integrate signaling from multiple plant immune receptors and are targeted by a Pseudomonas syringae effector. Cell Host Microbe *7*, 290-301.

Zhang, J., and Zhou, J.M. (2010). Plant immunity triggered by microbial molecular signatures. Mol Plant *3*, 783-793.

Zhang, K., Halitschke, R., Yin, C., Liu, C.J., and Gan, S.S. (2013). Salicylic acid 3-hydroxylase regulates Arabidopsis leaf longevity by mediating salicylic acid

catabolism. Proceedings of the National Academy of Sciences of the United States of America *110*, 14807-14812.

Zhou, J., He, P., and Shan, L. (2014). Ubiquitination of plant immune receptors. Methods in Molecular Biology *1209*, 219-231.

Zipfel, C., Robatzek, S., Navarro, L., Oakeley, E.J., Jones, J.D., Felix, G., and Boller, T. (2004). Bacterial disease resistance in Arabidopsis through flagellin perception. Nature *428*, 764-767.